Alma Mater Studiorum - Università di Bologna

DOTTORATO DI RICERCA IN FISICA

Ciclo XXVIII

Settore concorsuale di afferenza: 02/A2
Settore scientifico disciplinare: FIS/02

EMERGING GEOMETRY OF CORPUSCULAR BLACK HOLES

Presentata da **Andrea Giugno**

Coordinatore Dottorato
Prof. Gastone Castellani

Relatore
Prof. Roberto Casadio

Sessione II
Anno Accademico 2015/2016

Abstract

Quantum physics lends a view of space-time geometry as an emergent structure that shows classical features only at some observational level. The space-time manifold can be viewed as a purely theoretical arena, where quantum states and observables are defined, with the additional freedom of changing coordinates. We focus on spherically symmetric quantum sources, and determine the probability they are black holes. The gravitational radius is promoted to quantum mechanical operator acting on the "horizon wave-function". This formalism is applied to several sources with mass around the fundamental scale, as natural candidates of quantum black holes. This horizon quantum mechanics supports some features of BEC models of black holes. The Klein-Gordon equation for a toy graviton field coupled to a static matter current classically reproduces the Newtonian potential, while the corresponding quantum state is given by a coherent superposition of scalar modes. When N such bosons are self-confined in a volume of the size of the Schwarzschild radius, the horizon shows that their radius corresponds to a proper horizon whose related uncertainty is connected to the typical energy of Hawking modes: it is suppressed as N increases, contrarily to a single very massive particle. The spectrum of these systems is formed by a discrete ground state and a continuous Planckian distribution at the Hawking temperature representing the radiation. Assuming the internal scatterings give rise to the Hawking radiation, the N-particle state can be collectively described by a single-particle wave-function. The partition function follows together with the usual entropy law, with a logarithmic correction related to the Hawking component. The backreaction of radiating modes is also shown to reduce the Hawking flux, and eventually stop it.

Contents

Introduction

Untestable, undetectable and beyond reach, Black Holes (BHs) gained a prime role among the most interesting and debated theoretical models of modern phyisics. There is a robust indication that these dark vacancies in the space-time continuum are naturally originated when a very massive star ceases abruptly to exist. In the early stages, the leading characters in the field of stellar collapse were, indubitably, Oppenheimer and co-workers [1, 2]. They gave the start of a monumental amount of scientific literature on this subject, piercing the shroud on many enygmatic points in General Relativity (GR), and leaving many questions unanswered (see [3, 4] and references therein, for example).

Trying to describe the formation of BHs from a technical point of view naturally faces many issues, which happen to become much more involved once Quantum Mechanics (QM) comes into play. At any scale, one usually seeks the help of the famous Thorne's *hoop conjecture* [5], which claims that a BH appears whenever some certain energy (normally mass) M is entirely localised inside its own gravitational radius $R_{\rm H}$. In the most elementary cases, this is merely the Schwarzschild radius $R_{\rm H} = 2\,G_{\rm N}\,M$.

Initially conceived for classical, astrophysical BHs, this argument lacks of a rigorous experimental proof yet, but it has proved to possess a genuine reliability on any theoretical testing ground. In the classical description of vastly extended systems, the background metric and its related horizon structure are key points and GR succeeds in giving an accurate and consistent description of their properties. Nevertheless, when the characteristic length scale of the theory drops below the Planck one, this confidence quickly fades away. In fact, QM fails at providing a sharp answer to the position of physical objects, which in turn become fuzzily localised in space, and thus the statement of the hoop conjecture happens to be something to handle with care. In this range quantum effects are prominent and one shall also take into account the possible existence of new objects, usually named as "quantum black holes". Moreover, the hoop conjecture itself implies the suggestion that BHs may originate in a typical quantum situation, such as particle col-

lisions. Employing some suitable approximations (one over all is the neglect of total angular momentum), two particles can indeed collide with an impact parameter shorter than R_{H}, according to the amount of energy in the center of mass of the system.

One then predicts that a microscopic BH is formed, with relevant quantum properties. These fascinating objects cannot lack of a consistent quantum theory of gravity, in order to show their many features in proper fashion. Unfortunately, the scenario of physics is still waiting for such a wondeful theory and one needs to work under some approximations, which cannot avoid to be very restrictive sometimes. Quantum Field Theory (QFT) on curved space-time backgrounds has been realised for this scope: this theoretical apparatus stems from the assumption that the quantum fluctuations of gravity are small, or at least suppressed by the ones related to matter fields, and has produced outstanding results, like the renowned Hawking radiation [6, 7].

A new theoretical model was recently proposed by Dvali and Gomez [8], which allows to describe the quantum properties of BHs from an entirely new angle: large BHs are viewed as graviton condensates on the verge of a quantum phase transition and can be reliably described on flat space (or, in the arena of Newtonian gravitation), the geometry of space-time emerges as a collective effect [9]. In addition to that, we present some of the features of this model obtained from the "horizon wave-function formalism" (HWF). In this general approach, a wave-function for the gravitational radius can be associated with any localised QM particle [10, 11, 12, 13, 14, 15], which makes it easy to formulate in a quantitative way a condition for distinguishing BHs from regular particles. Among the added values, the formalism naturally leads to an effective Generalised Uncertainty Principle (GUP) [16] for the particle's position, and a decay rate for microscopic BHs.

This thesis is organised as follows: first, in Chapter 1, we will discuss some of the open problems affecting a quantum description of the gravitational interaction. In addition to that, we will explain some feature of ADM formalism, which bestows the space-time with some well-defined quantities, such as masses and energies in case of spherical symmetry. The most prominent between the spherical-symmetric models is the Oppenheimer-Snyder homogeneous collapsing system described in Section 1.1. The canonical quantisation of GR is further explained in Section 1.2 with some focus on the FRW minisuperspace approximation (Section 1.2.1) and the so-called problem of time (Section 1.2.2), stemming from the diffeomorphism invariance of the theory.

Chapter 2 introduces the reader to the formalism of the Horizon Wave Function (HWF) [17] and displays many of its interesting features. In particular, this tool is not only applied to the usual Schwarzschild solution, but also to BHs with more than one horizon, like Reissner-Nordström ones

(Section 2.3.2), and to BHs living in higher dimensional space-times (Section 2.3.4). Moreover, we will see how this construction correctly reproduces a GUP.

In Chapter 3, we discuss the corpuscular model of Refs. [8] and one of its possible field theoretic implementations in Section 3.1. (The particular case we consider there will allow us to make some conjectures regarding the BH formation from the gravitational collapse of a star). This formalism is then applied to specific models of corpuscular BHs and their Hawking radiation in Section 3.2 and collects results from Refs. [18] and [19].

Finally, some comments and speculations are summarised in Chapter 4.

Notation

Throughout the discussion of this thesis, we shall use the following notation.

- Speed of light $c = 1$
- Planck length $\ell_{\rm p}$ and mass $m_{\rm p}$
- Newton's constant $G_{\rm N} = \frac{\ell_{\rm p}}{m_{\rm p}}$
- Planck's constant $\hbar = \ell_{\rm p} m_{\rm p}$
- Schwarzschild radius $R_{\rm H} = \frac{2\ell_{\rm p} M}{m_{\rm p}}$
- $A_{\rm H} = 4\pi R_{\rm H}^2$
- GR = General Relativity
- QM = Quantum Mechanics
- QG = Quantum Gravity
- BH = Black Hole
- BEC = Bose-Einstein Condensate

Chapter 1

The road to quantising gravity

After Einstein introduced the theory of Special Relativity (SR) [20], we have grown accustomed to thinking of the space-time as the geometrical space where things happen. In this respect, SR just adds one dimension to the three-dimensional space of Newtonian physics, which is the natural arena for describing mathematically our intuitive notion of motion, or object displacements. However, we should not forget Einstein's first great achievement came from a rethinking of the concept of time and length as being related to actual measurements, which in turn require synchronised clocks. Quantum physics emerged around the same time from the very same perspective: a proper description of atoms and elementary particles, and other phenomena mostly occurring at microscopic scales, required a more refined analysis of how variables involved in such phenomena are actually measured. Since measuring means interacting with the system under scrutiny, the uncertainty principle due to a finite Planck constant then came out as a fact of life, like the Lorentz transformations come out from the finite speed of light. This gave rise to the mathematical structure of the complex Hilbert space of states, on which observables are given by operators with suitable properties, and the outcome of any measurements could then be predicted with at best a certain probability. In SR one can nonetheless think of the space-time coordinates as being labels of actual space-time points, observables in principle, as they implicitly define an inertial observer.

Then came GR [21], which allows for the use of any coordinates to identify space-time points, in a way that let us describe physics again much closer to what experimentalists do. The price to pay is that space-time correspondingly becomes a manifold endowed with a general Lorentzian metric, which acts as the "potential" for the universal gravitational force. This metric, in practice, determines the causal structure that was before given by the fixed Minkowski metric, and BHs were found in this theory. The quantisation of

matter fields on these metric manifolds led to the discovery of paradoxes and other difficulties, which are often pinpointed as the smoking gun that these two theories, of Quantum matter (fields) and GR, are hard to unify. But if one looks back at how these two pillars of modern physics precisely emerged from the rethinking of the interplay between a physical system and the observer, the path to follow should become clear, at least ideally: one should give up as many assumptions as possible, and set up the stage for describing the most fundamental processes that involve both. In so doing, one preliminary question we can try to address is what are the best variables to use (for each specific system), regardless of what we have come to accept as "fundamental" or "elementary". The very concept of space-time, as a "real" entity, should be put through this rethinking process. If the aim of our quantum theory is to describe the motion of objects, the space-time geometry is just an effective picture that we can conveniently employ in classical GR, but which might be too difficult to describe fully in the quantum theory [22]. In fact, the first step in this construction should be to give a clear modelling of the detection process by which we observe something somewhere: which observables should we employ then, and what are the physical restrictions we expect on them? All we wrote above is in fact nothing new. Any attempt at quantising canonically the Einstein-Hilbert action [23, 24, 25] falls into this scheme, in which the space-time is just a mathematical arena, and the metric becomes the basic observable, along with matter variables. Unfortunately, a mathematical treatment of the so called "superspace" of wave-functions describing all the possible states of the metric is extremely complicated. In fact, DeWitt himself, in his famous 1967 paper [26], immediately reverted to a simplified formulation in order to apply it to cosmology. His choice was based on preserving isotropy and homogeneity of the universe at the quantum level, which leads to the Friedman-Robertson-Walker family of metrics, with one degree of freedom, the scale factor. The corresponding space of quantum states is greatly simplified and referred to as the FRW "minisuperspace".

A general property of the Einstein theory is that the gravitational interaction is always attractive and we are thus not allowed to neglect its effect on the causal structure of space-time if we pack enough energy in a sufficiently small volume. This can occur, for example, if two particles (for simplicity, of negligible spatial extension and total angular momentum) collide with an impact parameter b shorter than the Schwarzschild radius corresponding to the total center-of-mass energy E of the system, that is

$$b \leq 2\,\ell_{\rm p}\,\frac{E}{m_{\rm p}} \equiv r_{\rm H}\ . \tag{1.1}$$

This hoop conjecture [5] has been checked and verified theoretically in a

variety of situations, but it was initially formulated for BHs of (at least) astrophysical sizes [27, 28, 29], for which the very concept of a classical background metric and related horizon structure should be reasonably safe (for a review of some problems, see the bibliography in Ref. [30]). Whether the concepts involved in the above conjecture can also be trusted for masses approaching the Planck size, however, is definitely more challenging. In fact, for masses in that range, quantum effects may hardly be neglected (for a recent discussion, see, e.g., Ref. [31]) and it is reasonable that the picture arising from General Relativistic BHs must be replaced in order to include the possible existence of "quantum BHs". Although a clear definition of such objects is still missing, most would probably agree that their production cross-section should (approximately) comply with the hoop conjecture, and that they do not decay thermally (see, e.g., Refs. [32, 33, 34, 35, 36, 37]).

The main complication in studying the Planck regime is that we do not have any experimental insight thereof, which makes it very difficult to tell whether any theory we could come up with is physically relevant. We might instead start from our established concepts and knowledge of nature, and push them beyond the present experimental limits. If we set out to do so, we immediately meet with a conceptual challenge: how can we describe a system containing both QM objects (such as the elementary particles of the Standard Model) and classically defined horizons? The aim of this review is precisely to show how one can introduce an operator (observable) for the gravitational radius, and define a corresponding HWF [10], which can be associated with any localised Quantum Mechanical particle or source [38, 39]. This horizon quantum mechanics (HQM) then provides a quantitative (albeit probabilistic) condition that distinguishes a BH from a regular particle. Since this "transition" occurs around the Planck scale, the HQM represents a simple tool to investigate properties of (any models of) quantum BHs in great generality. We shall also review how the HQM naturally leads to an effective GUP [11, 16, 40, 41, 42] for the particle position, a decay rate for microscopic BHs [11], and a variety of other results for BHs with mass around the fundamental Planck scale [37].

1.1 Gravitational collapse

Leaving aside for a moment the issues of a quantum-mechanical description of gravity, we introduce some open questions encoded in the geometry of trapped surfaces. In order to discuss the relevant properties of a classical horizon, we start by writing down the most general metric for a spherically

symmetric space-time as [43]

$$\mathrm{d}s^2 = g_{ij}(x^k)\,\mathrm{d}x^i\,\mathrm{d}x^j + r^2(x^k)\left(\mathrm{d}\theta^2 + \sin^2\theta\,\mathrm{d}\phi^2\right) \ , \tag{1.2}$$

where r is the areal coordinate and $x^i = (x^0, x^1)$ are coordinates on surfaces where the angles θ and ϕ are constant. It is clear that all the relevant physics takes place on the radial-temporal plane and we can safely set $x^0 = t$ and $x^1 = r$ from now on. Heuristically, we can think of a (local) "apparent horizon" as the place where the escape velocity equals the speed of light, and we expect its location be connected to the energy in its interior by simple Newtonian reasoning. More technically, in GR, an apparent horizon occurs where the divergence of outgoing null congruences vanishes and the radius of this trapping surface in a spherically symmetric space-time is thus determined by

$$g^{ij}\,\nabla_i r\,\nabla_j r = 0 \ , \tag{1.3}$$

where $\nabla_i r$ is the covector perpendicular to surfaces of constant area $\mathcal{A} = 4\,\pi\,r^2$. But then GR makes it very hard to come up with a sensible definition of the amount of energy inside a generic closed surface. Moreover, even if several proposals of mass functions are available [44], there is then no simple relation between these mass functions and the location of trapping surfaces. Accidentally, spherical symmetry is powerful enough to overcome all of these difficulties, in that it allows to uniquely define the total Misner-Sharp mass as the integral of the classical matter density $\rho = \rho(x^i)$ weighted by the flat metric volume measure,

$$m(t,r) = \frac{4\,\pi}{3}\int_0^r \rho(t,\bar{r})\,\bar{r}^2\,\mathrm{d}\bar{r} \ , \tag{1.4}$$

as if the space inside the sphere were flat. This Misner-Sharp function represents the active gravitational mass [1] inside each sphere of radius r and also determines the location of trapping surfaces, since Einstein equations imply that

$$g^{ij}\,\nabla_i r\,\nabla_j r = 1 - \frac{2\,M}{r} \ , \tag{1.5}$$

where $M = \ell_{\mathrm{p}}\,m/m_{\mathrm{p}}$. Due to the high non-linearity of gravitational dynamics, it is still very difficult to determine how a matter distribution evolves in time and forms surfaces obeying Eq. (1.3), but we can claim that a classical

[1] Roughly speaking, it is the sum of both matter energy and its gravitational potential energy.

trapping surface is found where the gravitational radius $R = 2\,M$ equals the comoving areal radius r, that is

$$R_{\rm H} \equiv 2\,M(t,r) = r\ , \tag{1.6}$$

which is nothing but a generalisation of the hoop conjecture (1.1) to continuous energy densities. Of course, if the system is static, the above radius will not change in time and the rapping surface becomes a permanent proper horizon (which is the case we shall mostly consider in the following).

On the other hand, one of the most relevant scenarios where we expect a quantum theory of gravitation could lead to strong predictions is the collapse of compact objects and the possible formation of BHs. This physical process cannot be realistically modelled as isotropic or homogeneous in all of its aspects, both because of the high non-linearity of the underlying relativistic dynamics and for the presence of many mechanisms, e.g. generating outgoing radiation [45, 46, 47, 48]. After the seminal papers of Oppenheimer, the literature on the subject has grown immensely, but many issues are still open in GR (see, e.g. Ref. [49, 50], and references therein).

This is not to mention the conceptual and technical difficulties one faces when the quantum nature of the collapsing matter is taken into account. As we mentioned, assuming quantum gravitational fluctuations are small, one can describe matter by means of QFT on the curved background spacetime [51]. However, the use of a fixed background is directly incompatible with the description of a self-gravitating system representing a collapsing object, for which the evolution of the background and possible emergence of non-trivial causal structures cannot be reliably addressed perturbatively.

In order to introduce the Oppenheimer-Snyder model, we write g_{ij} inside (1.2) as

$$g_{ij} = \begin{pmatrix} -e^{2\lambda} & 0 \\ 0 & e^{2\nu} \end{pmatrix}\ , \tag{1.7}$$

and we use a general function $R = R(r,t)$ to describe the dynamics of the areal radius.

We compute the related Einstein tensor $G_{\mu\nu}$, whose relevant components

are

$$
\begin{aligned}
G_{tt} &= \frac{M'}{R^2\,R'}\,e^{2\lambda} - \frac{2\dot{R}}{R\,R'}\left(\dot{R}' - \dot{R}\lambda' - \dot{\nu}\,R'\right) \ , && (1.8)\\
G_{rr} &= -\frac{\dot{M}}{R^2\,\dot{R}}\,e^{2\nu} - \frac{2R'}{R\,\dot{R}}\left(\dot{R}' - \dot{R}\lambda' - \dot{\nu}\,R'\right) \ , && (1.9)\\
G_{tr} &= -\frac{2}{R}\left(\dot{R}' - \dot{R}\lambda' - \dot{\nu}R'\right) && (1.10)\\
G_{\theta\theta} &= R\,e^{-2\nu}\left[\left(\lambda'' + \lambda'^2 - \lambda'\nu'\right)R + R'' + R'(\lambda' - \nu')\right]\\
&\quad -R\,e^{-2\lambda}\left[\left(\ddot{\nu} + \dot{\nu}^2 - \dot{\lambda}\dot{\nu}\right)R + \ddot{R} + \dot{R}(\dot{\nu} - \dot{\nu})\right] \ , && (1.11)\\
G_{\phi\phi} &= \sin^2\theta\,G_{\theta\theta} \ , && (1.12)
\end{aligned}
$$

where the dot denotes the derivative with respect to the proper time t, while the prime is respect the comoving radius r. If we consider a model of dust, the energy-momentum tensor of a perfect fluid

$$T_{\mu\nu} = \mathrm{diag}(\rho, p_r, p_\theta, p_\phi) \tag{1.13}$$

satisfies the condition $p_r = p_\theta = p_\phi = 0$ and the field equations become

$$\rho = \frac{M'}{R^2\,R'} \ , \qquad 0 = -\frac{\dot{M}}{R^2\,\dot{R}} \ . \tag{1.14}$$

From the latter we obtain that the mass function, *i.e.* the amount of matter enclosed within the comoving radius r, does not change with time.

Equations (1.10) and (1.11) can be combined in order to get

$$\dot{R}' = \dot{R}\,\lambda' + \dot{\nu}\,R' \ , \tag{1.15}$$

which result in the Misner-Sharp mass equation

$$\dot{R}^2 = \frac{M}{R} + f(r) \ . \tag{1.16}$$

With all the considerations above, the metric of can be safely set as

$$ds^2 = -dt^2 + \frac{R'^2}{1 + f(r)}dr^2 + R^2 d\Omega^2 \ . \tag{1.17}$$

There is the gauge freedom to fix the scaling of the areal function $R(t, r)$ encoding its variation in a scaling factor a

$$R(t, r) = r\,a(t) \ , \tag{1.18}$$

where homogeneity and isotropy demand a to be function of t alone. The scale factor is in turn fixed by some conditions.

For instance it is reasonable to impose that, at the initial time $t_i = 0$, the horizon is comoving with the observer

$$R(r, 0) = r \ , \tag{1.19}$$

that is to say $a(r, t_i) = 1$. In addition to that, we have for dust

$$\rho = \frac{M'}{r^2} \ , \tag{1.20}$$

whose mass profile is shaped as $M(r) = r^3 \bar{M}(r)$, with $\bar{M}$ smooth enough to avoid divergences in the center. In particular, since the system is homogeneous, the latter function can only be a constant because ρ does not depend on r. Moreover, the function $f(r)$ sets the inital conditions of the constituents of the collapsing shell and we choose

$$f(r) = r^2 \, \phi \tag{1.21}$$

for convenience.

It follows that Eq. (1.16) becomes

$$\dot{a}^2(t) = \frac{\bar{M}}{a(t)} + \phi \ , \tag{1.22}$$

where $\dot{a} < 0$ since the dust collapses, and the associated density is

$$\rho = \frac{3\bar{M}}{a^3} \ . \tag{1.23}$$

The sign of ϕ in Eq. (1.22) is the same of the velocity of the shells at infinity and when the collapse is marginally bound ($\phi = 0$) the equation of motion is analitically solvable.

However, for what it will follow, it is necessary to note that the free collapse is doomed to end in a singularity, where

$$\rho = \infty \quad \Longrightarrow \quad a(t_s) = 0 \ . \tag{1.24}$$

In addition to that, the dust will eventually cross the event horizon, whose geometry is determined by Eq. (1.5), and the system will become a BH.

With this simple model we took a spherical regular cloud made of homogeneous dust and followed its collapse. At a given instant of time the horizon and the central singularity form and the structure of a BH arises. We recall

that this description stems from many assumptions, such as the spherical symmetry of the system and the absence of phenomena like rotations. Anyway, the determination of the horizon, having the interior solution is not so straightforward. In fact, this requires the knowledge of the global structure of the spacetime, since it does not depend on the observer.

Using only GR we still have to understand many features of collapse models. If we pile up enough mass within a fixed radius we obtain a BH. Nevertheless the process that leads to the formation of the BH is dynamical and the structure of the horizon during collapse is not well understood. Most likely GR is not enough in the strong field regime and one needs to account for microphysics or modifications to the theory. These modifications will affect the crucial elements of BHs, again, the singularity and the horizons.

1.2 Canonical quantisation of gravity

The earliest attempts at quantising GR, performed during the 1950s and 1960s, started from a quite natural choice for configuration variables, namely the components of the three-metric h_{ij} describing the intrinsic geometry on a spatial slice Σ of the total space-time $\mathcal{M}$. In contrast to that, the so-called covariant approaches take a fixed fiducial background geometry and regard the curved space-time of GR as a perturbation given by a massless graviton field. The advantage of the canonical way, however, is that the full metric itself gains the status of field and the causal structure shall not be fixed a priori.

The technical work starts from writing down GR in the so-called Hamiltonian form, since the procedure of quantisation is quite explicit once a theory is cast in this fashion. In the canonical description, one designates a set of configuration variables q^n, with canonically conjugate momenta π_n, which describe the state of the system at some time in a suitable phase space. The evolution of these parameters is ruled by the Hamiltonian $H(q^n, \pi_n)$, which gives the physically allowed motions in phase space as a family of orbits.

Once the universe $\mathcal{M}$ has been foliated in arbitrary $3-$dimensional spacelike hypersurfaces, the momenta conjugated to h_{ij} effectively encode the rate at which the metric changes. From the $4-$dimensional perspective, this mechanism is directly related to the extrinsic curvature of Σ. This approach is known as geometrodynamics since it views GR as describing the dynamics of spatial geometry.

Following the standard procedure, we can start a canonical description of

gravity by means of the decomposition of the metric tensor

$$g_{\mu\nu} = \begin{pmatrix} -\mathcal{N}^2 + \mathcal{N}_k\mathcal{N}^k & \mathcal{N}_j \\ \mathcal{N}_i & h_{ij} \end{pmatrix} , \tag{1.25}$$

where the components enjoy

$$h_{ik}h^{kj} = \delta_i^j , \qquad \mathcal{N}^i = h^{ij}\mathcal{N}_j . \tag{1.26}$$

Above, the functions $\mathcal{N}$ and $\mathcal{N}_i$ are called lapse and shift functions, respectively. Denoting the covariant differentiation with respect to the 3−metric h_{ij} with a dot, one can define the quantity

$$K_{ij} = \frac{1}{2}\mathcal{N}^{-1}(\mathcal{N}_{i.j} + \mathcal{N}_{j.i} - h_{ij,0}) , \tag{1.27}$$

which is known as second fundamental form. It describes the curvature of the hypersurface $x^0 = constant$, viewed from the 4−dimensional embedding space-time. In contrast to the latter, the intrinsic curvature tensor ${}^{(3)}\mathcal{R}_{ij}$, only depends on h_{ij} on the hypersurface. With all these pieces, the Lagrangian reads

$$\begin{aligned} L &= \int \mathrm{d}\vec{x}\,\mathcal{L} = \frac{m_\mathrm{p}}{16\pi\ell_\mathrm{p}} \int \mathrm{d}\vec{x}\,\sqrt{-g}\;{}^{(4)}\mathcal{R} \\ &= \frac{m_\mathrm{p}}{16\pi\ell_\mathrm{p}} \int \mathrm{d}\vec{x}\,\mathcal{N}\,h\left(K_{ij}K^{ij} - K^2 + {}^{(3)}\mathcal{R}\right) , \end{aligned} \tag{1.28}$$

where

$$g = \det g_{\mu\nu} , \quad h = \det h_{ij} , \quad {}^{(3)}\mathcal{R} = h^{ij}\,{}^{(3)}\mathcal{R}_{ij} \quad \text{and} \quad K = h^{ij}K_{ij} . \tag{1.29}$$

The primary constraints are obtained computing the momenta

$$\pi = \frac{\delta L}{\delta \mathcal{N}_{,0}} = 0 , \qquad \pi^i = \frac{\delta L}{\delta \mathcal{N}_{i,0}} = 0 , \tag{1.30}$$

$$\pi^{ij} = \frac{\delta L}{\delta h_{ij,0}} = -\sqrt{h}(K^{ij} - h^{ij}K) , \tag{1.31}$$

conjugated to the lapse $\mathcal{N}$, the shift $\mathcal{N}_i$ and the metric h_{ij}, respectively. Since the "velocities" $\mathcal{N}_{,0}$ and $\mathcal{N}_{i,0}$ are independent from the momenta, one can assign arbitrary values to them, corresponding to the choice of different boundary conditions on the space-time coordinates.

The Cauchy problem is ill-defined since some of the field variables do not possess a related conjugate momenta, while the others are not at all

dynamically independent. Field equations themselves fail at being linearly independent, and some of them show no second time derivative. This issue is labeled as "problem of constraints" and arises from the general coordinate-transformation invariance group of the theory.

At this point, let us take a little step back, in order to explain this concept with a pedagogical argument. A typical example of constraint is Gauss' law in the ordinary Maxwell theory: in absence of charges, the electric field $\vec{E}(\vec{x})$ satisfies

$$\vec{\nabla} \cdot \vec{E}(\vec{x}) - 4\pi\rho(\vec{x}) = 0 \tag{1.32}$$

at every point $\vec{x}$. It follows that one of the three component is fixed everywhere in space, once the remaining two are specified. Not all components of the Maxwell equations generate a physical propagation of the fields, and the number of true degrees of freedom is reduced. On a quantum mechanical level, this mechanism stems from the $U(1)$ gauge invariance of QED.

In the case of GR, the constraints come from the fact that the full theory is invariant under the diffeomorphism

$$g_{\mu\nu}(x) \to g'_{\mu\nu}(x) = g_{\mu\nu}(x) + \xi_{\mu,\nu} + \xi_{\nu,\mu} \ , \tag{1.33}$$

for any covector $\xi_\mu(x)$. Heuristically, this gauge means that the metric solving the Einstein's equations can be dragged around, with its related matter fields, on $\mathcal{M}$. The new solution is physically equivalent, although mathematically distinct, from the original one.

As usual, we can compute the Hamiltonian as a Legendre transform of the Lagrangian (1.28), obtaining

$$H = \frac{m_{\rm p}}{16\pi\ell_{\rm p}} \int \mathrm{d}\vec{x} \, \left(\pi\mathcal{N}_{,0} + \pi^i\mathcal{N}_{i,0} + \mathcal{N}\mathcal{H} + \mathcal{N}_i\mathcal{H}^i\right) \ . \tag{1.34}$$

The quantity

$$\mathcal{H} \ = \ \sqrt{h}\left(K_{ij}K^{ij} - K^2 - {}^{(3)}\!\mathcal{R}\right) \ , \tag{1.35}$$

is called super-Hamiltonian density, while

$$\mathcal{H}^i \ = \ -2\pi^{ij}_{\ \ ,j} - h^{il}(2h_{jl,k} - h_{jk,l})\pi^{jk} \tag{1.36}$$

generates spatial diffeomorphisms along orbits defined by the shift function $\mathcal{N}_i(x)$.

There exist secondary constraints, which restrict the dynamical freedom of the field and which are insensitive to how the velocities have been fixed.

Since the primary constraints have to hold for any instant of time, their derivative with respect to the coordinate x^0 has to vanish. Realising the latter as a Poisson bracket with H, it follows

$$\mathcal{H}^i = 0 \ , \qquad \mathcal{H} = 0 \ . \tag{1.37}$$

In the classical (unquantised) canonical formulation of GR, the constraints do not imply any particular problem, besides defining suitable gauge invariant observables that commute with them. In fact, one fixes a background spacetime by means of a convenient choice of the functions $\mathcal{N}$ and $\mathcal{N}_i$, which does not interfere with the resulting geometry. An alternative selection of lapse and shift implies a different background on which to evolve the foreground.

When the theory moves to the quantum realm, however, the constraints involve a series of delicate problems, both conceptually and technically. The quantisation scheme promotes the configuration variables and their conjugated momenta to operators acting on a Hilbert space, while their classical Poisson-bracket relations become commutations and encode the quantum fuzziness linked to the Heisenberg's uncertainty principle. Eventually, the dynamical evolution is generated by the hamiltonian operator $\hat{H}$ acting on a vector $|\Psi\rangle$, which represents the quantum state of the system.

This simple procedure involves complicated classical functions of fields defined at the same spatial point. The perturbative non-renormalisability of QG suggests that the operator analogues of these expressions are very ill-defined. Furthermore, this issue is affected by the horrendous operator-ordering difficulties, which in turn arise when attempts are made to replace the classical constraints and Hamiltonians with operator equivalents.

In quantum gauge theories there are two possible approaches, according to whether constraining is done before or after quantisation. In the former case, the true degrees of freedom are selected and are the only ones to enjoy the promotion to operators during quantisation. Regardless the personal choice of the way in which the gauge is fixed, all these schemes involve the removal of redundant degrees of freedom by imposing some special conditions. Fixing a gauge in a general covariant theory is equivalent to specifying a particular coordinate system with respect to which the physical data is described (spatial coordinates) and with respect to which it evolves (time coordinate).

This procedure has to take care of the general question of the extent to which classical geometrical properties can be, or should be, preserved in the quantum theory. In fact, from the classical point of view, the way in which the separation of the canonical variables into physical and non-physical parts is performed does not prevent to write back the metric h_{ij} as a functional of the dynamical and non-dynamical modes.

It is not guaranteed that something similar could be done at the quantum level, and after promoting the 3−metric h_{ij} and its conjugate momentum to operators, with usual commutation rules

$$\left[\hat{h}_{ij}(x), \hat{\pi}^{kl}(y)\right] = -i\ell_{\rm p} m_{\rm p}\, \delta^{k}_{(i}\delta^{l}_{j)}\delta(x-y) \ , \tag{1.38}$$

one is faced with the additional concern that the resulting theory may well not be independent of the choice of gauge.

Because of these issues, the usual approach in canonical QG is to impose the constraints after quantizing. In this constraint quantization approach, due to Dirac, one treats the constraints themselves as a set of operators $\hat{C}^n$, and demands that physical states $|\Psi_{\rm phys}\rangle$ be those which are annihilated by them. More specifically, the physical states are solutions to the equations

$$\hat{C}^n\,|\Psi_{\rm phys}\rangle = 0 \ . \tag{1.39}$$

Concerning the first set of Eqs. (1.37), this results straightforwardly in the so-called diffeomorphism constraints

$$\hat{\mathcal{H}}^i\ |\Psi\rangle = -\left[\sqrt{h}\left(K^{ij} - h^{ij}K\right)\right]_{.j}\ |\Psi\rangle = 0 \ , \tag{1.40}$$

which are responsible for shifting data tangential to the initial surface. They are therefore related to the shift vector field $\mathcal{N}_i$. They guarantee that the wave functional is invariant under three-dimensional coordinate transformations. The configuration space of all three-metrics divided by three-dimensional diffeomorphisms is called superspace.

Making use of the DeWitt metric

$$G_{ijkl} = \frac{1}{2}h^{-1/2}\left(h_{ik}h_{jl} + h_{il}h_{jk} - h_{ij}h_{kl}\right) \ , \tag{1.41}$$

the constraint

$$\hat{\mathcal{H}}\ |\Psi\rangle = 0 \ , \tag{1.42}$$

gives the Wheeler-DeWitt equation

$$\left(16\pi\ell_{\rm p}^3 m_{\rm p}\, G_{ijkl}\,\frac{\delta^2}{\delta h_{ij}\,\delta h_{kl}} + \frac{m_{\rm p}}{16\pi\ell_{\rm p}}\,\sqrt{h}\,{}^{(3)}\!\mathcal{R}\right)|\Psi\rangle = 0 \ . \tag{1.43}$$

This constraint shows to be responsible for pushing data off the initial surface, and thus is related to the lapse function. In particular, this equation is rather central as it should encode (at least in principle) the dynamics at the quantum level.

1.2.1 FRW minisuperspace

In QG, the phase space is infinite dimensional as we are dealing with a field theory. An approximation which is sometimes taken is to only consider the largest wavelength modes of the order of the size of the universe when studying cosmological models. This is the minisuperspace approximation. The validity of this approximation holds as long as the adiabatic approximation holds. In order to assume the Friedmann universe to be closed, it must be filled with some form of energy, given either by matter or radiation. The related Hamiltonian density refines the constraint given by Eq. (1.42). Moreover, these new particles are distributed uniformly on a 3−sphere of radius $R(t)$, which can be recast as

$$R(t) = R\, a(t) \ , \tag{1.44}$$

by means of the gauge (1.18), where $R = R(t = 0)$. On this hypersphere, all the degrees of freedom are "frozen out" except one, corresponding to the time-varying scale factor $a(t)$.

The metric of the Friedmann universe is written from (1.2)

$$g_{\mu\nu} = \begin{pmatrix} -\mathcal{N}^2 & 0 \\ 0 & h^0_{ij} \end{pmatrix} \ , \tag{1.45}$$

setting $\mathcal{N}_i = 0$, while h^0_{ij} is the induced metric of a 3−sphere of unit radius $h_{ij} = R^2\, a^2\, h^0_{ij}$, whose Ricci scalar is just ${}^{(3)}\mathcal{R} = 6/R^2a^2$. The lagrangian (1.28) is accordingly obtained by integrating this metric over the volume of the sphere $2\pi^2 R^3$

$$L = \frac{3m_{\rm p}R^2}{4\ell_{\rm p}} \int {\rm d}a\, a \left[-\frac{R^2}{\mathcal{N}} (a_{,0})^2 + \mathcal{N} \right] . \tag{1.46}$$

The total Lagrangian $L_{\rm tot} = L + L_{\rm int}$ is completed with the addition of the effective Lagrangian describing the internal degrees of freedom of the material particles which form the universal dust. Their dynamical degrees of freedom may be described by the canonical coordinates q^i and the momenta obtained by proper time differentiation

$$\dot{q}^i = \frac{1}{\mathcal{N}}\, q^i_{,0} \ , \tag{1.47}$$

whose "freezing out" requires all the particles to be identical and in the identical coherent state. The effective Lagrangian density is thus

$$\mathcal{L}_{\rm int} \sim N\mathcal{N}\, l \left(q, \frac{q_{,0}}{\mathcal{N}} \right) \ , \tag{1.48}$$

where N is the total number of the particles of the universe and l is their single-particle lagrangian.

Defining

$$\Pi = \frac{\delta L}{\delta a_{,0}} = -\frac{3m_{\rm p}R^2}{2\ell_{\rm p}}\,\frac{a\,a_{,0}}{\mathcal{N}}\ , \tag{1.49}$$

the total Hamiltonian density is

$$\mathcal{H} + \mathcal{H}_{\rm int} \;=\; \pi\mathcal{N}_{,0} - \mathcal{N}\left(\frac{\ell_{\rm p}}{3m_{\rm p}R}\,\frac{\Pi^2}{a} + \frac{3m_{\rm p}}{4\ell_{\rm p}}R\,a - Nm\right)\ . \tag{1.50}$$

Here, the symbol m designates the internal Hamiltonian $p_i\dot{q}^i - l$ of the particles. In particular, such quantity is identified with the rest mass, provided the arbitrary zero point of l has been chosen correctly. At the quantum level, the condition

$$\pi = \frac{\delta L_{\rm tot}}{\delta\mathcal{N}_{,0}} = 0 \tag{1.51}$$

turns immediately to the analog of the Wheeler-deWitt equation (1.43) in the a-representation

$$\left(\frac{\ell_{\rm p}}{3m_{\rm p}R^3}\,a^{-1/4}\,\frac{\partial}{\partial a}\,a^{-1/2}\,\frac{\partial}{\partial a}\,a^{-1/4} - \frac{3m_{\rm p}}{4\ell_{\rm p}}R\,a + Nm\right)|\Psi\rangle = 0\ , \tag{1.52}$$

where m is now understood as the particle mass operator. For the arguments appearing in the following chapters, it is enough to determine the normalizable solutions of such equation in the WKB approximation for a suitable potential.

DeWitt [26] related Eq. (1.52) to the simple Schrödinger equation of a massive point particle moving in the one-dimensional potential

$$V(a) = \begin{cases} \infty & \text{if}\ \ a < 0\ , \\ \\ \dfrac{3m_{\rm p}}{4\ell_{\rm p}}R & \text{if}\ \ a > 0\ , \end{cases} \tag{1.53}$$

with energy Nm and boundary conditions $\Psi(a=0) = 0$. Moreover, it is possible to estimate the energy spectrum of the system

$$Nm \sim \sqrt{n + \frac{3}{4}} \tag{1.54}$$

from the phase integral condition

$$\begin{aligned} n + \frac{3}{4} &= -\frac{R}{2\pi} \oint \Pi \, \mathrm{d}a \\ &= \frac{3 m_{\mathrm{p}} R^2}{2\pi \ell_{\mathrm{p}}} \int_0^{a_{\max}} \sqrt{a \left(a_{\max} - a \right)} \, \mathrm{d}a \ . \end{aligned} \tag{1.55}$$

In the last equation

$$a_{\max} = \frac{4\ell_{\mathrm{p}}}{3 m_{\mathrm{p}}} R \, N m \tag{1.56}$$

is the maximum value of the scale factor which allows the wave-function $\Psi\left(a(t)\right)$ to be normalizable, *i.e.* not to have an asymptotically exponential behaviour. At this point we may take back a closed Friedmann universe as a realistic model, since it has a maximum radius of expansion in the classical theory, and realise that the quantum number n is huge, roughly $n \sim 10^{120}$.

If we take into account all the degrees of freedom of the universe (whose number is pushed to infinity in a field theory) the value of n will be greater of many orders of magnitude. To our purpose, anyway, it is sufficient to note that the minisuperspace approximation is able to capture a vast amount of information from the fondamental full theory of QG and plug it into a reliable semiclassical approximation.

1.2.2 A problem to solve... in time

Let us conclude this brief introduction on the open questions of QG with the problem of time (for an excellent review, see [52] and references therein). All approaches to canonical QG deal with the infamous “problem of time" in one form or another. As we saw, GR is invariant under diffeomeorphisms and the background coordinates are stripped of their physical nature. Anyway, once the manifold $\mathcal{M}$ is foliated, the slices Σ on which the configuration variables live inevitably include time, in the same way they do with space.

Furthermore, the geometrical nature of time implies the fact that it must be a solution of the Einstein's field equations, while the space-time geometry is a dynamical variable. From the point of view of Σ it is nothing but a label which is freely chosen, and not a physical parameter which rules the causal evolution of gravitational models. However, one shall take into account that it is possible to solve field equations first and then isolate a variable, for each solution, from within the emerging phase space that is designated to play the role of time.

The existence of the super-Hamiltonian constraint $\mathcal{H} = 0$ reflects the inclusion of an ordinary time variable in the data, since constraints take

into account of the general covariance of the theory. The resulting Wheeler-DeWitt equation is accountable for describing time-evolution in the classical theory. Yet, the quantum counterpart (1.43) of this argument, descending from the quantum constraint (1.42), would in principle point out that the true physical states of the system do not evolve at all: there is no t. To be more accurate, any physical wave-function cannot depend on this now unphysical coordinate. Any possible "Schrödinger equation", therefore, falls into being a constraint rather than the key ingredient of dynamics.

If the constraints are not satisfied by the canonical initial data then the evolution of these inputs with respect to the appropriate equations will not generate a physically possible spacetime for choices of lapse $\mathcal{N}$ and shift $\mathcal{N}_i$. Nonetheless, when the constraints are satisfied then the various choices of these functions will always generate the same spacetime metric $g_{\mu\nu}(x)$.

For what follows, we try to override the deep technical details and just settle with the main concept stemming from the problem of time during the constrained quantisation of gravity.

In the approach which the theory is constrained before quantisation, the problem is to quantise an action principle in which the canonical variables $h_{ij}(x)$ and $\pi^{ij}(x)$ are subject to the constraints (1.37) and where all non-dynamical variables have been formerly removed. This procedure aims at retrieving a sort of "Schrödinger equation"

$$-im_{\mathrm{p}}\ell_{\mathrm{p}}\frac{\partial}{\partial t}\left|\Psi\right\rangle = \hat{H}\left|\Psi\right\rangle \ , \tag{1.57}$$

where the internal time t has already been identified as a suitable functional of the canonical variables, which satisfy their related constraints. Among all the possible strategies, this is rather "old-school", since its sought output strongly traces the classical time of quantum physics, in order to maintain the consistency of the theoretical setup.

On the contrary, if one decides to constrain after quantising, the constraints (1.42) are imposed at the quantum level and select vectors belonging to the physical sector of the total Hilbert space. The identification of a sensible time coordinate is therefore made at the end of this operation and contributes to give a reasonable interpretation on physical grounds, with much emphasis on the probabilistic side of the matter. However, the resulting outcome of this construction is not strongly linked to the starting quantum structure as in the previous approach.

We conclude this paragraph stressing out that both of the approaches are affected by the problem of time also at a functional level. In the scheme in which the identification of t is carried out before quantisation, there may appear some anomalies in the algebra given by the local Hamiltonians associated

with the generalised Schrödinger equation. Of course, any of such anomalies is meant to affect this equation with troublesome inconsistencies. In the other quantisation procedure, the space-time diffeomorphism sub-group $Diff(\mathcal{M})$, which quotients the total symmetry group of the theory, generates a Lie algebra, whose quantum version can be anomalous.

Eventually, in both ways, the undelying algebra is not endorsed to close, and the coherence of the classical time evolution may not be recovered.

Chapter 2

Horizon Quantum Mechanics

The very first attempt at solving Einstein's field equations resulted in the discovery of the Schwarzschild metric [53, 54]

$$\mathrm{d}s^2 = -f\,\mathrm{d}t^2 + f^{-1}\,\mathrm{d}r^2 + r^2\left(d\theta^2 + \sin^2\theta\,d\phi^2\right)\ , \tag{2.1}$$

with

$$f = 1 - \frac{2\,M}{r}\ , \tag{2.2}$$

and the appearance of the characteristic length $R_{\mathrm{H}} = 2\,M$ associated to the source. In fact, given a spherically symmetric matter source, the Schwarzschild radius R_{H} measures the area of the event horizon, which makes the interior of the sphere causally disconnected from the outer portion of space-time. At the same time, QM naturally associates a Compton-de Broglie wavelength to a particle. This is the minimum resolvable length scale, according to the Heisenberg uncertainty principle, and it can be roughly understood as the threshold below which quantum effects cannot be neglected. It is clear that any attempt at quantising gravity should regard those two lengths on somewhat equal grounds.

Anyway, the picture lacks of any mass threshold, since the classical theory does not yield a lower limit for the function M. Therefore, it seems that one can set the area of the trapping surface to be arbitrarily small and eventually have BHs of vanishingly small mass.

2.1 Compton length and BH mass threshold

As we mentioned above, quantum mechanics provides a length cut-off through the uncertainty in the spatial localisation of a particle. It is roughly given

by the Compton length

$$\lambda_m \simeq \ell_{\rm p} \frac{m_{\rm p}}{m} = \frac{\ell_{\rm p}^2}{M} \tag{2.3}$$

if, for the sake of simplicity, we consider a spin-less point-like source of mass m. It is a well-established fact that quantum physics is a more fundamental description of the laws of nature than classical physics. This means that $R_{\rm H}$ only makes sense when it is not "screened" by λ_m, that is

$$R_{\rm H} \geq \lambda_m \ , \tag{2.4}$$

and, equivalently, the BH mass must satisfy

$$m \geq m_{\rm p} \ , \tag{2.5}$$

or $M \geq \ell_{\rm p}$. We want to remark that the Compton length (2.3) can also be thought of as a quantity which rules the quantum interaction of m with the local geometry. Although it is likely that the particle's self-gravity will affect it, we still safely assume the flat space condition (2.5) as a reasonable order of magnitude estimate.

In light of recent developments, the common argument that quantum gravity effects should become relevant only at scales of order $m_{\rm p}$ or higher appears to be somewhat questionable, since the condition (2.5) implies that a classical description of a gravitational system with $m \gg m_{\rm p}$ should be fairly accurate (whereas for $m \sim m_{\rm p}$ the judge remains out). This is indeed the idea of "classicalization" in a nutshell, as it was presented in Refs. [55, 56] and, before that, of models with a minimum length and gravitationally inspired GUPs [57]. The latter are usually presented as fundamental principles for the reformulation of quantum mechanics in the presence of gravity, following the canonical steps that allow to bring a theory to the quantum level. In this picture, gravity would then reduce to a "kinematic effect" encoded by the modified commutators for the canonical variables. In this review, we shall instead follow a different line of reasoning: we will start from the introduction of an auxiliary wave-function that describes the horizon associated with a given localised particle, and retrieve a modified uncertainty relation as a consistent result [11].

2.2 Horizon Wave-Function

We are now ready to formulate the quantum mechanical description of the gravitational radius in three spatial dimensions in a general fashion [10]. For

the reasons listed above, we shall only consider quantum mechanical states representing *spherically symmetric* objects, which are *localised in space*. Since we want to put aside a possible time evolution for the moment (see Section 2.4), we also choose states *at rest* in the given reference frame or, equivalently, we suppose that every function is only taken at a fixed instant of time. According to the standard procedure, the particle is consequently described by a wave-function $\psi_{\rm S} \in L^2(R^3)$, which we assume can be decomposed into energy eigenstates,

$$|\psi_{\rm S}\rangle = \sum_E C(E)\ |\psi_E\rangle \ . \tag{2.6}$$

As usual, the sum over the variable E represents the decomposition on the spectrum of the Hamiltonian,

$$\hat{H}\ |\psi_E\rangle = E\ |\psi_E\rangle \ , \tag{2.7}$$

regardless of the specific form of the actual Hamiltonian operator $\hat{H}$. Note though that the relevant Hamiltonian here should be the analogue of the flat space energy that defines the Misner-Sharp mass (1.4). Once the energy spectrum is known, we can invert the expression of the Schwarzschild radius in Eq. (1.1) in order to get

$$E = m_{\rm p}\,\frac{r_{\rm H}}{2\,\ell_{\rm p}} \ . \tag{2.8}$$

We then define the (unnormalised) HWF as

$$\psi_{\rm H}(r_{\rm H}) = C\,(m_{\rm p}\,r_{\rm H}/2\,\ell_{\rm p}) \ , \tag{2.9}$$

whose normalisation is fixed by means of the Schrödinger scalar product in spherical symmetry,

$$\langle\,\psi_{\rm H}\mid\phi_{\rm H}\,\rangle = 4\,\pi\int_0^\infty \psi^*_{\rm H}(r_{\rm H})\,\phi_{\rm H}(r_{\rm H})\,r_{\rm H}^2\,{\rm d}r_{\rm H} \ . \tag{2.10}$$

In this conceptual framework, we could naively say that the normalised wave-function $\psi_{\rm H}$ yields the probability for an observer to detect a gravitational radius of areal radius $r = r_{\rm H}$ associated with the particle in the quantum state $\psi_{\rm S}$. The sharply defined classical radius $R_{\rm H}$ is thus replaced by the expectation value of the operator $\hat{r}_{\rm H}$. Since the related uncertainty is in general not zero, this gravitational quantity will necessarily be "fuzzy", like the position of the source itself. In any case, we stress that the observational meaning of the HQM will appear only after we introduce a few derived quantities.

In fact, we recall that we aimed at introducing a quantitative way of telling whether the source is a BH or a regular particle. Given the wave-function $\psi_{\rm H}$ associated with the quantum state $\psi_{\rm S}$ of the source, the probability density for the source to lie inside its own horizon of radius $r = r_{\rm H}$ will be the product of two factors, namely

$$\mathcal{P}_<(r < r_{\rm H}) = P_{\rm S}(r < r_{\rm H})\, \mathcal{P}_{\rm H}(r_{\rm H}) \ . \tag{2.11}$$

The first term,

$$P_{\rm S}(r < r_{\rm H}) = \int_0^{r_{\rm H}} \mathcal{P}_{\rm S}(r)\, {\rm d}r = 4\,\pi \int_0^{r_{\rm H}} |\psi_{\rm S}(r)|^2\, r^2\, {\rm d}r \ , \tag{2.12}$$

is the probability that the particle resides inside the sphere of radius $r = r_{\rm H}$, while the second term,

$$\mathcal{P}_{\rm H}(r_{\rm H}) = 4\,\pi\, r_{\rm H}^2\, |\psi_{\rm H}(r_{\rm H})|^2 \ , \tag{2.13}$$

is the probability density that the value of the gravitational radius is $r_{\rm H}$. Finally, it seems natural to consider the source is a BH if it lies inside its horizon, regardless of the size of the latter. The probability that the particle described by the wave-function $\psi_{\rm S}$ is a BH will then be given by the integral of (2.11) over all possible values of the horizon radius $r_{\rm H}$, namely

$$P_{\rm BH} = \int_0^\infty \mathcal{P}_<(r < r_{\rm H})\, {\rm d}r_{\rm H} \ , \tag{2.14}$$

which is the main outcome of the HQM.

In the following, we shall review the application of this construction to some simple, yet intriguing examples, in which the source is represented by Gaussian wave-functions. We anticipate that such states show very large horizon fluctuations and are not good candidates for describing astrophysical BHs [11] (for which extended models instead provide a better semiclassical limit [9]), but appear well-suited for investigating BHs around the fundamental Planck scale as unstable bound states [37].

2.2.1 Alternative horizon quantizations

It is important to remark the differences of the HQM with respect to other approaches in which the gravitational degrees of freedom of (or on) the horizon are quantised according to the background field method [58] (see, e.g. Refs. [59, 60, 61, 62, 63, 64, 65]). In general, such attempts consider linear perturbations of the metric on this surface [63], and apply the standard quantum field construction [51], which is what one would do with free

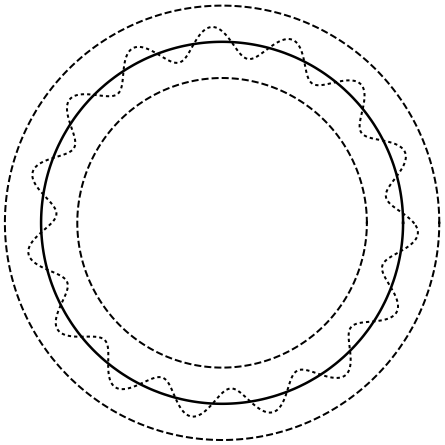

Figure 2.1: Pictorial view of the HQM radial fluctuations (dashed lines) and quantum field theoretic fluctuations (dotted line) around the classical horizon radius (solid line).

gravitons propagating on a fixed background. Of course, the fact that the horizon is a null surface implies that these perturbative modes enjoy several peculiar properties. For instance, they can be described by a conformal field theory [61], which one can view as the origin of the idea of BHs as holograms [64, 65].

In the HQM, one instead only describes those spherical fluctuations of the horizon (or, more, precisely, of the gravitational radius) which are determined by the quantum state of the source. These fluctuations therefore do not represent independent gravitational degrees of freedom, although one could suggest that they be viewed as collective perturbations in the zero point energy of the above-mentioned perturbative modes (see Fig. 2.1). In this respect, the HWF would be analogous to the quantum mechanical state of a hydrogen atom, whereas the perturbative degrees of freedom would be the quantum field corrections that lead to the Lamb shift.

Let us finally point out that the HQM also differs from other quantisations of the canonical degrees of freedom associated with the Schwarzschild BH metric [66, 67, 68, 69, 70, 71], in that the quantum state for the matter source plays a crucial role in defining the HWF. The HQM is therefore complementary to most of the approaches one usually encounters in the literature. In fact, it can be combined with perturbative approaches, like it was done in Ref. [37], to show that the poles in the dressed graviton propagator [36] can indeed be viewed as (unstable) quantum BHs.

2.3 Spherically symmetric Gaussian sources

We can make the previous formal construction more explicit by describing the massive particle at rest in the origin of the reference frame with the spherically symmetric Gaussian wave-function [10, 11, 13]

$$\psi_{\rm S}(r) = \frac{e^{-\frac{r^2}{2\,\ell^2}}}{(\ell\,\sqrt{\pi})^{3/2}} \ . \tag{2.15}$$

We shall often consider the particular case when the width ℓ (related to the uncertainty in the spatial size of the particle) is roughly given by the Compton length (2.3) of the particle,

$$\ell = \lambda_m \simeq \ell_{\rm p}\,\frac{m_{\rm p}}{m} \ . \tag{2.16}$$

Even though our analysis holds for independent values of ℓ and m, one expects that $\ell \geq \lambda_m$ and Eq. (2.16) is therefore a limiting case of maximum localisation for the source. It is also useful to recall that the corresponding wave-function in momentum space is given by

$$\tilde{\psi}_{\rm S}(p) = \frac{e^{-\frac{p^2}{2\,\Delta^2}}}{(\Delta\,\sqrt{\pi})^{3/2}} \ , \tag{2.17}$$

with $p^2 = \vec{p}\cdot\vec{p}$ being the square modulus of the spatial momentum, and the width

$$\Delta = m_{\rm p}\,\frac{\ell_{\rm p}}{\ell} \simeq m \ . \tag{2.18}$$

Note that the mass m is not the total energy of the particle, and $m < \langle\,\hat{H}\,\rangle$ if the spectrum of $\hat{H}$ is positive definite.

2.3.1 Neutral spherically symmetric BHs

In order to relate the momentum p to the total energy E, the latter being the analogue of the Misner-Sharp mass (1.4), we simply and consistently assume the relativistic mass-shell equation in flat space-time,

$$E^2 = p^2 + m^2 \ . \tag{2.19}$$

From Eq. (2.8), and fixing the normalisation in the inner product (2.10), we then obtain the HWF [10, 11, 13]

$$\psi_{\rm H}(r_{\rm H}) = \frac{1}{4\,\ell_{\rm p}^3}\sqrt{\frac{\ell^3}{\pi\,\Gamma\left(\frac{3}{2},1\right)}}\,\Theta(r_{\rm H}-R_{\rm H})\,e^{-\frac{\ell^2\,r_{\rm H}^2}{8\,\ell_{\rm p}^4}} \ , \tag{2.20}$$

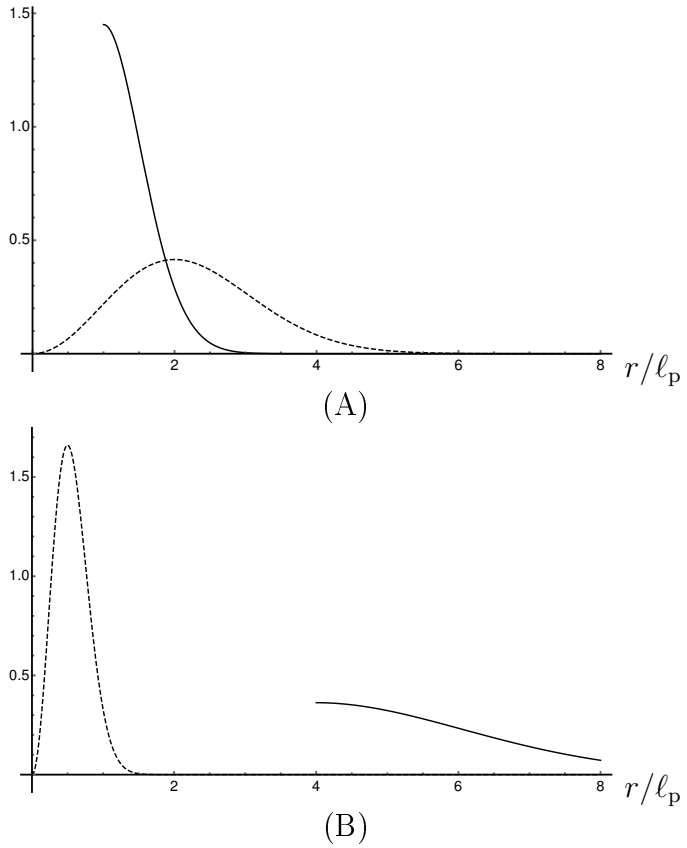

Figure 2.2: Probability densities $\mathcal{P}_{\rm H}$ in Eq. (2.13) (solid line) and $\mathcal{P}_{\rm S}$ (dashed line) for $m = m_{\rm p}/2$ (upper panel) and $m = 2\,m_{\rm p}$ (lower panel), assuming $m \sim \ell^{-1}$.

where we defined $R_{\rm H} = 2\,\ell_{\rm p}\,m/m_{\rm p}$ and the Heaviside step function appears in the above equation because $E \geq m$. Finally,

$$\Gamma(s,x) = \int_x^\infty t^{s-1}\,e^{-t}\,{\rm d}t\ , \tag{2.21}$$

is the upper incomplete Gamma function. In general, one has two parameters, the particle mass m and the Gaussian width ℓ. The HWF will therefore depend on both and so will the probability $P_{\rm BH} = P_{\rm BH}(\ell, m)$, which can be computed only numerically [13] (see also section 2.4).

As we mentioned previously, it seems sensible to assume $\ell \gtrsim \lambda_m$. In particular, the condition $\ell \sim m^{-1}$ in Eq. (2.16) precisely leads to a BH mass threshold of the form given in Eq. (2.5). We indeed expect that the particle will be inside its own horizon if $\langle\,\hat{r}^2\,\rangle \lesssim \langle\,\hat{r}^2_{\rm H}\,\rangle$, and Eq. (2.5) then follows straightforwardly from $\langle\,\hat{r}^2\,\rangle \simeq \ell^2$ and $\langle\,\hat{r}^2_{\rm H}\,\rangle \simeq \ell^4_{\rm p}/\ell^2$. For example, this

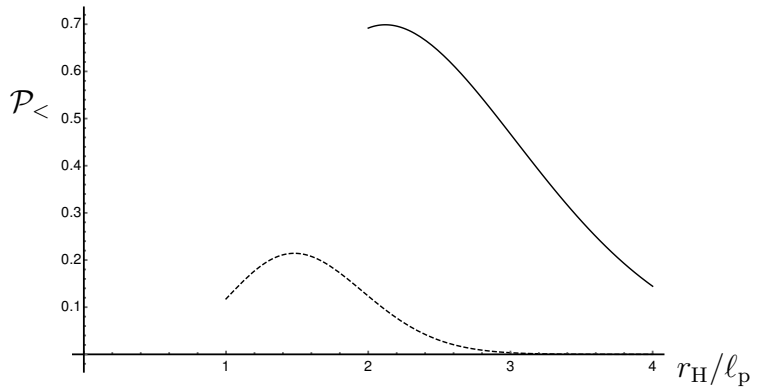

Figure 2.3: Probability density $\mathcal{P}_<$ in Eq. (2.22) that particle is inside its horizon of radius $r_{\rm H} \geq R_{\rm H} = 2\,\ell_{\rm p}\,m/m_{\rm p}$, for $\ell = \ell_{\rm p}$ (solid line) and for $\ell = 2\,\ell_{\rm p}$ (dashed line), assuming $m \sim \ell^{-1}$.

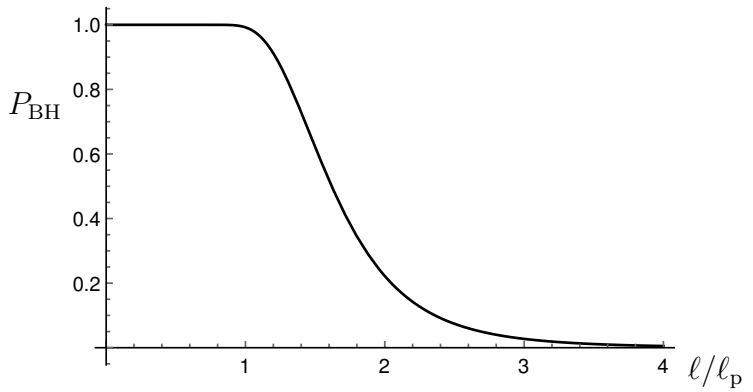

Figure 2.4: Probability $P_{\rm BH}$ in Eq. (2.23) that particle of width $\ell \sim m^{-1}$ is a BH.

conclusion is illustrated in Fig. 2.2, where the density $\mathcal{P}_{\rm H}$ is plotted along with the probability density $\mathcal{P}_{\rm S} = 4\,\pi\,r^2\,|\psi_{\rm S}(r)|^2$ for $m < m_{\rm p}$ and $m > m_{\rm p}$. In the former case, the horizon is more likely found within a smaller radius than the particle's, with the opposite situation occurring in the latter. As a matter of fact, the probability density (2.11) can be explicitly computed,

$$\mathcal{P}_< = \frac{\ell^3}{2\,\sqrt{\pi}\,\ell_{\rm p}^6}\,\frac{\gamma\left(\frac{3}{2},\frac{r_{\rm H}^2}{\ell^2}\right)}{\Gamma\left(\frac{3}{2},1\right)}\,\Theta(r_{\rm H}-R_{\rm H})\,e^{-\frac{\ell^2 r_{\rm H}^2}{4\,\ell_{\rm p}^4}}\,r_{\rm H}^2\ , \tag{2.22}$$

where $\gamma(s,x) = \Gamma(s) - \Gamma(s,x)$ is the lower incomplete Gamma function. One can integrate the density (2.22) for $r_{\rm H}$ from $R_{\rm H}$ to infinity and the

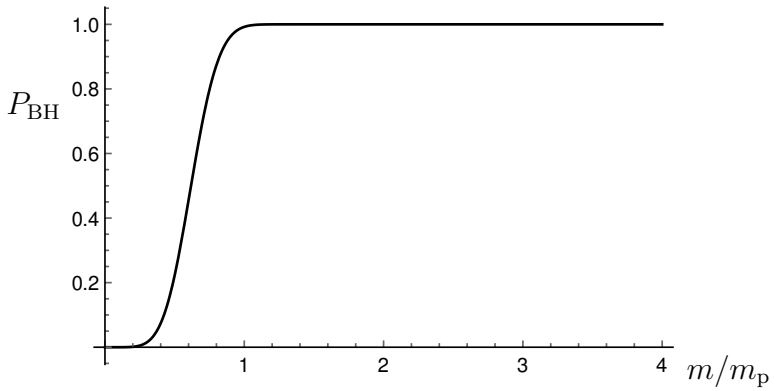

Figure 2.5: Probability $P_{\rm BH}$ in Eq. (2.23) that particle of mass $m \sim \ell^{-1}$ is a BH.

probability (2.14) for the particle to be a BH is finally given by

$$P_{\rm BH}(\ell) = \mathrm{erf}\left(\frac{2\ell_{\rm p}^2}{\ell^2}\right) + \frac{\sqrt{\pi}}{2}\,\frac{\mathrm{erfc}\left(\frac{2\ell_{\rm p}^2}{\ell^2}\right)}{\Gamma\left(\frac{3}{2},1\right)} - \frac{2\ell_{\rm p}^2/\ell^2}{\sqrt{\pi}\,\Gamma\left(\frac{3}{2},1\right)}\,\frac{\left(3+\frac{4\ell_{\rm p}^4}{\ell^4}\right)}{\left(1+\frac{4\ell_{\rm p}^4}{\ell^4}\right)^2}\,e^{-\left(1+\frac{4\ell_{\rm p}^4}{\ell^4}\right)} - \frac{2\sqrt{\pi}}{\Gamma\left(\frac{3}{2},1\right)}\,T\left(\frac{2\sqrt{2}\ell_{\rm p}^2}{\ell^2},\frac{\ell^2}{2\ell_{\rm p}^2}\right)\,, \tag{2.23}$$

where T is the Owen's function (A.7) [1]. Since we are assuming that $\ell/\ell_{\rm p} = m_{\rm p}/m$, this probability can also be written as a function of the mass m as

$$P_{\rm BH}(m) = \mathrm{erf}\left(\frac{2m^2}{m_{\rm p}^2}\right) + \frac{\sqrt{\pi}}{2}\,\frac{\mathrm{erfc}\left(\frac{2m^2}{m_{\rm p}^2}\right)}{\Gamma\left(\frac{3}{2},1\right)} - \frac{2m^2/m_{\rm p}^2}{\sqrt{\pi}\,\Gamma\left(\frac{3}{2},1\right)}\,\frac{\left(3+\frac{4m^4}{m_{\rm p}^4}\right)}{\left(1+\frac{4m^4}{m_{\rm p}^4}\right)^2}\,e^{-\left(1+\frac{4m^4}{m_{\rm p}^4}\right)} - \frac{2\sqrt{\pi}}{\Gamma\left(\frac{3}{2},1\right)}\,T\left(\frac{2\sqrt{2}m^2}{m_{\rm p}^2},\frac{m_{\rm p}^2}{2m^2}\right)\,. \tag{2.24}$$

In Fig. 2.3, we plot the probability density (2.22), for different values of the Gaussian width $\ell \sim m^{-1}$. It is already clear that such a probability decreases with m (eventually vanishing below the Planck mass). In fact, in Fig. 2.4, we show the probability (2.23) that the particle is a BH as a function of the width $\ell \sim m^{-1}$, and in Fig. 2.5 the same probability as a function of the particle mass $m \sim \ell^{-1}$. From these plots of $P_{\rm BH}$, we can immediately

[1] More detailed calculations of cumbersome integrals are given in A. In this particular case, the variable $x = \ell\, r_{\rm H}/2\,\ell_{\rm p}^2$, and we made use of Eq. (A.8) with $A = 2\,\ell_{\rm p}^2/\ell^2$.

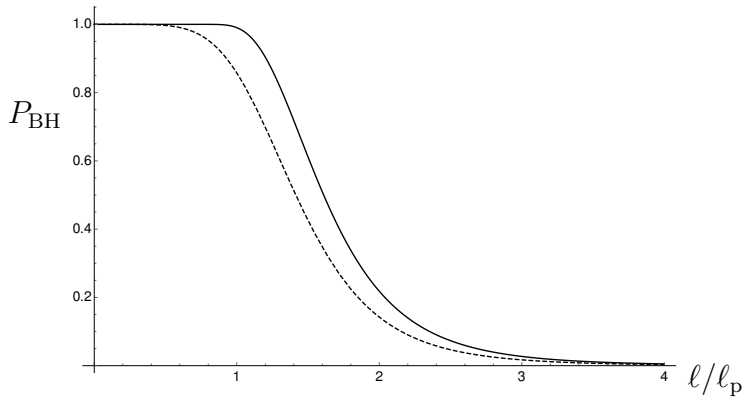

Figure 2.6: Plot of exact $P_{\rm BH}$ in Eq. (2.23) (straight line) and its approximation in Eq. (2.26) (dashed line).

infer that the particle is most likely a BH, namely $P_{\rm BH} \simeq 1$, for $\ell \lesssim \ell_{\rm p}$ or - equivalently - $m \gtrsim m_{\rm p}$. We have therefore derived the condition (2.5) from a totally Quantum Mechanical picture.

We conclude by recalling that a simple analytic approximation is obtained by taking the limit $R_{\rm H} \to 0$ in Eq. (2.20), namely [10, 11, 13]

$$\psi_{\rm H}(r_{\rm H}) = \left(\frac{\ell}{2\sqrt{\pi}\,\ell_{\rm p}^2}\right)^{3/2} e^{-\frac{\ell^2\, r_{\rm H}^2}{8\ell_{\rm p}^4}} \ , \tag{2.25}$$

from which follows the approximate probability

$$P_{\rm BH}(\ell) = \frac{2}{\pi}\left[\arctan\left(2\,\frac{\ell_{\rm p}^2}{\ell^2}\right) - \frac{2\,\ell^2\,(\ell^4/\ell_{\rm p}^4 - 4)}{\ell_{\rm p}^2\,(4+\ell^4/\ell_{\rm p}^4)^2}\right] \ . \tag{2.26}$$

Fig. 2.6 shows graphically that this approximation slightly underestimates the exact probability in Eq. (2.23).

Effective GUP and horizon fluctuations

From the Gaussian wave-function (2.15), we easily find that the uncertainty in the particle's size is given by

$$\begin{aligned} \Delta r^2 &\equiv 4\,\pi \int_0^\infty |\psi_{\rm S}(r)|^2\, r^4\, {\rm d}r - \left(4\,\pi \int_0^\infty |\psi_{\rm S}(r)|^2\, r^3\, {\rm d}r\right)^2 \\ &= \Delta_{\rm QM}\,\ell^2 \ , \end{aligned} \tag{2.27}$$

where

$$\Delta_{\rm QM} = \frac{3\,\pi - 8}{2\,\pi} \ . \tag{2.28}$$

Analogously, the uncertainty in the horizon radius results in

$$\begin{aligned}\Delta r_{\rm H}^2 &\equiv 4\,\pi\int_0^\infty |\psi_{\rm H}(r_{\rm H})|^2\, r_{\rm H}^4\,{\rm d}r_{\rm H} - \left(4\,\pi\int_0^\infty |\psi_{\rm H}(r_{\rm H})|^2\, r_{\rm H}^3\,{\rm d}r_{\rm H}\right)^2 \\ &= 4\,\ell_{\rm p}^4\left[\frac{E_{-\frac{3}{2}}(1)}{E_{-\frac{1}{2}}(1)} - \left(\frac{E_{-1}(1)}{E_{-\frac{1}{2}}(1)}\right)^2\right]\frac{1}{\ell^2}\ , \end{aligned} \tag{2.29}$$

where

$$E_n(x) = \int_1^\infty \frac{e^{-xt}}{t^n}\,{\rm d}t\ , \tag{2.30}$$

is the generalised exponential integral. Since

$$\begin{aligned}\Delta p^2 &\equiv 4\,\pi\int_0^\infty |\psi_{\rm S}(p)|^2\, p^4\,{\rm d}p - \left(4\,\pi\int_0^\infty |\psi_{\rm S}(p)|^2\, p^3\,{\rm d}p\right)^2 \\ &= \Delta_{\rm QM}\,\frac{\ell_{\rm p}^2}{\ell^2}\,m_{\rm p}^2\ , \end{aligned} \tag{2.31}$$

we can write the width of the Gaussian as $\ell^2 = \Delta_{\rm QM}\,\ell_{\rm p}^2\,m_{\rm p}^2/\Delta p^2$, and, finally, assume the total radial uncertainty is a linear combination of Eqs. (2.27) and (2.29), thus obtaining [11]

$$\begin{aligned}\frac{\Delta R}{\ell_{\rm p}} &\equiv \frac{\Delta r + \xi\,\Delta r_{\rm H}}{\ell_{\rm p}} \\ &= \Delta_{\rm QM}\,\frac{m_{\rm p}}{\Delta p} + \xi\,\Delta_{\rm H}\,\frac{\Delta p}{m_{\rm p}}\ , \end{aligned} \tag{2.32}$$

where ξ is an arbitrary coefficient (presumably of order one), and

$$\Delta_{\rm H}^2 = \frac{4}{\Delta_{\rm QM}}\left[\frac{E_{-\frac{3}{2}}(1)}{E_{-\frac{1}{2}}(1)} - \left(\frac{E_{-1}(1)}{E_{-\frac{1}{2}}(1)}\right)^2\right]\ . \tag{2.33}$$

This GUP is plotted in Fig. 2.7 (for $\xi = 1$), and is precisely of the kind considered in Ref. [16], leading to a minimum measurable length

$$\Delta R = 2\,\sqrt{\xi\,\Delta_{\rm H}\,\Delta_{\rm QM}}\,\ell_{\rm p} \simeq 1.15\,\sqrt{\xi}\,\ell_{\rm p}\ , \tag{2.34}$$

obtained for

$$\Delta p = \sqrt{\frac{\Delta_{\rm QM}}{\xi\,\Delta_{\rm H}}}\,m_{\rm p} \simeq 0.39\,\frac{m_{\rm p}}{\sqrt{\xi}}\ . \tag{2.35}$$

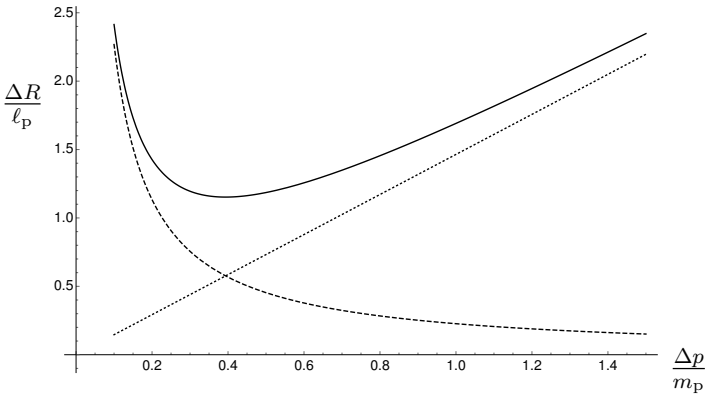

Figure 2.7: Uncertainty relation (2.32) (solid line) as a combination of the Quantum Mechanical uncertainty (dashed line) and the uncertainty in horizon radius (dotted line).

Of course, this is not the only possible way to define a combined uncertainty, but nothing forces us to consider a GUP instead of making direct use of the HWF.

One of the main conclusions for the HQM of Gaussian states can now be drawn from Eq. (2.29), that is

$$\Delta r_{\rm H} \sim \ell^{-1} \sim m \ , \tag{2.36}$$

which means the size of the corresponding horizon shows fluctuations of magnitude $\Delta r_{\rm H} \sim r_{\rm H} \sim R_{\rm H}$. This is clearly not acceptable for BHs with mass $m \gg m_{\rm p}$, which we expect to behave (semi)classically. In other words, the classical picture of a BH as the vacuum geometry generated by a (infinitely) thin matter source does not seem to survive in the quantum description, and one is led to consider alternative models for astrophysical size BHs [9, 18, 19, 72, 73, 74, 75, 76, 77, 78].

Quantum BH evaporation

One of the milestones of contemporary theoretical physics is the discovery that BHs radiate thermally at a characteristic temperature [6, 7]

$$T_{\rm H} = \frac{m_{\rm p}^2}{8\,\pi\,m} \ . \tag{2.37}$$

However, if we try to extrapolate this temperature to vanishingly small mass M, we see that $T_{\rm H}$ diverges.

One can derive improved BH temperatures for $m \simeq m_{\rm p}$ from the GUP (see Refs. [11, 79, 80, 81, 82, 83, 84, 85, 86] for detailed computations). Here, we just recall that one obtains [2]

$$m = \frac{m_{\rm p}^2}{8\,\pi\,T} + 2\,\pi\,\xi\,T \ , \tag{2.38}$$

with the condition $\xi > 0$, which is necessary for the existence of a minimum BH mass (see Fig. 2.8). We remark that this is consistent with our previous analysis, since we stated repeatedly that a particle with a mass significantly smaller than $m_{\rm p}$ should not be a BH, i.e. $P_{\rm BH} \ll 1$ whenever $m \ll m_{\rm p}$. It is straightforward to extremise (2.38) and get

$$m_{\rm min} = \sqrt{\xi}\,m_{\rm p} \ , \qquad T_{\rm max} = \frac{m_{\rm p}}{4\,\pi\,\sqrt{\xi}} \ . \tag{2.39}$$

Moreover, we can invert (2.38) in order to obtain $T = T(m)$ and consider the "physical" branch, which reproduces the Hawking behaviour $T = 0$ for $m \gg m_{\rm p}$. When $0 < \xi < 1$ we can expand the result for m around $m_{\rm p}$, hence

$$\begin{aligned} \frac{T}{m_{\rm p}} &= \frac{1}{4\,\pi\,\xi\,m_{\rm p}}\left(m - \sqrt{m^2 - \xi\,m_{\rm p}^2}\right) \\ &= \frac{1-\sqrt{1-\xi}}{4\,\pi\,\xi}\left(1 - \frac{m - m_{\rm p}}{\sqrt{1-\xi}\,m_{\rm p}}\right) + \mathcal{O}\left[(1 - m/m_{\rm p})^2\right] \ . \end{aligned} \tag{2.40}$$

We note that such an expansion for T is well-defined even for $\xi < 0$, suggesting that the microscopic structure of the space-time may be arranged as a lattice [87]. In the same approximation, we can also expand the canonical decay rate

$$-\frac{{\rm d}m}{{\rm d}t} = \frac{8\,\pi^3\,m^2\,T^4}{15\,m_{\rm p}^5\,\ell_{\rm p}} \tag{2.41}$$

$$\simeq \beta\,\frac{m^2}{m_{\rm p}\,\ell_{\rm p}} + \mathcal{O}(m - m_{\rm p}) \ , \tag{2.42}$$

where $4 \cdot 10^{-5} < \beta < 7 \cdot 10^{-4}$ when $0 < \xi < 1$ [11].

The reader may deem unlikely that an object with a mass of the order of $m_{\rm p}$ can be faithfully described by the same standard thermodynamics which arises from a (semi-)classical description of BHs. On the other hand, the HQM is specifically designed to hold in a quantum regime. We can therefore

[2] The parameter ξ here is analogue, but not necessarily equal, to the parameter ξ in Eq. (2.32).

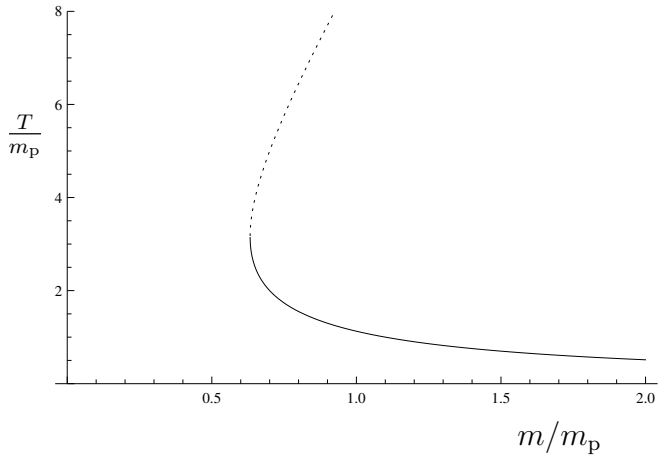

Figure 2.8: Temperature vs. mass according to Eq. (2.38) with $\beta = 1/10$: solid line reproduces the Hawking behaviour for large $m \gg m_{\rm p}$; dotted line is the unphysical branch, and their meeting point represents the BH with minimum mass.

guess that the decay of a Planck size BH will be related to the probability $P_{\rm T}$ that the particle is found outside its own horizon [3] [11]. Of course, if the mass $m \ll m_{\rm p}$, the HWF tells us the particle is most likely not a BH to begin with, so the above interpretation must be restricted to $m \simeq m_{\rm p}$ (see again Fig. 2.5). We first define the complementary probability density

$$\mathcal{P}_{>}(r > r_{\rm H}) = P_{\rm S}(r > r_{\rm H})\, \mathcal{P}_{\rm H}(r_{\rm H}) \ , \tag{2.43}$$

where now

$$P_{\rm S}(r > r_{\rm H}) = 4\,\pi \int_{r_{\rm H}}^{\infty} |\psi_{\rm S}(r)|^2\, r^2\, {\rm d}r = \frac{2}{\sqrt{\pi}}\, \Gamma\left(\frac{3}{2}, \frac{r_{\rm H}^2}{\ell^2}\right) \ . \tag{2.44}$$

Upon integrating the above probability density over all values of $r_{\rm H}$, we then obtain

$$P_{\rm T}(m) \simeq a - b\, \frac{m - m_{\rm p}}{m_{\rm p}} \ , \tag{2.45}$$

where $a \simeq 0.008$ and $b \simeq 0.14$ are positive constants. We can accordingly estimate the amount of particle's energy outside the horizon as

$$\Delta m \simeq m\, P_{\rm T} \simeq a\, m + \mathcal{O}(m - m_{\rm p}) \ . \tag{2.46}$$

[3] The subscript T stands for tunnelling, which alludes to the understanding of the Hawking emission as a tunnelling process through the horizon [88].

On the other hand, from the time-energy uncertainty relation, $\Delta E\,\Delta t \simeq m_{\rm p}\,\ell_{\rm p}$, one gets the typical emission time

$$\Delta t \simeq \frac{\ell_{\rm p}^2}{\Delta r_{\rm H}} \simeq \ell \ , \tag{2.47}$$

employing (1.1) and (2.29). Putting the two pieces together, we find that the flux emitted by a Planck size black hole would satisfy [11]

$$-\frac{\Delta m}{\Delta t} \simeq a\,\frac{m}{\ell} \simeq a\,\frac{m^2}{m_{\rm p}\,\ell_{\rm p}} \ , \tag{2.48}$$

whose functional behaviour agrees with the result (2.42) obtained from a GUP.

There is a large discrepancy between the numerical coefficients in Eq. (2.42) and those in Eq. (2.48). First, we note that Eq. (2.41) holds in the canonical ensemble of statistical mechanics, and the disparity may therefore arise because a Planck mass particle cannot be consistently described by standard thermodynamics, which in turn requires the BH is in quasi-equilibrium with its own radiation [88, 89]. In fact, the canonical picture does not even enforce energy conservation, which is instead granted in the microcanonical formalism [90, 91]. However, the HQM is insensitive to thermodynamics and it is therefore remarkable that the HQM and the GUP yield qualitatively similar results. In any case, the above analysis of BH evaporation is very preliminary and significant changes are to be expected when considering a better description of the microscopic structure of quantum BHs [18, 37, 74, 77, 78].

2.3.2 Electrically charged sources

An extension of the original HQM regards the case of electrically charged massive sources [92, 93, 94, 95, 96], and was obtained in Refs. [14, 15] from the Reissner-Nordström (RN) metric [97, 98]. The latter is of the form (2.1) with

$$f = 1 - \frac{2\,\ell_{\rm p}\,m}{m_{\rm p}\,r} + \frac{Q^2}{r^2} \ , \tag{2.49}$$

where m is again the ADM mass and Q is the charge of the source. In the following, it will be convenient to employ the specific charge

$$\epsilon = \frac{|Q|\,m_{\rm p}}{\ell_{\rm p}\,m} \ . \tag{2.50}$$

The case $\epsilon = 0$ reduces to the neutral Schwarzschild metric. For $0 < \epsilon < 1$, the above function f has two zeroes, namely

$$\begin{aligned} R_\pm &= \ell_{\rm p} \frac{m}{m_{\rm p}} \pm \sqrt{\left(\ell_{\rm p} \frac{m}{m_{\rm p}}\right)^2 - Q^2} \\ &= \ell_{\rm p} \frac{m}{m_{\rm p}} \left(1 \pm \sqrt{1-\epsilon^2}\right) \ , \end{aligned} \tag{2.51}$$

and the RN metric therefore describes a BH. Moreover, the two horizons coincide for $\epsilon = 1$ and the BH is said to be *extremal*, while the singularity is naked, i.e. accessible to an external observer, for $\epsilon > 1$.

Inner Horizon

The case $0 < \epsilon \leq 1$ was considered in Ref. [14], where the HQM was extended for the presence of more than one trapping surface. A procedure similar to the neutral case was followed for each of the two horizon radii (2.51): one initially determines the HWFs and then uses them to compute the probability for each horizon to exist. Eqs. (2.51) is lifted to the quantum level by introducing the operators $\hat{r}_\pm$ and $\hat{H}$, which replace their classical counterparts $R_\pm$ and m. Moreover, these operators are chosen to act multiplicatively on the respective wave-functions, whereas the specific charge ϵ remains a simple parameter (c-number) [4].

First we note the total energy $\hat{H}$ can be expressed in terms of the horizon radii as

$$\ell_{\rm p} \frac{\hat{H}}{m_{\rm p}} = \frac{\hat{r}_+ + \hat{r}_-}{2} \ , \tag{2.52}$$

and one also has

$$\hat{r}_\pm = \hat{r}_\mp \frac{1 \pm \sqrt{1-\epsilon^2}}{1 \mp \sqrt{1-\epsilon^2}} \ . \tag{2.53}$$

We then obtain the HWFs for r_+ and r_- by expressing p from the mass-shell relation (2.19) in terms of the eigenvalue E of $\hat{H}$ in Eq. (2.52), and then replacing one of the relations (2.53) into the wave-function representing the source in momentum space, as in Eq. (2.17). For the usual limiting

[4] As usual, going from the classical to the quantum realm is affected by ambiguities, and this choice is not unique.

case (2.16), $\ell \sim m^{-1}$, it is straightforward to obtain

$$\psi_{\rm H}(r_\pm) = \sqrt{\frac{1}{2\pi\,\Gamma\left(\frac{3}{2},1\right)}\left[\frac{\ell}{\ell_{\rm p}^2(1\pm\sqrt{1-\epsilon^2})}\right]^3}\,\Theta\left(r_\pm - R_\pm\right) \times \exp\left\{-\frac{\ell^2\,r_\pm^2}{2\ell_{\rm p}^4\,(1\pm\sqrt{1-\epsilon^2})^2}\right\}\,, \tag{2.54}$$

where the minimum radii are given by

$$R_\pm = \ell_{\rm p}\,\frac{m}{m_{\rm p}}\left(1\pm\sqrt{1-\epsilon^2}\right) = \frac{\ell_{\rm p}^2}{\ell}\left(1\pm\sqrt{1-\epsilon^2}\right)\,. \tag{2.55}$$

The probability densities for the source to be found inside each of the two horizons turn out to be

$$\mathcal{P}_{<\pm} = \frac{4}{\sqrt{\pi}\,\Gamma\left(\frac{3}{2},1\right)}\left[\frac{\ell}{\ell_{\rm p}^2(1\pm\sqrt{1-\epsilon^2})}\right]^3\,\Theta(r_\pm - R_\pm) \times\gamma\left(\frac{3}{2},\frac{r_\pm^2}{\ell^2}\right)\,\exp\left\{-\frac{\ell^2\,r_\pm^2}{\ell_{\rm p}^4\,(1\pm\sqrt{1-\epsilon^2})^2}\right\}\,r_\pm^2\,. \tag{2.56}$$

In the neutral case $\epsilon = 0$, $\mathcal{P}_{<-}$ is of course ill-defined, while $\mathcal{P}_{<+}$ equals the probability density (2.22), which means that r_+ becomes the Schwarzschild radius $r_{\rm H}$.

Fig. 2.9 shows the probability density $\mathcal{P}_{<+}$ for the massive source to reside inside the external horizon $r = r_+$ for two values of the width ℓ (above and below the Planck scale) and three values of the specific charge ϵ. The maximum of this function clearly decreases when ℓ increases above $\ell_{\rm p}$ or, equivalently, when m gets smaller than the Planck mass. Fig. 2.10 shows the analogous probability densities $\mathcal{P}_{<-}$ for the inner horizon $r = r_-$. Obviously, the smaller ϵ the smaller is the probability that a trapping surface occurs. Moreover, as we expected from the start, the density profiles coincide in the extremal case $\epsilon = 1$ (thick and thin dashed lines), because the two horizons merge.

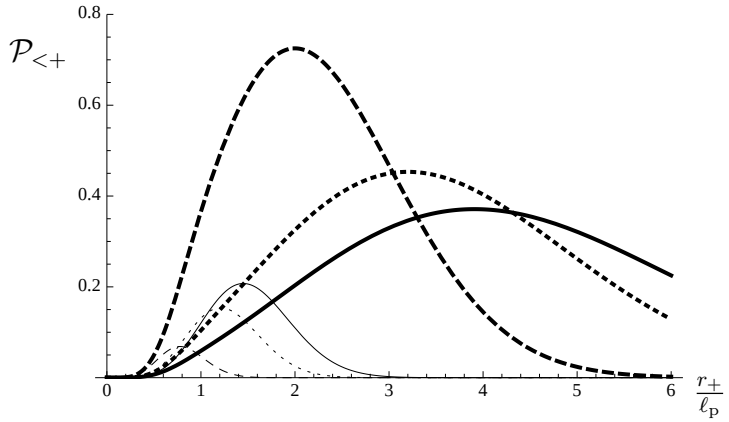

Figure 2.9: Probability density $\mathcal{P}_{<+}$ in Eq. (2.56) that the particle is inside its outer horizon $r = r_+$, for $\ell = \ell_{\rm p}/2$ (thick lines) and $\ell = 2\,\ell_{\rm p}$ (thin lines) with $\epsilon = 0.3$ (continuous lines), $\epsilon = 0.8$ (dotted lines) and $\epsilon = 1$ (dashed lines). For $\epsilon = 1$, the two horizons coincide and $\mathcal{P}_{<-} = \mathcal{P}_{<+}$.

Integrating over $r_\pm$, we obtain the probabilities [5]

$$\begin{aligned} P_{\rm BH\pm}(\ell,\epsilon) \;=\; & \mathrm{erf}\left[\frac{\ell_{\rm p}^2}{\ell^2}\left(1\pm\sqrt{1-\epsilon^2}\right)\right] + \frac{\sqrt{\pi}}{2}\,\frac{\mathrm{erfc}\left[\frac{\ell_{\rm p}^2}{\ell^2}\left(1\pm\sqrt{1-\epsilon^2}\right)\right]}{\Gamma\left(\frac{3}{2},1\right)} \\ & -\frac{\left(1\pm\sqrt{1-\epsilon^2}\right)\ell_{\rm p}^2/\ell^2}{\sqrt{\pi}\,\Gamma\left(\frac{3}{2},1\right)}\,\frac{3+\frac{\ell_{\rm p}^4}{\ell^4}\left(1\pm\sqrt{1-\epsilon^2}\right)^2}{\left[1+\frac{\ell_{\rm p}^4}{\ell^4}(1\pm\sqrt{1-\epsilon^2})^2\right]^2}\,e^{-\left[1+\left(1\pm\sqrt{1-\epsilon^2}\right)^2\frac{\ell_{\rm p}^4}{\ell^4}\right]} \\ & -\frac{2\sqrt{\pi}}{\Gamma\left(\frac{3}{2},1\right)}\,T\left[\sqrt{2}\frac{\ell_{\rm p}^2}{\ell^2}\left(1\pm\sqrt{1-\epsilon^2}\right),\frac{\ell^2}{\ell_{\rm p}^2\left(1\pm\sqrt{1-\epsilon^2}\right)}\right]\,. \end{aligned} \tag{2.57}$$

where T is again the Owen's function (A.7).

Fig. 2.11 shows how these probabilities vary with the parameter ϵ for values of ℓ above or below the Planck scale. For the outer horizon, it is clear that $P_{\rm BH+} \simeq 1$ for widths $\ell \lesssim \ell_{\rm p}$ (mass larger than $m_{\rm p}$). On the contrary, when $\ell \gtrsim \ell_{\rm p}$ (or $m \lesssim m_{\rm p}$), the probability sensibly decreases as the specific charge ϵ approaches 1 from below. We see that this probability is does not exactly vanish even when ℓ exceeds the Planck length $\ell_{\rm p}$. As an example, for $\ell = 2\,\ell_{\rm p}$, corresponding to $m = m_{\rm p}/2$, we find $0.15 \lesssim P_{\rm BH+}(\epsilon) \lesssim 0.2$ for a large interval of values of the specific charge. $P_{\rm BH+}$ only falls below 0.1 right before the BH becomes maximally charged ($\epsilon \simeq 1$). As far as the inner

[5] It is convenient to define $x_\pm = \ell\, r_\pm/\ell_{\rm p}^2(1\pm\sqrt{1-\epsilon^2})$, and use again Eq. (A.8), with $A = (1\pm\sqrt{1-\epsilon^2})\,\ell_{\rm p}^2/\ell^2$.

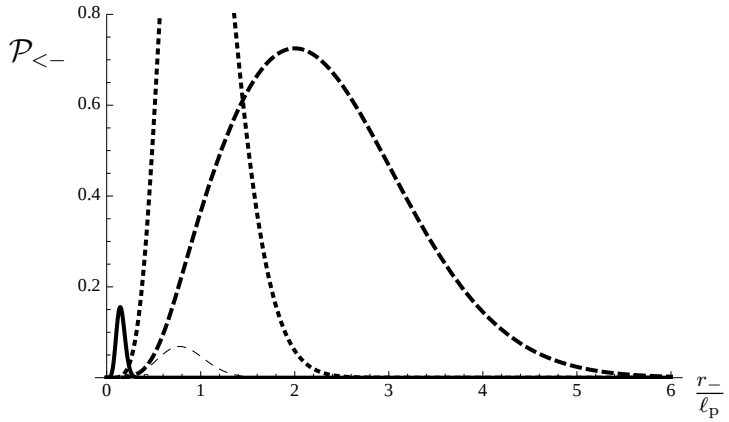

Figure 2.10: Probability density $\mathcal{P}_{<-}$ in Eq. (2.56) that particle is inside its inner horizon $r = r_-$, for $\ell = \ell_p/2$ (thick lines) and $\ell = 2\,\ell_p$ (thin lines) with $\epsilon = 0.3$ (continuous lines), $\epsilon = 0.8$ (dotted lines) and $\epsilon = 1$ (dashed lines). For $\epsilon = 1$, the two horizons coincide and $\mathcal{P}_{<-} = \mathcal{P}_{<+}$.

horizon is concerned, the scenario is profoundly different. The same plot shows that the probability $P_{\rm BH-} \ll 1$ for small values of ϵ and increases with this parameter. However, the role of ℓ is prominent because the sharper the Gaussian packet is localised in space (or the more massive it is), the smaller the value of ϵ for which this probability becomes significant. To summarise, there is an appreciable range of values of the specific charge ϵ for which the inner horizon is not likely to exist ($P_{\rm BH-} \ll 1$), while the system is a BH ($P_{\rm BH+} \simeq 1$).

The probabilities $P_{\rm BH\pm}$ as functions of the width ℓ are shown in Fig. 2.12 and as functions of the mass m in Fig. 2.13, for $\epsilon = 0.3$, 0.8 and 1. It is evident that smaller values of ϵ allow for $P_{\rm BH+}$ to approach 1 for smaller masses m. The specular situation happens when studying the inner probability $P_{\rm BH-}$. If we focus on the smallest specific charge considered here, $\epsilon = 0.3$, we notice that both probabilities are close to 1 only around $m \simeq 6\,m_p$, and not at the naively expected scale $m \simeq m_p$. Hence, there exists a non-negligible interval in the possible values of m (around the Planck scale) for $\epsilon < 1$ in which

$$P_{\rm BH+} \simeq 1 \quad \text{and} \quad P_{\rm BH-} \ll 1 \ . \tag{2.58}$$

In this interval, the system is most likely a BH, because it is the outer horizon which dictates this property, while the inner horizon is still not very likely to exist. Lowering the value of ϵ this range grows larger, while it narrows and eventually vanishes when approaching the maximally charged limit $\epsilon = 1$.

We conclude by remarking that we could have guessed this result. In fact, the smaller ϵ, the more the system looks like a neutral (Schwarzschild)

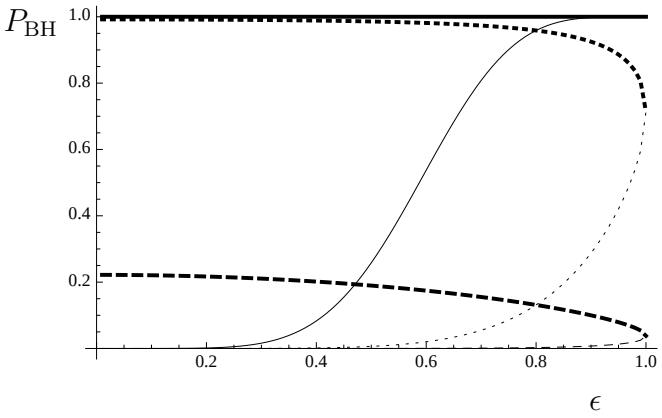

Figure 2.11: Probability $P_{\rm BH+}$ in Eq. (2.57) for the particle to be a BH (thick lines) and $P_{\rm BH-}$ in Eq. (2.57) for the particle to be inside its inner horizon (thin lines) as functions of ϵ for $\ell = \ell_{\rm p}/2$ (continuous line), $\ell = \ell_{\rm p}$ (dotted line) and $\ell = 2\,\ell_{\rm p}$ (dashed line). For $\epsilon = 1$ the two probabilities merge.

BH, since the mass becomes the dominant parameter and the presence of charge is (at most) a small perturbation. However, the existence of an inner horizon at $r = R_-$ is phenomenologically very important, because of the possible instability known as *mass inflation* [99, 100, 101] related to the specific features of such a Cauchy horizon. Eq. (2.58) suggests that this instability should not always occur for $0 < \epsilon \leq 1$, even when the particle is (most likely) a BH.

Quantum Cosmic Censorship

Overcharged sources with $\epsilon > 1$ were analysed in Ref. [15]. We recall that the cosmic censorship [49] was conjectured in order to exclude such naked singularities from General Relativity. It is therefore interesting to investigate whether quantum physics supports this view or can introduce modifications of any kind. The analysis is developed by assuming that the overcharged regime $\epsilon > 1$ is reached by continuing analytically the HWF from the case $0 < \epsilon \leq 1$. It is clear that this choice is again not unique, but it should be consistent at least when the specific charge is not much greater than the classical limiting threshold $\epsilon = 1$.

The first issue that needs to be taken into consideration for $\epsilon > 1$ is that the operators $\hat{r}_\pm$ directly obtained from Eq. (2.53) are not Hermitian. This could in principle be a reason to give up any observables corresponding to $\hat{r}_\pm$ in this classically forbidden region. Nonetheless, one can follow through and construct a Hermitian radial operator using only the real parts of the

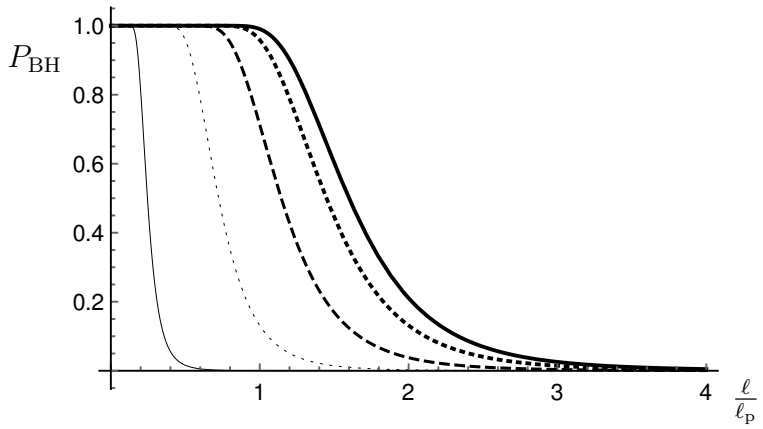

Figure 2.12: Probability $P_{\rm BH+}$ for the particle to be a BH (thick lines) and $P_{\rm BH-}$ for the particle to be inside its inner horizon (thin lines), in Eq. (2.57), as functions of ℓ, for $\epsilon = 0.3$ (continuous line), $\epsilon = 0.8$ (dotted line) and $\epsilon = 1$ (dashed line). For $\epsilon = 1$ thick and thin dashed lines overlap.

multiplicative operators $\hat{r}_\pm$. By continuing analytically Eq. (2.54) for $\epsilon > 1$, the square modulus of the HWF becomes [15]

$$|\psi_{\rm H}(r_{\rm H})|^2 = \mathcal{N}^2 \, \exp\left\{-\frac{2-\epsilon^2}{\epsilon^4}\,\frac{\ell^2\, r_{\rm H}^2}{\ell_{\rm p}^4}\right\} \ , \tag{2.59}$$

where $r_{\rm H}$ now replaces both r_+ and r_- (which in fact merge at $\epsilon = 1$) and $\mathcal{N}$ is a normalisation factor. It so happens that this HWF is still normalisable in the Schrödinger scalar product (2.10) if $r_{\rm H}$ is a real variable and for specific charge values in the range

$$1 < \epsilon^2 < 2 \ . \tag{2.60}$$

This suggests that there must be a quantum obstruction forbidding the system from crossing $\epsilon^2 = 2$. We will discuss this issue more completely after determining the full HWF.

One also needs to modify the step function in Eq. (2.54) when the system enters the overcharged regime. First, we note that the real part of the complex Eq. (2.55) is the same for r_+ and r_-, and set

$$R_{\rm H} = {\rm Re}\left[\frac{\ell_{\rm p}^2}{\ell}\left(1 \pm \sqrt{1-\epsilon^2}\right)\right] = \frac{\ell_{\rm p}^2}{\ell} \ . \tag{2.61}$$

We can then show that the continuity property which leads to Eq. (2.59) extends to $\hat{r}_{\rm H}$ when $r_{\rm H}$ is bounded from below by $R_{\rm H}$. In fact, we can compute

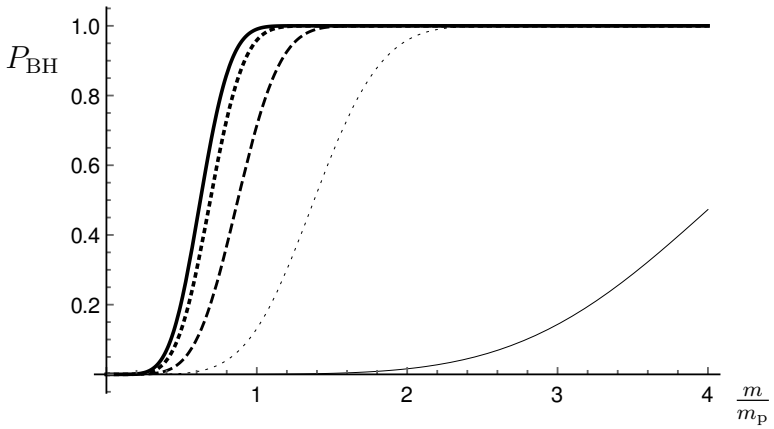

Figure 2.13: Probability $P_{\rm BH+}$ for the particle to be a BH (thick lines) and $P_{\rm BH-}$ for the particle to be inside its inner horizon (thin lines), in Eq. (2.57), as functions of m, for $\epsilon = 0.3$ (continuous line), $\epsilon = 0.8$ (dotted line) and $\epsilon = 1$ (dashed line). For $\epsilon = 1$ thick and thin dashed lines overlap.

the expectation value

$$\langle\, \hat{r}_{\rm H}\, \rangle = 4\,\pi \int_{R_{\rm H}}^{\infty} |\psi_{\rm H}(r_{\rm H})|^2\, r_{\rm H}^3\, {\rm d}r_{\rm H} \;= \frac{\epsilon^2}{\sqrt{2-\epsilon^2}}\, \frac{\Gamma\left(2, \frac{2-\epsilon^2}{\epsilon^4}\right)}{\Gamma\left(\frac{3}{2}, \frac{2-\epsilon^2}{\epsilon^4}\right)}\, R_{\rm H}\ , \qquad (2.62)$$

and observe that this expression matches the analogous expressions from the regime $0 < \epsilon \leq 1$,

$$\langle\, \hat{r}_{\pm}\, \rangle = 4\,\pi \int_{R_{\pm}}^{\infty} |\psi_{\pm}(r_{\pm})|^2\, r_{\pm}^3\, {\rm d}r_{\pm} = \frac{\Gamma\,(2,1)}{\Gamma\left(\frac{3}{2},1\right)}\, R_{\pm}\ , \qquad (2.63)$$

in the limit $\epsilon = 1$, namely

$$\lim_{\epsilon \searrow 1} \langle\, \hat{r}_{\rm H}\, \rangle = \frac{\Gamma\,(2,1)}{\Gamma\left(\frac{3}{2},1\right)}\, \frac{\ell_{\rm p}^2}{\ell} = \lim_{\epsilon \nearrow 1} \langle\, \hat{r}_{\pm}\, \rangle\ . \qquad (2.64)$$

Moreover, the same holds for the corresponding uncertainties, that is

$$\Delta r_{\rm H}^2(\ell, \epsilon \to 1^+) = \Delta r_{\pm}^2(\ell, \epsilon \to 1^-)\ . \qquad (2.65)$$

We omit the details here [15], and just remark that, for $\epsilon = 1$, the width of the Gaussian $\ell > \langle\, \hat{r}_{\rm H}\, \rangle$ for $m < \sqrt{\Gamma\left(\frac{3}{2},1\right)/\Gamma(2,1)}\, m_{\rm p} \simeq 0.8\, m_{\rm p}$. The gravitational fluctuations in the size of the source will thus be subdominant when its mass is sensibly smaller than the Planck mass $m_{\rm p}$, like in the neutral case.

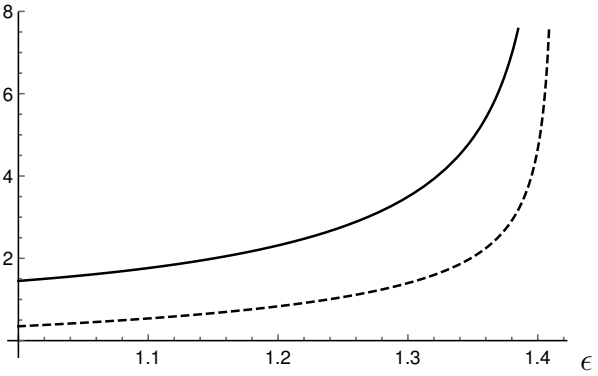

Figure 2.14: Expectation value $\langle\, \hat{r}_{\rm H} \,\rangle$ (solid line) and its uncertainty $\Delta r_{\rm H}$ (dashed line), in units of $\ell_{\rm p}$, as functions of the specific charge $1 < \epsilon^2 < 2$ and $\ell = \ell_{\rm p}$ ($m = m_{\rm p}$).

Let us now consider what happens when approaching the critical specific charge $\epsilon^2 = 2$. One may have already noticed that

$$\langle\, \hat{r}_{\rm H} \,\rangle \simeq \frac{8}{\sqrt{\pi\ (2-\epsilon^2)}}\,\frac{\ell_{\rm p}^2}{\ell}\ , \tag{2.66}$$

so that the ratio $\langle\, \hat{r}_{\rm H} \,\rangle/\ell$ diverges in the limit $\epsilon^2 \to 2$, regardless of the mass $m = m_{\rm p}\,\ell_{\rm p}/\ell$. Moreover, since

$$\Delta r_{\rm H} \simeq \sqrt{3\,\pi/8 - 1}\,\langle\, \hat{r}_{\rm H} \,\rangle \simeq 0.4\,\langle\, \hat{r}_{\rm H} \,\rangle\ , \tag{2.67}$$

the uncertainty $\Delta r_{\rm H}$ shows the same behaviour for $\epsilon^2 \to 2$ (see also Fig. 2.14).

In the same way that led to Eq. (2.57), we can obtain the probability $P_{\rm BH}$ that the particle is a BH for ϵ in the allowed range (2.60),

$$P_{\rm BH} = \frac{4}{\sqrt{\pi}\,\Gamma\left(\frac{3}{2},\,\frac{2-\epsilon^2}{\epsilon^4}\right)}\int_{\frac{\sqrt{2-\epsilon^2}}{\epsilon^2}}^{\infty}\gamma\left(\frac{3}{2},\,\frac{\epsilon^4}{2-\epsilon^2}\,\frac{\ell_{\rm p}^4}{\ell^4}\,x^2\right)e^{-x^2}\,x^2\,{\rm d}x\ , \tag{2.68}$$

where $x \equiv \sqrt{2-\epsilon^2}\,\ell\,r_{\rm H}/\epsilon^2\,\ell_{\rm p}^2$.

This probability is computed numerically and plotted in Fig. 2.15 as a function of ϵ. One notes that, for a Gaussian width much smaller than $\ell_{\rm p}$, $P_{\rm BH} \simeq 1$ throughout the whole range of the specific charge, which extends a similar result for $0 < \epsilon \leq 1$. Nevertheless, even when ℓ significantly exceeds the Planck length, we see that the same result is obtained in the limit $\epsilon^2 \to 2$. It is important to recall that, when the system is far from the Planck scale, $\ell \gg \langle\, \hat{r}_{\rm H} \,\rangle$, quantum fluctuations in the particle's position dominate and

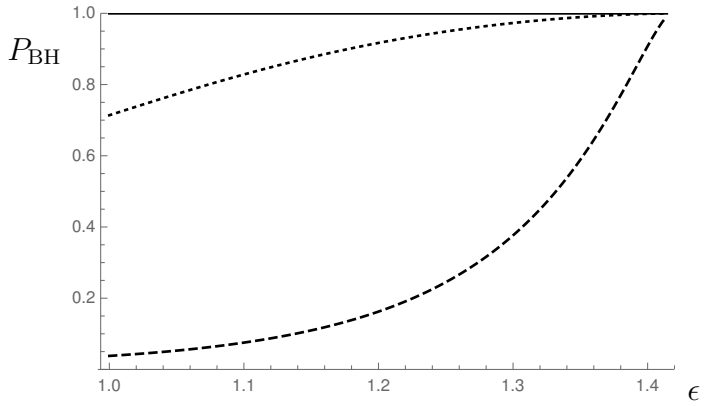

Figure 2.15: $P_{\rm BH}$ as a function of ϵ for $\ell = \ell_{\rm p}/2$ (solid line), $\ell = \ell_{\rm p}$ (dotted line) and $\ell = 2\,\ell_{\rm p}$ (dashed line). Cases with $\ell \ll \ell_{\rm p}$ are not plotted since they behave the same as $\ell = \ell_{\rm p}/2$, i.e. an object with $1 < \epsilon^2 < 2$ must be a BH.

$P_{\rm BH} \ll 1$ accordingly. However, strong quantum fluctuations in the size of the horizon appear in the overcharged regime where the probability $P_{\rm BH}$ is large, since $\langle\, \hat{r}_{\rm H} \,\rangle$ and $\Delta r_{\rm H}$ blow up for $\epsilon^2 \to 2$.

Bearing all the limitations and ambiguities in the above analysis, the picture that emerges is that of a *quantum* version of the cosmic censorship: first of all it appears that (slightly) overcharged configurations may exist, but have a large probability of being BHs, rather than naked singularities; secondly, when the specific charge is larger than a critical value (here found to be $\epsilon \simeq 1.4$), there exist no well-behaved HWF and the gravitational radius of the system cannot be defined. Of course, one should not forget that assuming a Gaussian wave-function for the source already restricts these conclusions to masses of the order of the Planck scale, and not too much larger, as we recalled in section 2.3.1.

2.3.3 Particle collisions in $(1+1)$ dimensions

A straightforward extension of the HQM to a state containing two free particles colliding head-on in one-dimensional flat space was presented in Ref. [12], where both constituents are represented by Gaussian wave-functions centred around the positions X_i and having linear momentum P_i ($i = 1$ or 2),

$$\langle\, x_i; 0 \mid \psi_{\rm S}^{(i)} \,\rangle \equiv \psi_{\rm S}(x_i) = e^{-i\,\frac{P_i\,x_i}{m_{\rm p}\,\ell_{\rm p}}}\,\frac{e^{-\frac{(x_i - X_i)^2}{2\,\ell_i}}}{\sqrt{\pi^{1/2}\,\ell_i}}\ , \tag{2.69}$$

where dynamical phases are neglected since we will only consider "snapshots" of the collision. Like in the one-particle case, one switches to momentum

space in order to compute the spectral decomposition of the system,

$$\langle\, p_i; 0 \mid \psi_{\rm S}^{(i)} \,\rangle \equiv \psi_{\rm S}(p_i) = e^{-i\,\frac{p_i\,X_i}{m_{\rm p}\ell_{\rm p}}}\,\frac{e^{-\frac{(p_i-P_i)^2}{2\,\Delta_i}}}{\sqrt{\pi^{1/2}\,\Delta_i}}\ , \tag{2.70}$$

where the width $\Delta_i = m_{\rm p}\ell_{\rm p}/\ell_i$, and we will use the relativistic flat-space dispersion relation $E_i^2 = p_i^2 + m_i^2$, just like in the single particle case (2.19). It is particularly interesting to consider particles with masses $m_1 \simeq m_2 \ll m_{\rm p}$, so that the probability that they form a BH can be significant only in the ultra-relativistic limit $|P_i| \sim E_i \sim m_{\rm p}$, which implies

$$\ell_i \simeq \frac{\ell_{\rm p}\,m_{\rm p}}{|P_i|}\ , \qquad \Delta_i \simeq |P_i|\ . \tag{2.71}$$

The two-particle state can be written as

$$|\psi_{\rm S}^{(1,2)}\rangle = \prod_{i=1}^{2}\left[\int_{-\infty}^{+\infty}{\rm d}p_i\,\psi_{\rm S}(p_i,t)\ |p_i\rangle\right]\ , \tag{2.72}$$

and the coefficients in the spectral decomposition (2.6) are given by

$$C(E) = \int_{-\infty}^{+\infty}\int_{-\infty}^{+\infty}\psi_{\rm S}(p_1)\,\psi_{\rm S}(p_2)\,\delta(E-E_1-E_2)\,{\rm d}p_1\,{\rm d}p_2\ . \tag{2.73}$$

The HWF is defined in the rest frame of the possible BH, that is in the centre-of-mass coordinate system with $P_1 = -P_2 \equiv P > 0$. From $P \sim m_{\rm p} \gg m_1 \simeq m_2$, we can also set $X_1 \simeq -X_2 \equiv X > 0$. The unnormalised HWF is then given by [12]

$$\begin{aligned}\psi_{\rm H} \;=\;& e^{-\frac{m_{\rm p}r_{\rm H}^2}{16\ell_{\rm p}^2\,P}-\frac{X^2P^2}{\ell_{\rm p}^2m_{\rm p}^2}}\,{\rm Erf}\left(1+\frac{m_{\rm p}\,r_{\rm H}}{4\,\ell_{\rm p}\,P}+i\,\frac{XP}{\ell_{\rm p}\,m_{\rm p}}\right)\\ &-e^{-\frac{m_{\rm p}r_{\rm H}^2}{16\ell_{\rm p}^2\,P}-\frac{X^2P^2}{\ell_{\rm p}^2m_{\rm p}^2}}\,{\rm Erf}\left(1-\frac{m_{\rm p}\,r_{\rm H}}{4\,\ell_{\rm p}\,P}-i\,\frac{XP}{\ell_{\rm p}\,m_{\rm p}}\right)\\ &+2\,e^{-1-\frac{2iXP}{\ell_{\rm p}m_{\rm p}}-\frac{m_{\rm p}r_{\rm H}^2}{16\ell_{\rm p}^2P}}\cosh\left(\frac{m_{\rm p}r_{\rm H}}{2\,\ell_{\rm p}P}+i\,\frac{r_{\rm H}X}{2\,\ell_{\rm p}^2}\right)\,{\rm Erf}\left(\frac{m_{\rm p}r_{\rm H}}{4\,\ell_{\rm p}P}\right)\end{aligned}\ , \tag{2.74}$$

whose normalisation can be computed numerically for fixed X and P.

The energy of the system is solely determined by the momentum, and in fact we notice from Fig. 2.16 that $\mathcal{P}_{\rm H} = |\psi_{\rm H}(r_{\rm H})|^2$ does not vary much with

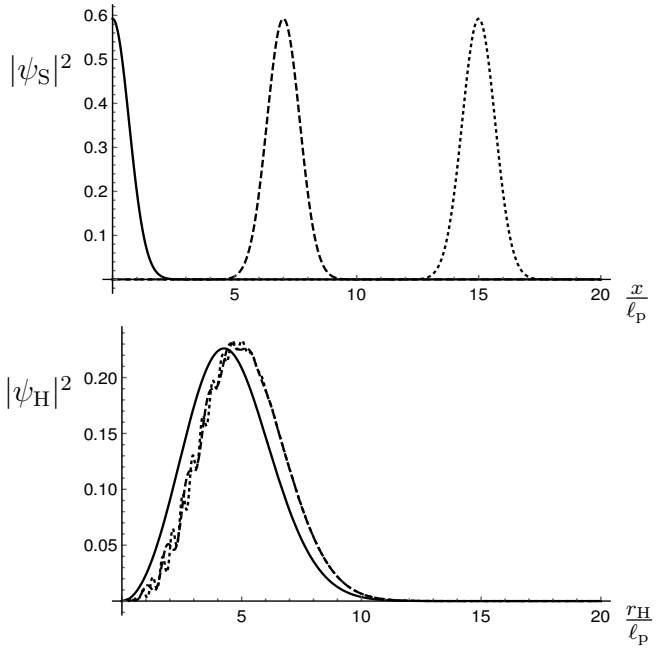

Figure 2.16: Top panel: square modulus of $\psi_{\rm S}$ for $P = m_{\rm p}$ and $X = 0$ (solid line) $X = 7\,\ell_{\rm p}$ (dashed line) and $X = 15\,\ell_{\rm p}$ (dotted line). Bottom panel: square modulus of $\psi_{\rm H}$ for $P = m_{\rm p}$ and $X = 0$ (solid line) $X = 7\,\ell_{\rm p}$ (dashed line) and $X = 15\,\ell_{\rm p}$ (dotted line). Particles are inside the horizon only for sufficiently small X.

X, but is clearly affected by P (see Fig. 2.17). Moreover, the peak of the probability density $\mathcal{P}_{\rm H}$ is always located around $r_{\rm H} \simeq 2\,\ell_{\rm p}\,(2P/m_{\rm p})$.

The final step is to compute the probability (2.14) that the two-particle system is a BH as a function of the distance X of each particle from the center-of-mass and the total energy $2P$ (see Fig. 2.18). One may argue that a rough estimate of the time evolution is given by considering this function along lines of constant P and decreasing X. In fact, it is easy to see that the probability increases to a maximum for $X = 0$, when the two particles overlap exactly. Hence, there is a large probability that the collision forms a BH, e.g. $P_{\rm BH}(X, 2P \gtrsim 2m_{\rm p}) \gtrsim 80\%$, when

$$X \lesssim 2\,\ell_{\rm p}\,(2P/m_{\rm p}) - \ell_{\rm p} = r_{\rm H}(2P) - \ell_{\rm p}\ . \tag{2.75}$$

The second term in the r.h.s. can be viewed as a quantum correction to the hoop formula (1.1) for $E \simeq 2P \gtrsim 2\,m_{\rm p}$, and becomes negligible for large (semi)classical BHs produced in collisions with $2P \gg m_{\rm p}$. Lowering P, we have that the region $P_{\rm BH}(X, 2P \lesssim 2m_{\rm p}) \gtrsim 80\%$ corresponds to the momenta satisfying $2P \gtrsim m_{\rm p}\,(1+X^2/9\,\ell_{\rm p}^2)$ and its boundary $P_{\rm BH}(X, 2P \lesssim 2m_{\rm p}) \simeq 80\%$

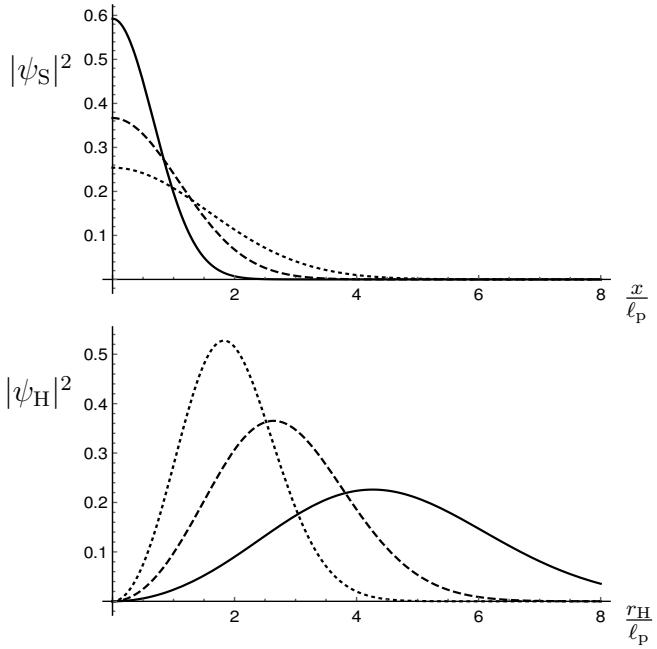

Figure 2.17: Top panel: square modulus of $\psi_{\rm S}$ for $X = 0$ and $P = m_{\rm p}$ (solid line) $P = 3\,m_{\rm p}/5$ (dashed line) and $P = 2\,m_{\rm p}/5$ (dotted line). Bottom panel: square modulus of $\psi_{\rm H}$ for $X = 0$ and $P = m_{\rm p}$ (solid line) $P = 3\,m_{\rm p}/5$ (dashed line) and $P = 2\,m_{\rm p}/5$ (dotted line). Particles' location is sharper the fuzzier (more spread) the horizon location and vice versa.

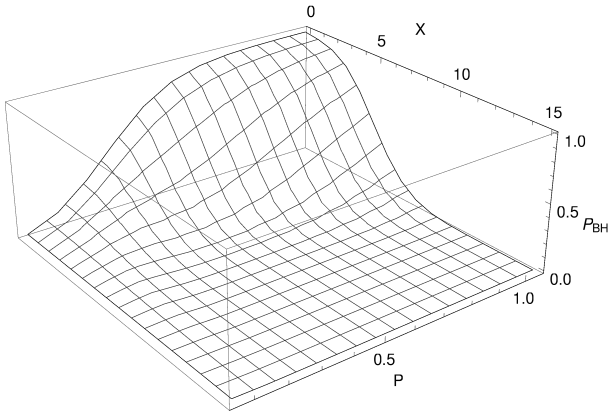

Figure 2.18: Probability the two-particle system is a BH as a function of X and P (in units of Planck length and mass respectively).

can be approximated by

$$2P - m_{\rm p} \simeq m_{\rm p}\, X^2/9\,\ell_{\rm p}^2 \ , \tag{2.76}$$

which crosses the axis $X = 0$ for $2P \simeq m_{\rm p}$. This curve represents a further correction to the hoop conjecture (1.1), and supports the conclusion that the mass of quantum BHs is bounded below by about $m_{\rm p}$. We should remark that, although these numerical values strongly depend on what probability $P_{\rm BH}$ is considered large enough, the slope in Eq. (2.75) agrees perfectly with Eq. (1.1). One can thus conclude that, despite the great simplifications assumed in this analysis, the HQM appears suitable to extend the hoop conjecture into the quantum description of BH formation.

2.3.4 Higher and lower dimensional models

The idea that the number of dimensions of space-time is not exactly four as we experience, was proposed in order to explain some puzzles of the Standard Model, like the hierarchy problem, or for consistence with string theory. Remarkably, in $D > 3$ spatial dimensions, the fundamental gravitational mass $m_D \ll m_{\rm p}$, and $\ell_D = \hbar/m_D \gg \ell_{\rm p}$, where

$$G_D = \frac{\ell_D^{D-2}}{m_D} \ . \tag{2.77}$$

This opens up the possibility of having much lighter BHs, possibly within the reach of current high-energy experiments [102, 103]. This happens both in the ADD [104, 105] and the Randall-Sundrum [106, 107] models (for a comprehensive, see Ref. [108]). In Ref. [109] the HQM probability that BHs form in the ADD scenario was computed, with some interesting consequences.

It is also instructive to study theories with less than three spatial dimensions, since the corresponding quantum theories are simpler and can be solved exactly [110]. In recent years, interest in such theories was also revived by the possibility that the number of spatial dimensions effectively decreases when approaching $\ell_{\rm p}$, regardless of the model under consideration. This effect is called "spontaneous dimensional reduction" and has been extended to various contexts, most of which with special focus on the energy dependence of the spectral dimension, including causal dynamical triangulations [111, 112, 113] and non-commutative geometry inspired mechanisms [114, 115, 116, 117]. An alternative approach is built on the claim that the effective dimensionality of space-time increases as the ambient energy scale decreases [118, 119, 120, 121, 122, 123].

$(1+D)$-dimensional Schwarzschild metric

In D spatial dimensions, the generalised Schwarzschild metric is given by

$$\mathrm{d}s^2 = -\left(1-\frac{R_D}{r^{D-2}}\right)\mathrm{d}t^2 + \left(1-\frac{R_D}{r^{D-2}}\right)^{-1}\mathrm{d}r^2 + r^{D-1}\,\mathrm{d}\Omega_{D-1}\ , \quad (2.78)$$

where the classical horizon radius is

$$R_D = \left(\frac{2\,G_{\mathrm{D}}\,m}{|D-2|}\right)^{\frac{1}{D-2}} = \begin{cases} \dfrac{1}{2\,G_1\,m} & \text{if } \ D=1 \\ \\ \left(\dfrac{2\,G_{\mathrm{D}}\,m}{D-2}\right)^{\frac{1}{D-2}} & \text{if } \ D>2\ . \end{cases} \quad (2.79)$$

Note that $D=2$ is excluded because in that case there exists no asymptotically flat BH, and we do not want to include a cosmological constant.

The source of the gravitational field is still described by a Gaussian wavefunction, that is

$$\psi_{\mathrm{S}}(r) = \frac{e^{-\frac{r^2}{2\,\ell^2}}}{(\ell\,\sqrt{\pi})^{D/2}}\ , \quad (2.80)$$

whose momentum space counterpart is

$$\tilde{\psi}_{\mathrm{S}}(p) = \frac{e^{-\frac{p^2}{2\,\Delta^2}}}{(\Delta\,\sqrt{\pi})^{D/2}}\ , \quad (2.81)$$

where $\Delta = m_D\,\ell_D/\ell$ and, taking again Eq. (2.16), $\ell \sim m^{-1}$, we recover $\Delta \simeq m$. As in $D=3$, we assume the relativistic mass-shell relation in flat space (2.19), and, for $D>3$, one obtains the HWF

$$\begin{aligned} \psi_{\mathrm{H}} \ = \ & \left\{\frac{D-2}{\ell_D^{\,D}\,\pi^{D/2}}\left[\frac{(D-2)\,\ell}{2\,\ell_D}\right]^{\frac{D}{D-2}}\ \frac{\Gamma\left(\frac{D}{2}\right)}{\Gamma\left(\frac{D}{2D-4},1\right)}\right\}^{1/2} \\ & \times\Theta(r_{\mathrm{H}}-R_D)\,\exp\left\{-\frac{(D-2)^2}{8}\,\frac{\ell^2\,r_{\mathrm{H}}^{2(D-2)}}{\ell_D^{2(D-1)}}\right\}\ , \end{aligned} \quad (2.82)$$

whose normalisation was fixed in the scalar product

$$\langle\,\psi_{\mathrm{H}}\mid\phi_{\mathrm{H}}\,\rangle = \Omega_{D-1}\int_0^\infty \psi^*_{\mathrm{H}}(r_{\mathrm{H}})\,\phi_{\mathrm{H}}(r_{\mathrm{H}})\,r_{\mathrm{H}}^{D-1}\,\mathrm{d}r_{\mathrm{H}}\ , \quad (2.83)$$

where Ω_{D-1} is the volume of the $D-$sphere.

For $D = 1$, there is an important change of sign in the argument of the step function. In fact, the generalisation (1.6) of the hoop conjecture (1.1) is now satisfied when $0 \leq r_{\rm H} \leq R_1$ and the HWF reads

$$\psi_{\rm H} = \sqrt{\frac{2/\ell}{\Gamma\left(-\frac{1}{2}, 1\right)}}\, \Theta(R_1 - r_{\rm H})\, \exp\left\{-\frac{\ell^2}{8\, r_{\rm H}^2}\right\} \ , \tag{2.84}$$

which otherwise is the same as (2.82) with $D = 1$.

BH probability

It is straightforward to write down the probability for the particle to be inside a D-dimensional ball of radius $r_{\rm H}$,

$$P_{\rm S}(r < r_{\rm H}) = \Omega_{D-1} \int_0^{r_{\rm H}} |\psi_{\rm S}(r)|^2\, r^{D-1}\, {\rm d}r \ , \tag{2.85}$$

and the probability density that the gravitational radius equals $r_{\rm H}$ is

$$\mathcal{P}_{\rm H}(r_{\rm H}) = \Omega_{D-1}\, r^{D-1}\, |\psi_{\rm H}(r_{\rm H})|^2 \ . \tag{2.86}$$

Omitting the details, one then finds

$$\begin{aligned} \mathcal{P}_< \ &= \ \frac{2}{\ell_D^D} \left[\frac{(D-2)\,\ell}{2\,\ell_D}\right]^{\frac{D}{D-2}} \frac{D-2}{\Gamma\left(\frac{D}{2\,D-4}, 1\right)\Gamma\left(\frac{D}{2}\right)}\, \Theta(r_{\rm H} - R_D) \\ &\quad \times \gamma\left(\frac{D}{2}, \frac{r_{\rm H}^2}{\ell^2}\right) \exp\left\{-\frac{(D-2)^2}{4}\, \frac{\ell^2\, r_{\rm H}^{2(D-2)}}{\ell_D^{2(D-1)}}\right\} r_{\rm H}^{D-1} \end{aligned} \tag{2.87}$$

and the BH probability is

$$\begin{aligned} P_{\rm BH} \ &= \ \frac{2(D-2)}{\Gamma\left(\frac{D}{2D-4}, 1\right)\Gamma\left(\frac{D}{2}\right)} \\ &\quad \times \int_1^\infty \gamma\left(\frac{D}{2}, \left[\frac{2}{D-2}\, \left(\frac{\ell_D}{\ell}\right)^{D-1}\right]^{\frac{2}{D-2}} x_D^2\right) e^{-x_D^{2(D-2)}}\, x_D^{D-1}\, {\rm d}x_D \end{aligned} \tag{2.88}$$

where we defined $x_D^{D-2} = (D-2)\,\ell\, r_{\rm H}^{D-2}/2\,\ell_D^{D-1}$. Eq. (2.88) depends, as usual, on the Gaussian width ℓ, but also on the number D of spatial dimensions (with $D = 3$ reproducing Eq. (2.23)). Since the above integral cannot be performed analytically for a general D, in Fig. 2.19 we show the numerical dependence on ℓ of the above probability for different spatial dimensions, and compare it with the approximation obtained by taking the limit $R_D \to 0$.

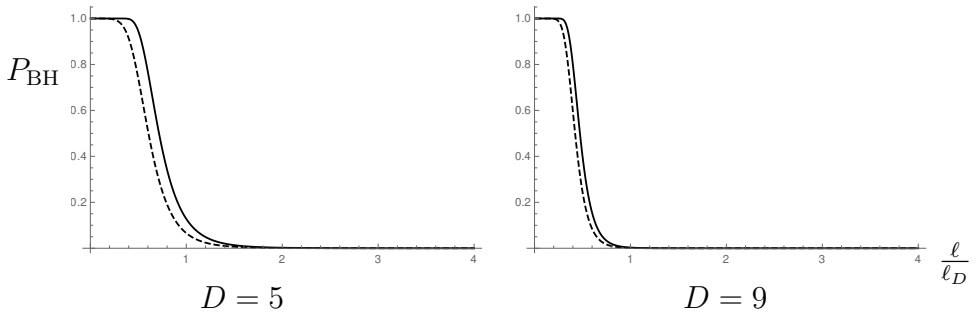

Figure 2.19: Probability $P_{\rm BH}(\ell)$ of a particle to be a BH (straight line) compared to its analytical approximation (dashed line), for $D = 5$ and 9.

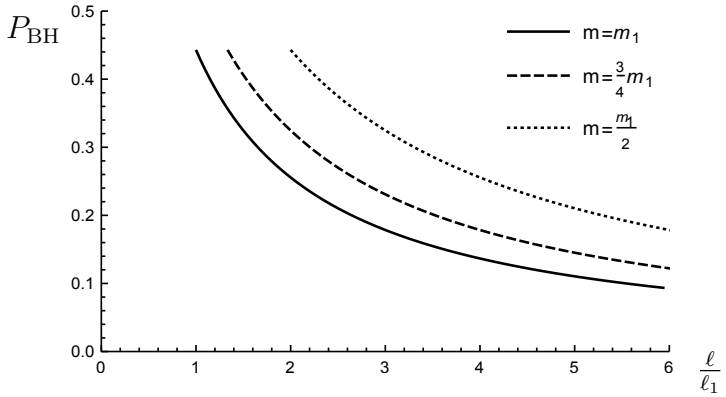

Figure 2.20: Probability $P_{\rm BH}(\ell, m)$ for a particle to be a BH in $D = 1$, for $m = m_1$ (solid line), $m = 3\,m_1/4$ (dashed line) and $m = m_1/2$ (dotted line).

The most important fact here is that the probability $P_{\rm BH} = P_{\rm BH}(m, D)$ at a given m decreases significantly for increasing D, and for large values of D a particle of mass $m \simeq m_D$ is most likely not a BH. This result should have a strong impact on the number of BHs produced in particle collisions. In fact, one expects the effective production cross-section $\sigma(E) \sim P_{\rm BH}(E)\,\sigma_{\rm BH}(E)$, where $\sigma_{\rm BH} \sim 4\,\pi\,E^2$ is the usual expression following from Eq. (1.1). Since $P_{\rm BH}$ can be very small, $\sigma(E) \ll \sigma_{\rm BH}(E)$ for $D > 4$, and much less BHs should be produced than estimated previously [103].

For $D = 1$ and $\ell = \lambda_m$, we can integrate the density

$$\mathcal{P}_{\rm H} = \frac{2/\ell}{\Gamma\left(-\frac{1}{2}, 1\right)}\,\Theta(R_1 - |r_{\rm H}|)\,{\rm erf}\left(\frac{r_{\rm H}}{\ell}\right)\,\exp\left\{-\frac{\ell^2}{4\,r_{\rm H}^2}\right\}\,, \qquad (2.89)$$

obtained from Eq. (2.84), and find

$$P_{\rm BH} = \frac{1}{\Gamma\left(-\frac{1}{2},1\right)} \int_0^1 {\rm erf}\left(\frac{x_1}{2}\right) e^{-\frac{1}{x_1^2}}\, {\rm d}x_1 \simeq 0.44 \ , \tag{2.90}$$

where $x_1 = 2\, r_{\rm H}/\ell$, which can also be obtained from Eq. (2.88) by setting $D = 1$. This last equation reveals a striking difference between $D = 1$ and higher-dimensional space-times. The maximum probability that a BH may form is independent of the mass of the source. This result is supported by the fact that the one-dimensional gravitational constant $G_1 = \hbar$ and

$$\langle\, \hat{r}_{\rm H} \,\rangle \simeq R_1(m) \simeq \lambda_m \ , \tag{2.91}$$

for any possible mass, and hence no source can be treated in a classical way. Moreover, for more general cases with $\ell > \lambda_m$, particles with masses considerably lower than the mass scale m_1 still have a relatively large probability to be BHs (see Fig. 2.20) [109]. Another important feature of the HWF in $D = 1$ is that

$$\Delta r_{\rm H} \simeq \ell \simeq \Delta p^{-1} \ , \tag{2.92}$$

that is the uncertainty in the horizon radius shows the same dependence on the momentum uncertainty found in the Heisenberg relation. This implies that we cannot obtain a GUP in $D = 1$ by combining (linearly) the above the two uncertainties, unlike in the three-dimensional case (2.32). In fact, all of these results agree with the notion that two-dimensional BHs are strictly quantum objects [117].

GUP from HWF in higher dimensions

For $D > 3$, we have

$$\langle\, \hat{r} \,\rangle = \frac{2^{1-D}\sqrt{\pi}\,(D-1)!}{\Gamma\left(\frac{D}{2}\right)^2}\, \ell \tag{2.93}$$

and

$$\langle\, \hat{r}^2 \,\rangle = \frac{D}{2}\, \ell^2 \ . \tag{2.94}$$

Moreover,

$$\Delta p = \sqrt{A_D}\, m = \sqrt{A_D}\, m_D\, \frac{\ell_D}{\ell} \ , \tag{2.95}$$

so that

$$\frac{\Delta r}{\ell_D} = \sqrt{A_D}\,\frac{\ell}{\ell_D} = A_D\,\frac{m_D}{\Delta p}\ , \tag{2.96}$$

where

$$A_D \equiv \frac{D}{2} - \left(\frac{2^{1-D}\sqrt{\pi}}{\Gamma\left(\frac{D}{2}\right)^2}\,(D-1)!\right)^2\ . \tag{2.97}$$

From the HWF (2.82), we likewise obtain the expectation values

$$\langle\,\hat{r}_{\rm H}\,\rangle = \frac{{\rm E}_{\frac{D-5}{2D-4}}(1)}{{\rm E}_{\frac{D-4}{2D-4}}(1)}\,R_D \tag{2.98}$$

and

$$\langle\,\hat{r}^2_{\rm H}\,\rangle = \frac{{\rm E}_{\frac{D-6}{2D-4}}(1)}{{\rm E}_{\frac{D-4}{2D-4}}(1)}\,R^2_D\ , \tag{2.99}$$

in terms of the exponential integral (2.30), so that

$$\frac{\Delta r_{\rm H}}{\ell_D} = C_D\,\left(\frac{\ell_D}{\ell}\right)^{\frac{1}{D-2}} = B_D\,\left(\frac{\Delta p}{m_D}\right)^{\frac{1}{D-2}}\ , \tag{2.100}$$

where $B_D = A_D^{-\frac{2}{D-2}}\,C_D$ and

$$C_D = \sqrt{\frac{{\rm E}_{\frac{D-6}{2D-4}}(1)}{{\rm E}_{\frac{D-4}{2D-4}}(1)} - \left(\frac{{\rm E}_{\frac{D-5}{2D-4}}(1)}{{\rm E}_{\frac{D-4}{2D-4}}(1)}\right)^2}\,\left(\frac{2}{D-2}\right)^{\frac{1}{D-2}}\ . \tag{2.101}$$

By combining the two uncertainties (2.96) and (2.100) linearly, one finally finds

$$\frac{\Delta r}{\ell_D} = A_D\,\frac{m_D}{\Delta p} + \xi\,B_D\,\left(\frac{\Delta p}{m_D}\right)^{\frac{1}{D-2}}\ , \tag{2.102}$$

where, like before, the coefficient ξ is a dimensionless parameter.

Fig. 2.21 shows the total uncertainty Δr for different numbers of spatial dimensions (and $\xi = 1$). It is clear that in higher dimensions, one obtains the same qualitative behaviour as in $D = 3$, with Eq. (2.102) being again minimised by a length L_D corresponding to an energy scale M_D, which we plot in Figs. 2.22 and 2.23 as functions of the parameter ξ. From these plots we can infer that, for every value of D considered here, the assumption $M_D \simeq m_D$ makes large values of ξ significant, whilst the opposite happens if we set $L_D \simeq \ell_D$.

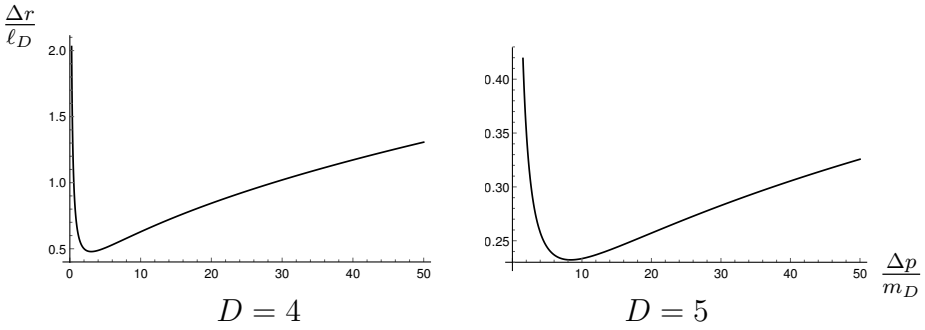

Figure 2.21: Uncertainty Δr as function of Δp for $D = 4$ and 5 and $\xi = 1$.

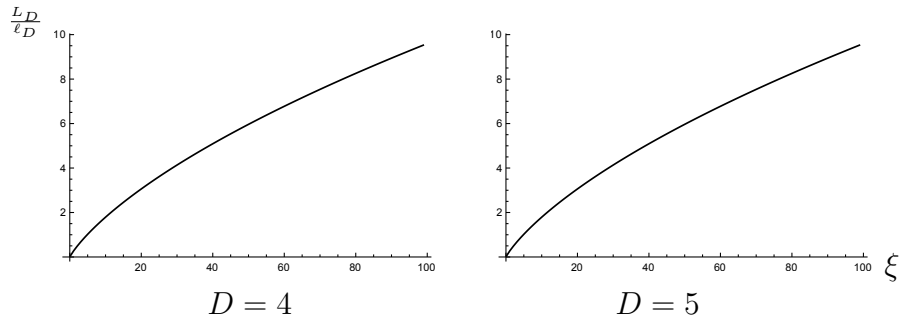

Figure 2.22: Minimum scale L_D as function of the parameter ξ for $D = 4$ and 5.

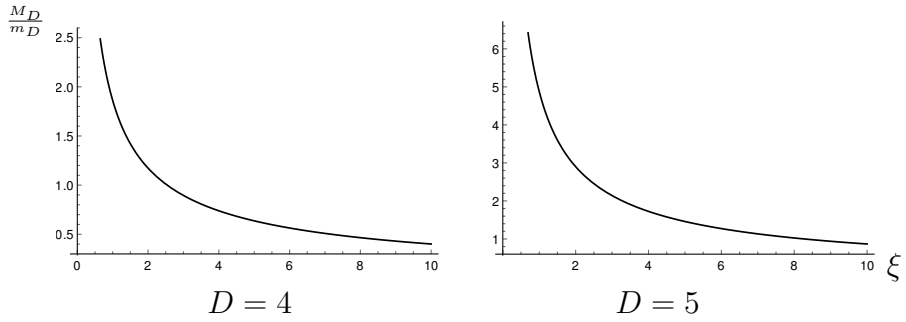

Figure 2.23: Minimum scale M_D as function of the parameter ξ for $D = 4$ and 5.

2.4 Causal time evolution

So far, time evolution was not considered. In the case of the two colliding wave-packets, one could sort of infer how the probability for the system of particles to form a BH evolves by looking at the plot representing this probability as a function of the distance between the two particles. However,

in this crude approximation, nothing would forbid the two particles from crossing each other, and the probability $P_{\rm BH}$ to reach one and then decrease. How a non-negligible BH probability could affect the evolution of a quantum state was addressed in Ref. [13] for the usual spherically symmetric Gaussian wave-packet (2.15). In order to simplify the analysis, all Standard Model interactions are neglected and the point of view is taken of an observer placed at a very large distance from this particle. It seems therefore sensible to assume that, if the particle is not a BH ($P_{\rm BH} \ll 1$), the time evolution is governed by the standard Schrödinger equation with the Hamiltonian $H = E$ of the mass-shell Eq. (2.19). If instead the system is a BH ($P_{\rm BH} \simeq 1$), no evolution should appear to occur at all (Hawking evaporation is also neglected in this toy model). The pictured considered in Ref. [13] is therefore of a BH as a "frozen star" [6].

When the wave-packet $\psi_{\rm S}$ does not fall into one of the above two limiting conditions, the evolution for arbitrarily "short" time intervals δt is taken to be described by means of the combination

$$\psi_{\rm S}(r, t+\delta t) = \left[\mu_{\rm H}(t)\,\hat{\mathbb{I}} + \bar{\mu}_{\rm H}(t)\,e^{-\frac{i\,\delta t}{m_{\rm p}\ell_{\rm p}}\hat{H}}\right]\psi_{\rm S}(r,t)\ , \tag{2.103}$$

where $\hat{\mathbb{I}}$ is the identity operator and the coefficients

$$\mu_{\rm H}(t) \simeq P_{\rm BH}(t) \simeq 1 - \bar{\mu}_{\rm H}(t)\ , \tag{2.104}$$

so that the two limiting behaviours are included by construction and unitarity is preserved,

$$1 = \mu_{\rm H}^2 + \bar{\mu}_{\rm H}^2 + 2\,\bar{\mu}_{\rm H}\,\mu_{\rm H}\,\cos\left(\frac{\delta t}{m_{\rm p}\ell_{\rm p}}\,\hat{H}\right) \simeq (\mu_{\rm H} + \bar{\mu}_{\rm H})^2\ , \tag{2.105}$$

for δt sufficiently short (see below about this very important point). In this limit, Eq. (2.103) results in the effective Schrödinger equation

$$i\,m_{\rm p}\ell_{\rm p}\,\frac{\delta\psi_{\rm S}(r,t)}{\delta t} \simeq [1 - P_{\rm BH}(t)]\,\hat{H}\,\psi_{\rm S}(r,t)\ , \tag{2.106}$$

which reproduces the standard quantum mechanical evolution in the limit $P_{\rm BH} \to 0$. Since the (now time-dependent) probability $P_{\rm BH} = P_{\rm BH}(t)$ is determined by the entire wave-function $\psi_{\rm S} = \psi_{\rm S}(r,t)$ and its associated HWF, the apparently trivial correction it introduces is instead non-local, and cannot be reproduced by means of a local interaction term of the form $H_{\rm int} = H_{\rm int}(r,t)$.

[6] Historically, this name was commonly used for gravitationally collapsed objects before the term BH was introduced [63].

This insight makes it evident that it will be generally very hard to solve Eq. (2.106) for a finite time interval.

By employing the spectral decomposition at fixed time t,

$$\psi_{\rm S}(r,t) = \sum_E C_E(t)\, j_0(E,r) \ , \tag{2.107}$$

where j_0 is a spherical Bessel function of the first kind, Eq. (2.103) can be written as

$$i\, m_{\rm p}\ell_{\rm p}\, \delta C_E(t) \simeq [1 - P_{\rm BH}(t)]\, E\, C_E(t)\, \delta t \ . \tag{2.108}$$

One can now determine $\delta C_E(t)$ provided $\psi_{\rm S}(t)$ is known, and reconstruct both $\psi_{\rm S}$ and $\psi_{\rm H}$ at the time $t + \delta t$, in order to proceed to the next time step.

If $\psi_{\rm S}(r, t = 0)$ is the Gaussian wave-function (2.15), the corresponding $P_{\rm BH}(t = 0) = P_{\rm BH}(\ell, m)$ discussed in Section 2.3.1, and this state will likely be a BH only if $m \gtrsim m_{\rm p}$ and $\ell \lesssim \ell_{\rm p}$. In particular, by setting $E \simeq m_{\rm p}$, we expect the evolution equation (2.108) holds for

$$\delta t \lesssim \ell_{\rm p} \frac{m_{\rm p}}{E} \simeq \ell_{\rm p} \ , \tag{2.109}$$

and even shorter intervals for modes with energy $E \gg m_{\rm p}$, which is a form of the natural duality $(E > m_{\rm p}) \Leftrightarrow (\delta t < \ell_{\rm p})$. One can now solve Eq. (2.108) with a time step satisfying (2.109), and subsequently obtain the wave-function $\psi_{\rm S}(r, t = \delta t)$ by inverting the decomposition (2.107). Fig. 2.24 shows the probability density $\mathcal{P}_{\rm S} = 4\,\pi\, r^2\, |\psi_{\rm S}(r,t)|^2$ at $t = 0$ and $t = \delta t = \ell_{\rm p}$ for $m = 3\, m_{\rm p}/4$ and $\ell = \lambda_m = 4\,\ell_{\rm p}/3$. One can make a comparison with the density arising from the standard free evolution during the same interval of time $\delta t = \ell_{\rm p}$. In this case, the initial state is characterised by the minimum gravitational radius $R_{\rm H} = 1.5\,\ell_{\rm p}$ given in Eq. (1.6), the expectation value of the energy $\langle\, E\,\rangle \simeq 1.15\, m_{\rm p}$, the Schwarzschild radius $\langle\, \hat{r}_{\rm H}\,\rangle \simeq 2.3\,\ell_{\rm p}$, and initial probability $P_{\rm BH} \simeq 0.8$. One immediately notices that the modified evolution makes the packet more confined than the usual quantum mechanical one. However, since the packet will keep on spreading, it is reasonable to guess that $P_{\rm BH}(t + \delta t) < P_{\rm BH}(t)$, and the effect of the horizon will mitigate over time.

Longer time evolutions can be obtained by discretising the time as $t = n\,\delta t$, where n is a positive integer and the time step δt is bounded by (2.109) for all relevant energies E in the spectrum (2.107). In Ref. [13] a numerical approach was employed in order to keep all these features under control. Fig. 2.25 shows the probability densities $\mathcal{P}_{\rm S}$ and $\mathcal{P}_{\rm H}$ for $m = 3\, m_{\rm p}/4$ and $\ell = \lambda_m = 4\,\ell_{\rm p}/3$, at the time $t = 10\,\delta t = 10\,\ell_{\rm p}$. The broadening of $\mathcal{P}_{\rm S}$ is

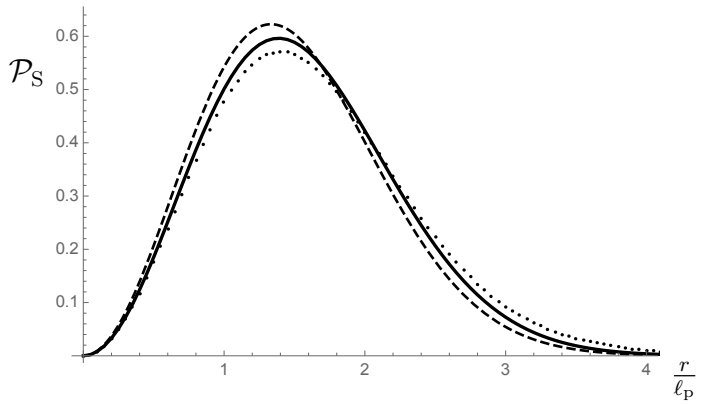

Figure 2.24: Time-evolution of the probability density for the initial Gaussian packet (2.15) with $m = 3\,m_p/4$ and $\ell = \lambda_m = 4\,\ell_p/3$ (dashed line) according to standard quantum mechanics (dotted line) compared to its causal evolution (2.106) (solid line) for $\delta t = \ell_p$.

clearly slower than in the standard quantum evolution, but still leads to a decreasing BH probability density. The time evolution of the BH probability is displayed in Fig. 2.26 for $\lambda_m = \ell = \ell_p$, $4\,\ell_p/3$ and $2\,\ell_p$. As usual, whenever the Gaussian width exceeds the Planck length, $\ell > \ell_p$, the BH probability tends to vanish very fast. A possible interpretation of this result is that the initial quantum BH decays and its own Hawking radiation is simulated by the widening of the wave-function [13].

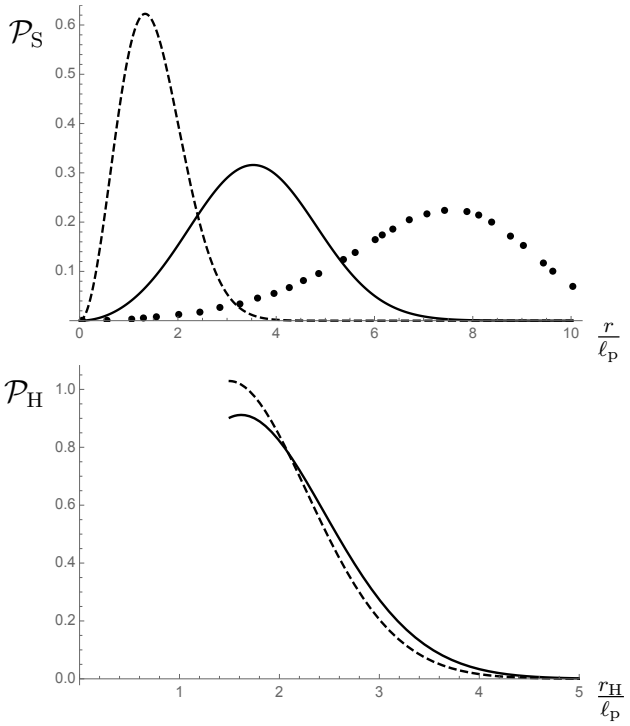

Figure 2.25: Upper panel: probability density from the final wave-packet $\psi_{\rm S}(r, 10\,\ell_{\rm p})$ with $\ell = 4\,\ell_{\rm p}/3$ from the modified evolution (2.106) (solid line) compared to the freely evolved packet (dotted line) and initial packet $\psi_{\rm S}(r, 0)$ (dashed line). Bottom panel: horizon probability density for the Gaussian particle in the upper panel at $t = 0$ (dotted line) and $t = 10\,\ell_{\rm p}$ (solid line). Note that $\psi_{\rm H}(r_{\rm H} < R_{\rm H}, t) = 0$, for $R_{\rm H} \equiv 1.5\,\ell_{\rm p}$.

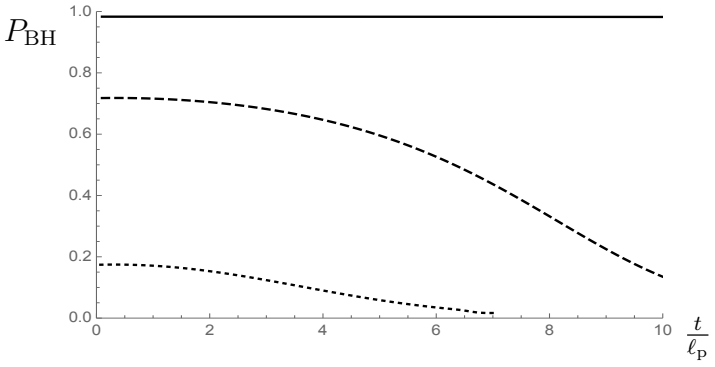

Figure 2.26: Time-evolution of the probability $P_{\rm BH}$ for the Gaussian wave-function (2.15) for $\ell = \ell_{\rm p}$ (solid line), $\ell = 4\,\ell_{\rm p}/3$ (dashed line) and $\ell = 2\ell_{\rm p}$ (dotted line).

Chapter 3

Corpuscular model

The simple and intuitive corpuscular model recently introduced by Dvali and Gomez in Refs. [73], and widely developed in Refs. [19, 124, 125, 126, 127, 128, 129, 130, 131], puts gravitation under a new light. The model is based on the assumption that the classical geometry should be viewed as an effective description of a quantum state with a large graviton occupation number, where gravitons play the role of space-time quanta, very much like photons are light quanta in a laser beam. Unlike photons, which do not interact with each other via quantum electrodynamics, graviton-graviton interaction is mediated by gravitation itself, whose attractive nature can thus lead to form a ball of superposed gravitational quanta. When such a superposition is a ground-state, the gravitational field is effectively a Bose-Einstein condensate (BEC): Dvali and Gomez conjectured this is precisely what happens inside BHs. Even when considering a strong gravitational regime, as expected to happen at the verge of BH formation, the whole construction can be nicely explained under Newtonian approximation. The Newtonian potential at a distance r generated by a system of N gravitons, each with effective mass m (so that the total mass $M = N\,m$) is

$$V_{\rm N}(r) \simeq -\frac{G_{\rm N}\,M}{r} = -\frac{\ell_{\rm p}\,N\,m}{r\,m_{\rm p}}\ . \tag{3.1}$$

This potential can be strong enough to confine the gravitons themselves inside a finite volume where they are all superposed on each other. The gravitons effective mass m can be related to their characteristic quantum mechanical size via the Compton/de Broglie wavelength $\lambda_m \simeq \frac{\hbar}{m} = \ell_{\rm p}\,\frac{m_{\rm p}}{m}$. If one assumes that the interaction is negligible outside the ball of gravitons and constant inside, with average interaction distance $r = \lambda_m$, the potential simplifies to

$$V_{\rm N}(r) \simeq -\frac{G_{\rm N}\,M}{\lambda_m}\Theta(\lambda_m - r) := V_{\rm N}(\lambda_m)\ , \tag{3.2}$$

which results in an average potential energy per graviton

$$U_m \simeq m\, V_{\rm N}(\lambda_m) := -N\,\alpha\, m \ , \tag{3.3}$$

where

$$\alpha = \frac{\ell_{\rm p}^2}{\lambda_m^2} = \frac{m^2}{m_{\rm p}^2} \ , \tag{3.4}$$

is the gravitational coupling.

One can think of virtually superposing gravitons one by one, thus strengthening their reciprocal attraction, until they find themselves confined inside a deep enough "potential well" from which they cannot escape. The condition for the gravitons to be "marginally bound" is reached when each single graviton has just not enough energy $E_K = m$ to escape the potential well,

$$E_K + U \simeq 0 \ . \tag{3.5}$$

At this point, one has created a BH solely out of condensed gravitational quanta. When this condition is reached, the gravitons are "maximally packed", and their number satisfies

$$N\,\alpha \simeq 1 \ . \tag{3.6}$$

The effective graviton mass correspondingly scales as

$$m \simeq \frac{m_{\rm p}}{\sqrt{N}} \ , \tag{3.7}$$

while the total mass of the BH scales like [1]

$$M = N\, m \simeq \sqrt{N}\, m_{\rm p} \ . \tag{3.8}$$

Moreover, the horizon's size, namely the Schwarzschild radius

$$R_{\rm H} = 2\,\ell_{\rm p}\frac{M}{m_{\rm p}} \ , \tag{3.9}$$

is spontaneously quantised as commonly expected [132], that is

$$R_{\rm H} \simeq \sqrt{N}\,\ell_{\rm p} \ . \tag{3.10}$$

[1] This scaling relation had been already found in [133] without fully understanding its role in the case of BH formation.

This simple, purely gravitational BH [2] can now be shown to emit purely gravitational Hawking radiation. In a first order approximation, reciprocal $2 \to 2$ graviton scatterings inside the condensate will give rise to a depletion rate

$$\Gamma \sim \frac{1}{N^2}\, N^2\, \frac{1}{\sqrt{N}\,\ell_{\rm p}}\ , \tag{3.11}$$

where the factor N^{-2} comes from α^2, the second factor is combinatoric (there are about N gravitons scattering with other $N-1 \simeq N$ gravitons), and the last factor comes from the characteristic energy of the process $\Delta E \sim m$. The amount of gravitons in the condensate will then decrease according to [73]

$$\dot{N} \simeq -\Gamma \simeq -\frac{1}{\sqrt{N}\,\ell_{\rm p}} + O(N^{-1})\ . \tag{3.12}$$

As explained in Refs. [73], this emission of gravitons reproduces the purely gravitational part of the Hawking radiation and contributes to the shrinking of the BH according to the standard results

$$\dot{M} \simeq m_{\rm p}\,\frac{\dot{N}}{\sqrt{N}} \sim -\frac{m_{\rm p}}{N\,\ell_{\rm p}} \sim -\frac{m_{\rm p}^3}{\ell_{\rm p}\,M^2}\ . \tag{3.13}$$

From this flux one can then read off the "effective" Hawking temperature

$$T_{\rm H} \simeq \frac{m_{\rm p}^2}{8\,\pi\,M} \sim m \sim \frac{m_{\rm p}}{\sqrt{N}}\ , \tag{3.14}$$

where the last expression is precisely the approximate value we shall use throughout.

3.1 Scalar toy-gravitons coupled to a source

The model presented in the previous section is very simple and leads to very "reasonable" properties, but in its original form lacks some features that might make it even more appealing. For example, the connection with the usual geometrical picture of GR is not immediate, and the horizon "emerges" from a classical mechanical condition (the binding condition of Eq. (3.5)), rather than from relativistic considerations (as it happens in the case of the hoop conjecture).

[2] This model is only made of gravitational energy, with no contribution from other particle species. For some preliminary results regarding the role of baryons, see Ref. [134].

Trying to understand the corpuscular theory of Dvali and Gomez, using different tools can be of some help. In Refs. [18], QFT was proposed in order to model a self-sustained graviton system. To simplify the description, the authors consider scalar toy-gravitons instead of regular gravitons, which allows to employ the Klein-Gordon equation for a real and massless scalar field ϕ coupled to a real scalar current J in Minkowski space-time,

$$\Box\phi(x) = q\, J(x) \ , \tag{3.15}$$

where $\Box = \eta^{\mu\nu}\,\partial_\mu\,\partial_\nu$ and q is a dimensionless coupling. One then also assumes that the current is time-independent, $\partial_0 J = 0$. In momentum space, with $k^\mu = (k^0, \mathbf{k})$, this leads to

$$k^0\,\tilde{J}(k^\mu) = 0 \tag{3.16}$$

which is solved by the distribution

$$\tilde{J}(k^\mu) = 2\,\pi\,\delta(k^0)\,\tilde{J}(\mathbf{k}) \ , \tag{3.17}$$

where $\tilde{J}^*(\mathbf{k}) = \tilde{J}(-\mathbf{k})$. For the spatial part, exact spherical symmetry is assumed, so that the analysis is restricted to functions of the kind $f(\mathbf{x}) = f(r)$, with $r = |\mathbf{x}|$. Classical spherically symmetric solutions of Eq. (3.15) can be formally written as

$$\phi_{\rm c}(r) = q\,\Box^{-1} J(r) \ , \tag{3.18}$$

and they can be found more easily in momentum space. The latter is defined by the integral trasnformation

$$\tilde{f}(k) = 4\,\pi \int_0^{+\infty} dr\, r^2\, j_0(kr)\, f(r) \ , \tag{3.19}$$

where

$$j_0(kr) = \frac{\sin(kr)}{k\,r} \ , \tag{3.20}$$

is a spherical Bessel function of the first kind and $k = |\mathbf{k}|$. This gives the solution

$$\tilde{\phi}_{\rm c}(k) = -q\,\frac{\tilde{J}(k)}{k^2} \ . \tag{3.21}$$

For example, for a current with Gaussian profile,

$$J(r) = \frac{e^{-r^2/(2\,\sigma^2)}}{(2\,\pi\,\sigma^2)^{3/2}} \ , \tag{3.22}$$

one finds

$$\tilde{J}(k) = e^{-k^2\sigma^2/2} \tag{3.23}$$

and the corresponding classical scalar field is given by

$$\begin{aligned} \phi_{\rm c}(r) &= -\frac{q}{2\,\pi^2}\int_0^{+\infty} {\rm d}k\, j_0(kr)\, e^{-k^2\sigma^2/2} \\ &= -\frac{q}{4\,\pi\,r}\,{\rm erf}\left(\frac{r}{\sqrt{2}\,\sigma}\right) , \end{aligned} \tag{3.24}$$

where erf is the error function. At large distances from the source J, when $r \gg \sigma$, the field ϕ reproduces the classical Newtonian potential (3.1), i.e.

$$V_{\rm N} = \frac{4\,\pi}{q}\, G_{\rm N}\, M\, \phi_{\rm c} \simeq -\frac{G_{\rm N}\, M}{r} \tag{3.25}$$

In the quantum theory, the classical configurations (3.18) are replaced by coherent states. To prove this statement, one can start with the normal-ordered quantum Hamiltonian density in momentum space,

$$\hat{\mathcal{H}} = k\, \hat{a}_k'^{\dagger}\, \hat{a}_k' + \tilde{\mathcal{H}}_g \ , \tag{3.26}$$

where $\tilde{\mathcal{H}}_g$ is the ground state energy density,

$$\tilde{\mathcal{H}}_g = -q^2\, \frac{|\tilde{J}(k)|^2}{2\,k^2} \ , \tag{3.27}$$

and the standard ladder operators are shifted according to

$$\hat{a}_k' = \hat{a}_k + q\, \frac{\tilde{J}(k)}{\sqrt{2\,k^3}} \ . \tag{3.28}$$

The source-dependent ground state $|g\rangle$ is annihilated by the shifted annihilation operator,

$$\hat{a}_k'\, |g\rangle = 0 \ , \tag{3.29}$$

and is a coherent state in terms of the standard field vacuum,

$$\hat{a}_k\, |g\rangle = -q\, \frac{\tilde{J}(k)}{\sqrt{2\,k^3}}\, |g\rangle = g(k)\, |g\rangle \ \ , \tag{3.30}$$

with $g = g(k)$ being an eigenvalue of the shifted annihilation operator. This results in

$$|g\rangle = e^{-N/2} \exp\left\{\int \frac{k^2\, {\rm d}k}{2\,\pi^2}\, g(k)\, \hat{a}_k^{\dagger}\right\} |0\rangle \ \ , \tag{3.31}$$

with N representing the expectation value of the number of quanta in the coherent state,

$$\begin{aligned} N &= \int \frac{k^2\,\mathrm{d}k}{2\,\pi^2}\,\langle g|\,\hat{a}_k^\dagger\,\hat{a}_k\,|g\rangle \\ &= \frac{q^2}{(2\,\pi)^2}\int \frac{\mathrm{d}k}{k}\,|\tilde{J}(k)|^2\ , \end{aligned} \tag{3.32}$$

from which the occupation number is found to be

$$n_k = \Big(\frac{q}{2\,\pi}\Big)^2\,\frac{|\tilde{J}(k)|^2}{k}\ . \tag{3.33}$$

It is now straightforward to verify that the expectation value of the field in the state $|g\rangle$ coincides with its classical value,

$$\begin{aligned} \langle g|\,\hat{\phi}_k\,|g\rangle &= \frac{1}{\sqrt{2\,k}}\,\langle g|\,\Big(\hat{a}_k + \hat{a}_{-k}^\dagger\Big)\,|g\rangle \\ &= \frac{1}{\sqrt{2\,k}}\,\langle g|\,\Big(\hat{a}'_k + \hat{a}'^\dagger_{-k}\Big)\,|g\rangle - q\,\frac{\tilde{J}(k)}{k^2} \\ &= \tilde{\phi}_{\mathrm{c}}(k)\ , \end{aligned} \tag{3.34}$$

thus $|g\rangle$ is a realisation of the Ehrenfest theorem.

It is important to note that Eq. (3.32) presents a UV divergence if the source has infinitely thin support, and an IR divergence if the source contains modes of vanishing momenta (which would only be physically consistent with an eternal source). Because to this, the state $|g\rangle$ and the number N are not mathematically well-defined in general. Anyway, the UV divergence can be cured, for example, by using a Gaussian distribution like the one in Eq. (3.22), while the IR divergence can be eliminated if the scalar field is massive or the system is enclosed within a finite volume (so that allowed modes are also quantised).

3.1.1 Black holes as self-sustained quantum states

One can now analyse a "star", made of ordinary matter whose density is distributed according to

$$\rho = M\,J\ , \tag{3.35}$$

where M is the total (proper) energy of the star. Its Newtonian potential energy is given by $U_M = M\,V_{\mathrm{N}}$, so that ϕ_{c} is accordingly determined by Eq. (3.25) and the quantum state of $\hat{\phi}$ by Eq. (3.34).

During the formation of a BH, the gravitons are expected to dominate the dynamics over the matter source [73]. Then, one can assume the matter contribution is negligible, and the source J in the r.h.s. of Eq. (3.15) is thus provided by the gravitons themselves. This source, consisting of gravitons, is roughly confined in a finite spherical volume $\mathcal{V} = 4\,\pi\,R^3/3$ (this is a crucial feature for the "classicalization" of gravity [55, 56] and requires an attractive self-interaction for the scalar field to admit bound states). The energy density (3.35) must then be equal to the average energy density inside the volume $\mathcal{V}$, which in turn is given by the average potential energy of each graviton in $\mathcal{V}$, times the number of gravitons: $N\,U_m/\mathcal{V}$. [3] This assumption is qualitatively the same as the marginally bound condition (3.5) with $N\,E_{\rm K} \sim J$. After some simple substitutions one finds

$$J \simeq -\frac{3\,N\,G_{\rm N}\,m}{q\,R^3}\,\phi_{\rm c}\ , \tag{3.36}$$

inside the volume $\mathcal{V}$, where m is the energy of each of the N scalar gravitons. Using this condition into Eq. (3.21), one finds

$$\frac{3\,N\,G_{\rm N}\,m}{R^3\,k^2} = \frac{3\,R_{\rm H}}{2\,R^3\,k^2} \simeq 1\ , \tag{3.37}$$

where

$$R_{\rm H} = 2\,G_{\rm N}\,M \tag{3.38}$$

is the classical Schwarzschild radius of the object. One can infer that a self-sustained system of gravitons will contain only the modes with momentum numbers $k = k_{\rm c}$ such that

$$R\,k_{\rm c} \simeq \sqrt{\frac{R_{\rm H}}{R}}\ , \tag{3.39}$$

where numerical coefficients of order one were dropped in line with the qualitative nature of the analysis.

This clearly does not happen in the Newtonian case, where the potential generated by an ordinary matter source would allow any momentum numbers. Ideally, this means that, if the gravitons represent the main self-gravitating source, the quantum state of the system must be given in terms of just one mode $\phi_{k_{\rm c}}$. A coherent state of the form in Eq. (3.31) requires a

[3] Each graviton interacts with the other $N-1$, so that the energy of each graviton is proportional to $(N-1)\,U_m$, but one can safely approximate $N-1 \simeq N$, given that N is considered large.

distribution of different momenta and cannot thus be built this way, i.e. by means of a strictly confined source. Furthermore, the relation (3.32) between N and the source momenta does not apply here. Instead, for very large N, all scalars are in the state $|k_{\rm c}\rangle$ and form a BEC.

Consider now that, for an ordinary star, the typical size is much greater than its Schwarzschild radius ($R \gg R_{\rm H}$) and therefore $k_{\rm c} \ll R^{-1}$. The corresponding de Broglie length $\lambda_{\rm c} \simeq k_{\rm c}^{-1} \gg R$, which conflicts with the assumption that the field represents a gravitating source only within a region of size R. However, in the "BH limit" $R \sim R_{\rm H}$, and recalling that $m = \hbar\, k$, one obtains

$$1 \simeq G_{\rm N}\, M\, k_{\rm c} = N\, \frac{m^2}{m_{\rm p}^2}\ , \tag{3.40}$$

which leads to the two scaling relations (3.8), namely $m = \hbar\, k_{\rm c} \simeq m_{\rm p}/\sqrt{N}$ and a consistent de Broglie length $\lambda_m \simeq \lambda_{\rm c} \simeq R_{\rm H}$. Therefore, an ideal system of self-sustained (toy) gravitons must be a BEC with a size that suggests it is a BH. All that remains to be proven is the existence of a horizon, or at least a trapping surface, in the given space-time.

The safest way to find trapping surfaces would require a general-relativistic solution for the self-gravitating BEC with given density and equation of state. Many authors faced this problem in the past decades. Self-gravitating boson stars in GR have been studied for example in Ref. [133], but only numerical solutions have been found, mostly generated by a Gaussian source [135, 136, 137, 138, 139, 140]. In the specific case presented here, QM crosses the way of GR because the BEC BH can be regarded to as a "giant soliton", and microscopic BHs are extremely dense, thus producing a (relatively) strong space-time curvature at very small scales. In these regimes it is uncertain whether a semiclassical approach is still valid, since the quantum fluctuations become relevant with respect to the surrounding space-time geometry. The HWF was precisely proposed in order to define the gravitational radius of any quantum system, and should therefore be very useful for investigating this issue.

To avoid misunderstandings, one needs to make some clarifications about the toy model presented above (where the field ϕ is totally confined inside a sphere of radius $R_{\rm H}$). The scaling relation (3.40) does not require the scalar field ϕ to vanish (or be negligible) outside the region of radius $R_{\rm H}$. Since the scalar field also provides the Newtonian potential (see Eq. (3.25)), the vanishing of the field outside $R_{\rm H}$ would imply there is no Newtonian potential outside the BEC, and this would conflict with the idea that the BEC is a gravitational source. To recover the classical Newtonian potential $V_{\rm N} \sim \phi$

outside the source, it is enough to relax the condition (3.36) for $r \gtrsim R_{\rm H}$ (where $J \simeq 0$), and properly match the (expectation) value of $\hat{\phi}$ with the Newtonian $\phi_{\rm c}$ from Eq. (3.25) at $r \gtrsim R_{\rm H}$. One then expects that for $r \gg R_{\rm H}$ and $N \gg 1$, the classical description is recovered and that the total mass M of the BH becomes the only relevant quantity. A hint of this can be found in the classical analysis of the outer ($r \gg \sigma \sim R_{\rm H}$) Newtonian scalar potential and its quantum counter-part, but also in the alternative description of gravitational scattering. Geodesic motion can be reproduced in the post-Newtonian expansion of the Schwarzschild metric by tree-level Feynman diagrams with graviton exchanges between a test probe and a (classical) large source [141] [4]. For $r \gg R_{\rm H}$, the source in this calculation is described by its total mass M, and quantum effects should then be suppressed by factors of $1/N$ [73].

3.2 BEC black hole horizons

When analysing the case of BEC BHs, one has to remember that these are composed of very large numbers of particles (the toy-gravitons) of very small effective mass $m \ll m_{\rm p}$ (thus very large de Broglie length, $\lambda_m \gg \ell_{\rm p}$), as opposed to the case of single massive particles studied in Refs. [11, 12, 13, 14, 15] and briefly reviewed in Section 2.3.1. According to Ref. [11], they cannot individually form (light) BHs. A generalisation of the formalism to a system of N such components is possible and will allow one to show that the total energy $E = M$ is sufficient to create a proper horizon.

In order to set the notation, consider a system of N scalar particles (our "toy gravitons"), $i = 1, \ldots, N$, whose dynamics is determined by a Hamiltonian H_i. If the particles are marginally bound according to Eq. (3.5), the single-particle Hilbert space can be assumed to contain the discrete ground state $|m\rangle$, defined by

$$\hat{H}_i \, |m\rangle = m \, |m\rangle \ , \tag{3.41}$$

and a gapless continuous spectrum of energy eigenstates $|\omega_i\rangle$, such that

$$\hat{H}_i \, |\omega_i\rangle = \omega_i \, |\omega_i\rangle \ , \tag{3.42}$$

with $\omega_i > m$. The continuous spectrum reproduces the particles that escape the BEC. Each particle is then assumed to be in a state given by a superposition of $|m\rangle$ and the continuous spectrum, namely

$$|\Psi_{\rm S}^{(i)}\rangle = \frac{|m\rangle + \gamma_1 \, |\psi_{\rm S}^{(i)}\rangle}{\sqrt{1+\gamma_1^2}} \ , \tag{3.43}$$

[4] For a similarly non-geometric derivation of the action of Einstein gravity, see Ref. [142].

where $\gamma_1 \in \mathbb{R}_+$ is a dimensionless parameter that weights the relative probability amplitude for each "toy graviton" to be in the continuum rather than ground state. The total wave-function will be given by the symmetrised product of N such states,

$$|\Psi_N\rangle \simeq \frac{1}{N!} \sum_{\{\sigma_i\}}^{N} \left[\bigotimes_{i=1}^{N} |\Psi_{\rm S}^{(i)}\rangle \right] \ , \tag{3.44}$$

where the sum is over all the permutations $\{\sigma_i\}$ of the N excitations. Since the interaction is included into terms proportional to powers of γ_1, the spectral decomposition of this N-particle state can be obtained by defining the total Hamiltonian simply as the sum of N single-particle Hamiltonians,

$$\hat{H} = \bigoplus_{i=1}^{N} \hat{H}_i \ . \tag{3.45}$$

The corresponding eigenvector for the discrete ground state with $M = N\,m$ is given by

$$\hat{H}\,|M\rangle = M\,|M\rangle \ , \tag{3.46}$$

and the eigenvectors for the continuum by

$$\hat{H}\,|E\rangle = E\,|E\rangle \ . \tag{3.47}$$

The spectral coefficients are computed by projecting $|\Psi_{\rm N}\rangle$ on these eigenvectors.

3.2.1 Black holes with no hair

The highly idealised case in Eq. (3.39) admits precisely one mode, given by

$$k_{\rm c} = \frac{\pi}{R_{\rm H}} = \frac{\pi}{2\sqrt{N}\,\ell_{\rm p}} \ , \tag{3.48}$$

so that, on the surface of the BH, $\phi_{k_{\rm c}}(R_{\rm H}) \simeq j_0(k_{\rm c}\,R_{\rm H}) = 0$, and the scalar field vanishes outside of $r = R_{\rm H}$,

$$\psi_{\rm S}(r_i) = \langle\, r_i \mid k_{\rm c}\,\rangle = \begin{cases} \mathcal{N}_{\rm c}\, j_0(k_{\rm c} r_i) & \text{for } r < R_{\rm H} \\ \\ 0 & \text{for } r > R_{\rm H} \ , \end{cases} \tag{3.49}$$

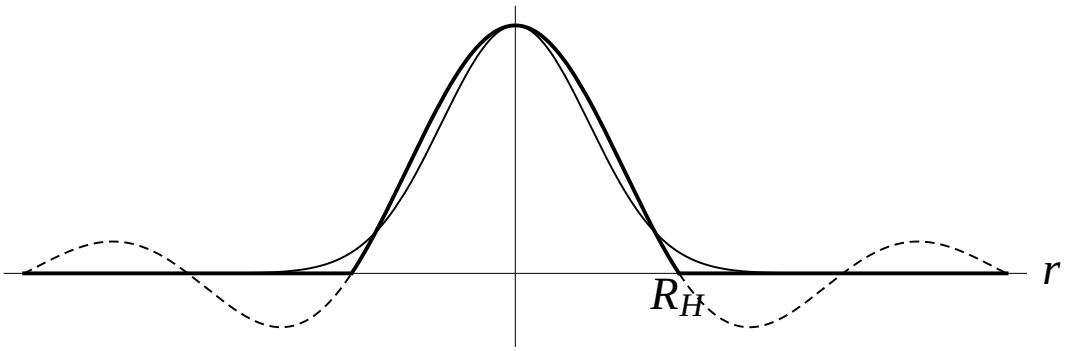

Figure 3.1: Scalar field mode of momentum number $k_{\rm c}$: ideal approximation in Eq. (3.49) (thick solid line) compared to exact $j_0(k_{\rm c}r)$ (dashed line). The thin solid line represents a Gaussian distribution of the kind considered in Ref. [77].

where $\mathcal{N}_{\rm c} = \sqrt{\pi/2\,R_{\rm H}^3}$ is a normalisation factor such that

$$4\,\pi\,\mathcal{N}_{\rm c}^2 \int_0^{R_{\rm H}} |j_0(k_{\rm c}r)|^2\,r^2\,{\rm d}r = 1\ . \tag{3.50}$$

This approximate mode is plotted in Fig. 3.1, and compared with a Gaussian distribution of the kind considered in Ref. [77].

It was noted before the end of Section 3.1.1 that a scalar field which vanishes everywhere outside $r = R_{\rm H}$ is inconsistent with the existence of an outer Newtonian potential, but one can still investigate the case for the sake of having a complete picture. A system of N such modes will be described by a wave-function which is the (totally symmetrised) product of $N \sim M^2$ equal modes and $\gamma_1 = 0$, that is

$$\Psi_{\rm N}(r_1, \ldots, r_N) = \frac{\mathcal{N}_{\rm c}^N}{N!} \sum_{\{\sigma_i\}} \prod_{i=1}^{N} j_0(k_{\rm c}r_i)\ . \tag{3.51}$$

This is clearly an eigenstate of the total Hamiltonian

$$\hat{H}\ |\Psi_{\rm N}\rangle = N\,\hbar\,k_{\rm c}\ |\Psi_{\rm N}\rangle = M\ |\Psi_{\rm N}\rangle\ \ , \tag{3.52}$$

and there exists only one non-vanishing coefficient in the spectral decomposition: $C(E) = 1$, for $E = N\,\hbar\,k_{\rm c} = M$, corresponding to a probability density for finding the horizon size between $r_{\rm H}$ and $r_{\rm H} + {\rm d}r_{\rm H}$

$$\begin{aligned} \mathcal{P}_{\rm H}(r_{\rm H}) &= 4\,\pi\,r_{\rm H}^2\ |\psi_{\rm H}(r_{\rm H})|^2 \\ &= \delta(r_{\rm H} - R_{\rm H})\ . \end{aligned} \tag{3.53}$$

This result, and the fact that all the excitations in the mode $k_{\rm c}$ are confined within the radius $R_{\rm H} \simeq \lambda_{\rm c}$, leads to the conclusion that the system is a BH,

$$\begin{aligned} P_{\rm BH} \;&\simeq\; 4\,\pi\,\mathcal{N}_{\rm c}^2 \int_0^\infty {\rm d}r_{\rm H}\,\delta(r_{\rm H}-R_{\rm H}) \int_0^{r_{\rm H}} |j_0(k_{\rm c}\,r)|^2\,r^2\,{\rm d}r \\ &=\; P_{\rm S}(r<R_{\rm H}) = 1\ . \end{aligned} \tag{3.54}$$

with the horizon located at its classical radius,

$$\langle\,\hat{r}_{\rm H}\,\rangle \equiv \langle\psi_{\rm H}|\,\hat{r}_{\rm H}\,|\psi_{\rm H}\rangle = R_{\rm H}\ , \tag{3.55}$$

and with absolutely negligible uncertainty

$$\Delta r_{\rm H}^2 \equiv \langle\psi_{\rm H}|\left(\hat{r}_{\rm H}^2 - R_{\rm H}^2\right)|\psi_{\rm H}\rangle \simeq 0\ . \tag{3.56}$$

The sharply vanishing uncertainty in $\langle\,\hat{r}_{\rm H}\,\rangle$ is an unphysical result, which is a consequence of considering the macroscopic BH as a pure quantum mechanical state built by superposing many wave-functions of the type (3.49). Also, a zero field at $r > R_{\rm H}$ cannot reproduce the Newtonian potential outside the BH, which clearly contradicts observations.

For a more realistic macroscopic BH (with $N \gg 1$), one therefore needs to consider the existence of more modes besides the ones with $k = k_{\rm c}$. In this case, the modes with $k = k_{\rm c}$ form a discrete spectrum (which comes from $k_{\rm c}$ being the minimum allowed momentum, in agreement with the idea of a BEC of gravitons), and must be treated separately. If modes with $k > k_{\rm c}$ exist, these would not be (marginally) trapped and could "leak out", thus representing a simple modelisation of the Hawking flux. They will form a continuous spectrum, which will lead to fuzziness in the horizon's location. The precise form of this part of the spectrum is however an open issue, and we will review several possibilities in the next sections.

3.2.2 Black hole with gaussian excited spectrum

Let us start assuming a continuous distribution in momentum space of each of the N scalar states given by half a Gaussian peaked around $k_{\rm c}$ (Fig. 3.2 displays a few modes above $k_{\rm c}$),

$$|\psi_{\rm S}^{(i)}\rangle = \mathcal{N}_\gamma \left(|k_{\rm c}\rangle + \gamma_1 \int_{k_{\rm c}}^\infty \frac{\sqrt{2}\,{\rm d}k_i}{\sqrt{\Delta_i\,\sqrt{\pi}}}\, e^{-\frac{\hbar^2(k_i-k_{\rm c})^2}{2\,\Delta_i^2}}\,|k_i\rangle \right)\ , \tag{3.57}$$

where $i = 1, \ldots, N$, the ket $|k\rangle$ denotes the eigenmode of eigenvalue k, and

$$\mathcal{N}_\gamma = \left(1+\gamma_1^2\right)^{-1/2} \tag{3.58}$$

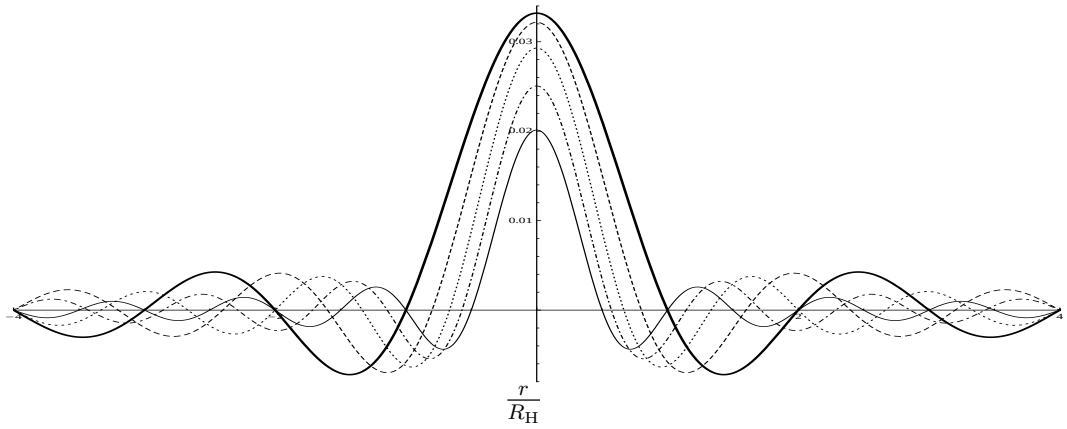

Figure 3.2: Modes of momentum number $k = k_{\rm c}$ (thick solid line), $k = (5/4)\,k_{\rm c}$ (dashed line), $k = (3/2)\,k_{\rm c}$ (dotted line), $k = (7/4)\,k_{\rm c}$ (dash-dotted line) and $k = 2\,k_{\rm c}$ (thin solid line). The relative weight is determined according to Eq. (3.57).

is a normalisation factor. Also, the width of the gaussians is $\Delta_i = m \simeq M/N \simeq m_{\rm p}/\sqrt{N}$, as calculated from the typical mode spatial size $k_{\rm c}^{-1} \sim \sqrt{N}\,\ell_{\rm p}$, and is the same for all particles. This is, of course, a necessary simplification needed in order to simplify the calculations. (More generally, one could assume a different width for each mode k_i.) Since $m = \hbar\,k_{\rm c}$ and $E_i = \hbar\,k_i$, one can also write

$$|\psi_{\rm S}^{(i)}\rangle = \mathcal{N}_\gamma \left(|m\rangle + \gamma_1 \int_m^\infty \frac{\sqrt{2}\,{\rm d}E_i}{\sqrt{m\,\sqrt{\pi}}}\, e^{-\frac{(E_i-m)^2}{2\,m^2}}\, |E_i\rangle \right) \ . \tag{3.59}$$

The total wave-function will be given by the symmetrised product of N

such states, and can be written by grouping equal powers of γ_1 as follows

$$
\begin{aligned}
|\Psi_{\rm N}\rangle \;\simeq\; & \frac{1}{N!}\sum_{\{\sigma_i\}}^{N}\left[\bigotimes_{i=1}^{N}|m\rangle\right] \\
& +\frac{\gamma_1}{N!}\left(\frac{2}{m\sqrt{\pi}}\right)^{1/2}\sum_{\{\sigma_i\}}^{N}\left[\bigotimes_{i=2}^{N}|m\rangle\otimes\int_m^\infty {\rm d}E_1\, e^{-\frac{(E_1-m)^2}{2\,m^2}}\,|E_1\rangle\right] \\
& +\frac{\gamma_1^2}{N!}\left(\frac{2}{m\sqrt{\pi}}\right)\sum_{\{\sigma_i\}}^{N}\left[\bigotimes_{i=3}^{N}|m\rangle\otimes\int_m^\infty {\rm d}E_1\, e^{-\frac{(E_1-m)^2}{2\,m^2}}\,|E_1\rangle\otimes\int_m^\infty {\rm d}E_2\, e^{-\frac{(E_2-m)^2}{2\,m^2}}\,|E_2\rangle\right] \\
& +\ldots \\
& +\frac{\gamma_1^J}{N!}\left(\frac{2}{m\sqrt{\pi}}\right)^{J/2}\sum_{\{\sigma_i\}}^{N}\left[\bigotimes_{i=J+1}^{N}|m\rangle\bigotimes_{j=1}^{J}\int_m^\infty {\rm d}E_j\, e^{-\frac{(E_j-m)^2}{2\,m^2}}\,|E_j\rangle\right] \\
& +\ldots \\
& +\frac{\gamma_1^N}{N!}\left(\frac{2}{m\sqrt{\pi}}\right)^{N/2}\sum_{\{\sigma_i\}}^{N}\left[\bigotimes_{i=1}^{N}\int_m^\infty {\rm d}E_i\, e^{-\frac{(E_i-m)^2}{2\,m^2}}\,|E_i\rangle\right]\;, \qquad (3.60)
\end{aligned}
$$

where the power of γ_1 clearly equals the number of bosons in an "excited" mode with $k > k_{\rm c}$. One can then identify two regimes, depending on the value of γ_1 (for further details, readers are directed to the Appendix A in Ref. [18]).

For $\gamma_1 \ll 1$, to leading order in γ_1, the spectral coefficient for $E \geq M$ is given by the term corresponding to just one particle in the continuum,

$$
C(E \geq M) \simeq \mathcal{N}_\gamma\left[\delta_{E,M}+\gamma_1\left(\frac{2}{m\sqrt{\pi}}\right)^{1/2} e^{-\frac{(E-M)^2}{2\,m^2}}\right]\;, \qquad (3.61)
$$

where $\delta_{A,B}$ is a Kronecker delta for the discrete part of the spectrum. The width $m \sim m_{\rm p}/\sqrt{N}$ is the typical energy of Hawking quanta emitted by a BH of mass $M \simeq \sqrt{N}\,m_{\rm p}$. The expectation value of the energy to next-to-leading order for large N and small γ_1 is

$$
\begin{aligned}
\langle\, E\,\rangle \;&\simeq\; \mathcal{N}_\gamma^2\left(M+\int_M^\infty E\,C^2(E)\,{\rm d}E\right) \\
&\simeq\; \sqrt{N}\,m_{\rm p}\left(1+\frac{\gamma_1^2/\sqrt{\pi}}{1+\gamma_1^2}\,\frac{1}{N}\right) \\
&\simeq\; \sqrt{N}\,m_{\rm p}\left(1+\frac{\gamma_1^2}{\sqrt{\pi}\,N}\right)\;, \qquad (3.62)
\end{aligned}
$$

and its uncertainty

$$\Delta E = \sqrt{\langle\, E^2 \,\rangle - \langle\, E \,\rangle^2} \simeq \frac{\gamma_1\, m_{\rm p}}{\sqrt{2\, N}} \ . \tag{3.63}$$

One can also calculate the ratio

$$\frac{\Delta E}{\langle\, E \,\rangle} \simeq \frac{\gamma_1}{\sqrt{2}\, N} \ , \tag{3.64}$$

where only the leading order in the large N expansion was kept. From the expression of the Schwarzschild radius $r_{\rm H} = 2\,\ell_{\rm p}\, E/m_{\rm p}$, one easily finds $\langle\, \hat{r}_{\rm H} \,\rangle \simeq R_{\rm H}$, with $R_{\rm H}$ given in Eq. (3.38), and

$$\frac{\Delta r_{\rm H}}{\langle\, \hat{r}_{\rm H} \,\rangle} \sim \frac{1}{N} \ , \tag{3.65}$$

which vanishes rapidly for large N. This case describes a macroscopic BEC BH with (very) little quantum hair, in agreement with Refs. [73], thus overcoming the problem of the large fluctuations $\Delta r_{\rm H} \sim \langle\, \hat{r}_{\rm H} \,\rangle$ which appear in the case of a single massive particle.

This "hair" is expected to represent the Hawking radiation field, and the connection with the thermal Hawking radiation will become more clear in Section 3.2.4, where a different form of the continuous spectrum will be employed

3.2.3 Quantum hair with no black hole

When $\gamma_1 \gtrsim 1$ and $N \gg 1$, all of the N particles are in the continuum, while the ground state $\phi_{k_{\rm c}}$ is totally depleted. The coefficient γ_1^N and any overall factors can be omitted in this case, and one finds

$$C(E \geq M) \simeq \int_m^\infty {\rm d}E_1 \cdots \int_m^\infty {\rm d}E_N \, \exp\left\{ -\sum_{i=1}^N \frac{(E_i - m)^2}{2\, m^2} \right\} \, \delta\left(E - \sum_{i=1}^N E_i \right) \tag{3.66}$$

along with $C(E < M) \simeq 0$. Note that, in this case the mass $M = N\, m$ still represents the minimum energy of the system corresponding to the "ideal" BH with all the N particles in the ground state $|k_{\rm c}\rangle$. For $N = M/m \gg 1$, this spectral function is estimated analytically in Ref. [18], and is given by

$$C(E \geq M) \simeq \sqrt{\frac{2}{\pi\, m^3}}\, (E - M)\, e^{-\frac{(E-M)^2}{4\, m^2}} \ , \tag{3.67}$$

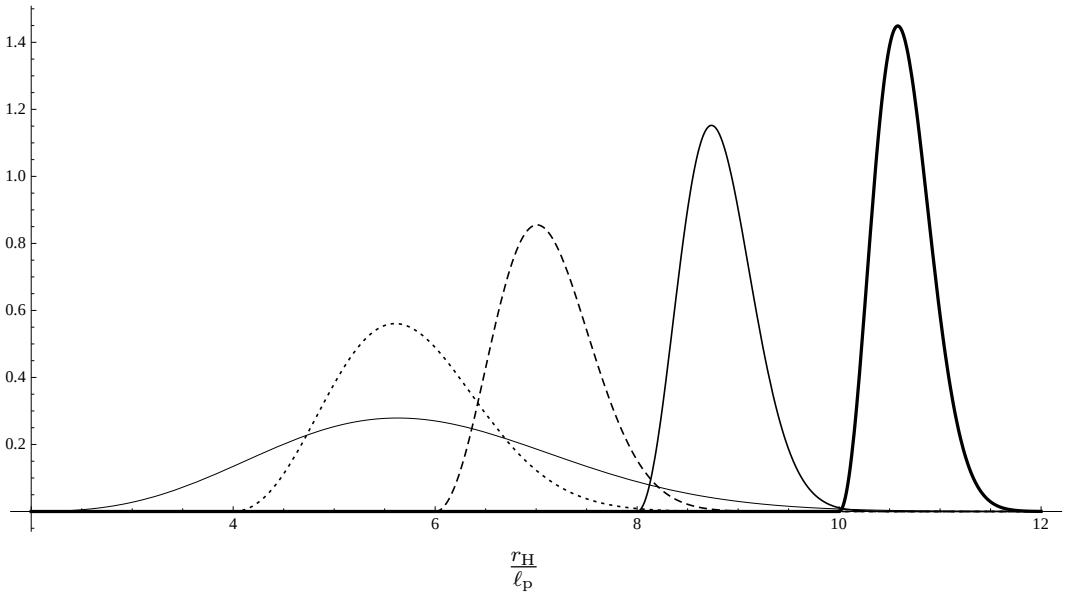

Figure 3.3: Probability density for the gravitational radius $r_{\rm H}$ for $N = 1$ ($R_{\rm H} = 2\,\ell_{\rm p}$; thin solid line), $N = 4$ ($R_{\rm H} = 4\,\ell_{\rm p}$; dotted line), $N = 9$ ($R_{\rm H} = 6\,\ell_{\rm p}$; dashed line), $N = 16$ ($R_{\rm H} = 8\,\ell_{\rm p}$; solid line) and $N = 25$ ($R_{\rm H} = 10\,\ell_{\rm p}$; thick solid line). The curves clearly become narrower the larger N.

which is peaked slightly above $E \simeq M = N\,m$, with a width $\sqrt{2}\,\Delta_i \sim m$, so that the (normalised) expectation value

$$\langle\, E \,\rangle \simeq \int_M^\infty E\, C^2(E)\, {\rm d}E = M + 2\,\sqrt{\frac{2}{\pi}}\, m \ , \tag{3.68}$$

consistently for a system built out of continuous modes. To be in the continuous part of the spectrum the energy of these modes must be (slightly) larger than m. For $N \gg 1$, however, $\langle\, E \,\rangle = M\,[1 + \mathcal{O}(N^{-1})]$, and the energy quickly approaches the minimum value M. This is also confirmed by the uncertainty

$$\Delta E \simeq \sqrt{\frac{3\,\pi - 8}{\pi}}\, m \ , \tag{3.69}$$

or $\Delta E \sim N^{-1/2}$.

The corresponding horizon wave-function is obtained by using $r_{\rm H} = 2\,\ell_{\rm p}\,E/m_{\rm p}$, and is approximately given by

$$\psi_{\rm H}(r_{\rm H} \geq 2\,\sqrt{N}\,\ell_{\rm p}) \simeq \left(r_{\rm H} - 2\,\sqrt{N}\,\ell_{\rm p}\right)\, e^{-\frac{\left(r_{\rm H} - 2\,\sqrt{N}\,\ell_{\rm p}\right)^2}{16\,\ell_{\rm p}^2/N}} \ , \tag{3.70}$$

and $\psi_{\rm H}(r_{\rm H} < 2\sqrt{N}\,\ell_{\rm p}) \simeq 0$. The probability density of finding the gravitational radius between $r_{\rm H}$ and $r_{\rm H} + {\rm d}r_{\rm H}$ is plotted in Fig. 3.3 for different values of N. The plot shows that for $N \sim 1$, the uncertainty in the size of the gravitational radius is large, but it decreases very fast with increasing N. The expectation value

$$\langle\, \hat{r}_{\rm H} \,\rangle \simeq 2\sqrt{N}\,\ell_{\rm p}\left(1 + \sqrt{\frac{2}{\pi}}\,\frac{2}{N}\right) = R_{\rm H}\left[1 + \mathcal{O}(N^{-1})\right] \ , \tag{3.71}$$

approaches (from above) the horizon radius of the ideal BH, $R_{\rm H} = 2\sqrt{N}\,\ell_{\rm p}$, for large N. Since $\langle\, \hat{r}_{\rm H} \,\rangle > R_{\rm H}$, one can safely view it as a trapping surface, whose uncertainty is proportional to the energy $m = m_{\rm p}/\sqrt{N}$, that is

$$\frac{\Delta r_{\rm H}}{\langle\, \hat{r}_{\rm H} \,\rangle} = \frac{\sqrt{\langle\, \hat{r}_{\rm H}^2 - \langle\, \hat{r}_{\rm H} \,\rangle^2 \,\rangle}}{\langle\, \hat{r}_{\rm H} \,\rangle} \simeq \frac{1}{N} \ , \tag{3.72}$$

which vanishes as fast as in the previous case for large N. This is also expected in a proper semiclassical regime [73].

It needs to be emphasised that cases with $\gamma_1 \not\ll 1$ do not describe a BEC BH, because most or all of the gravitons are in some excited mode with $k > k_{\rm c}$. However, one can think that these states may play a role either at the threshold of BH formation (before the gravitons condense into the ground state $|k_{\rm c}\rangle$ and form a BEC) or near the end of BH evaporation.

3.2.4 BEC with thermal quantum hair

In Section 3.2.2 it was shown that, for $\gamma_1 \ll 1$, the quantum state of N scalars is dominated by the configurations with just one boson in the continuum of excited states, while the remaining $N-1$ gravitons form the BEC. A Gaussian distribution was used to describe the continuous part of the spectrum, and it was found that the spectral function has a typical width of the order of the Hawking temperature,

$$T_{\rm H} = \frac{m_{\rm p}^2}{4\,\pi\,M} \simeq \frac{m_{\rm p}}{\sqrt{N}} \ , \tag{3.73}$$

or $T_{\rm H} \simeq m$. It is thus logical to ask what happens if the Gaussian distribution in Eq. (3.57) is replaced by a thermal spectrum at the temperature $T_{\rm H}$.

We hence start with a Planckian distribution [5] at the temperature $T_{\rm H} = m$

[5] Using a Boltzmann distribution for $N = 1$ is also possible. However, for $N > 1$, it is affected by infrared divergences.

for the continuum part, namely

$$|\psi_{\rm S}^{(i)}\rangle \;=\; \frac{\mathcal{N}_{\rm H}}{m^{3/2}}\int_m^\infty {\rm d}\omega_i\,\frac{(\omega_i-m)}{\exp\left\{\frac{\omega_i-m}{m}\right\}-1}\,|\omega_i\rangle$$
$$\equiv\; \mathcal{N}_{\rm H}\int_0^\infty {\rm d}\mathcal{E}_i\,G(\mathcal{E}_i)\;|\mathcal{E}_i\rangle\;\;, \tag{3.74}$$

where $\mathcal{N}_{\rm H}=\sqrt{3}/\sqrt{\pi^2-6\,\zeta(3)}\simeq 1.06$, the dimensionless variables

$$\mathcal{E}_i=\frac{\omega_i-m}{m}\;, \tag{3.75}$$

and the states $|\mathcal{E}_i\rangle=m^{1/2}\;|\omega_i\rangle$ were introduced, such that the identity in the continuum can be written as

$$\int_0^\infty {\rm d}\mathcal{E}_i\,|\mathcal{E}_i\rangle\,\langle\mathcal{E}_i|=\int_m^\infty {\rm d}\omega_i\,|\omega_i\rangle\,\langle\omega_i|=\mathbb{I}\;. \tag{3.76}$$

The "thermal hair" is again assumed to appear due to the scatterings between the scalars inside the BEC, therefore the parameter γ_1 should be related to the toy gravitons self-coupling α. In this exercise it is however kept as a free variable, so that one could relate it a posteriori to known features of the Hawking radiation.

Assuming that $\gamma_1\neq 0$ yields a good enough approximation of the leading effects due to these bosons self-interactions, the BEC can me treated as made of otherwise free scalars. The total wave-function of the system of N such bosons can again be written by collecting powers of γ_1,

$$\begin{aligned}
|\Psi_N\rangle \;\simeq\; & \frac{1}{N!}\sum_{\{\sigma_i\}}^N\left[\bigotimes_{i=1}^N|m\rangle\right]\\
&+\gamma_1\,\frac{\mathcal{N}_{\rm H}}{N!}\sum_{\{\sigma_i\}}^N\left[\bigotimes_{i=2}^N|m\rangle\otimes\int_0^\infty{\rm d}\mathcal{E}_1\,G(\mathcal{E}_1)\,|\mathcal{E}_1\rangle\right]\\
&+\gamma_1^2\,\frac{\mathcal{N}_{\rm H}^2}{N!}\sum_{\{\sigma_i\}}^N\left[\bigotimes_{i=3}^N|m\rangle\otimes\int_0^\infty{\rm d}\mathcal{E}_1\,G(\mathcal{E}_1)\,|\mathcal{E}_1\rangle\otimes\int_0^\infty{\rm d}\mathcal{E}_2\,G(\mathcal{E}_2)\,|\mathcal{E}_2\rangle\right]\\
&+\ldots\\
&+\gamma_1^J\,\frac{\mathcal{N}_{\rm H}^J}{N!}\sum_{\{\sigma_i\}}^N\left[\bigotimes_{i=J+1}^N|m\rangle\bigotimes_{j=1}^J\int_0^\infty{\rm d}\mathcal{E}_j\,G(\mathcal{E}_j)\,|\mathcal{E}_j\rangle\right]\\
&+\ldots\\
&+\gamma_1^N\,\frac{\mathcal{N}_{\rm H}^N}{N!}\sum_{\{\sigma_i\}}^N\left[\bigotimes_{i=1}^N\int_0^\infty{\rm d}\mathcal{E}_i\,G(\mathcal{E}_i)\,|\mathcal{E}_i\rangle\right]\;,
\end{aligned} \tag{3.77}$$

where the overall normalisation constant of $1/(1+\gamma_1^2)^{N/2}$ was omitted for the sake of simplicity.

For $E = M = N\,m$, on neglecting an overall normalisation factor, one obviously has

$$C(M) \simeq \frac{1}{N!}\,\langle M| \sum_{\{\sigma_i\}}^{N} \left[\bigotimes_{i=1}^{N} |m\rangle \right] = 1 \ . \tag{3.78}$$

For energies above the ground state, $E > M = N\,m$, the spectral coefficients are given by

$$C(E > M) = \langle\, E \mid \Psi_N \,\rangle \ , \tag{3.79}$$

and using the dimensionless variables (3.75), along with

$$\mathcal{E} = \frac{E - M}{m} \ , \tag{3.80}$$

one finds

$$\begin{aligned} C(\mathcal{E} > 0) \ &\simeq \ \gamma_1\,\mathcal{N}_{\rm H}\,G(\mathcal{E}) \\ &\quad +\gamma_1^2\,\mathcal{N}_{\rm H}^2 \int_0^\infty G(\mathcal{E}_1)\,G(\mathcal{E}-\mathcal{E}_1)\,{\rm d}\mathcal{E}_1 \\ &\quad +\ldots \\ &\quad +\gamma_1^N\,\mathcal{N}_{\rm H}^N \int_0^\infty G(\mathcal{E}_1)\,{\rm d}\mathcal{E}_1 \times \cdots \times \int_0^\infty G(\mathcal{E}_N)\,{\rm d}\mathcal{E}_N\,\delta\!\left(\mathcal{E} - \sum_{i=1}^{N} \mathcal{E}_i\right) \\ &\equiv \ \sum_{n=1}^{N} \gamma_1^n\,C_n(\mathcal{E}) \ , \end{aligned} \tag{3.81}$$

where all the coefficients in this expression can be written as

$$C_n = \mathcal{N}_{\rm H}^n \int_0^\infty G(\mathcal{E}_1)\,{\rm d}\mathcal{E}_1 \times \cdots \times \int_0^\infty G(\mathcal{E}_{n-1})\,{\rm d}\mathcal{E}_{n-1}\,G\!\left(\mathcal{E} - \sum_{i=1}^{n-1} \mathcal{E}_i\right) \ . \tag{3.82}$$

Each integral in $\mathcal{E}_i$ is peaked around $\mathcal{E}_i = 0$, so that one can approximate

$$G\!\left(\mathcal{E} - \sum_{i=1}^{n-1} \mathcal{E}_i\right) = \frac{\mathcal{E} - \sum_{i=1}^{n-1} \mathcal{E}_i}{\exp\left\{\mathcal{E} - \sum_{i=1}^{n-1} \mathcal{E}_i\right\} - 1} \simeq \frac{\mathcal{E}}{\exp\{\mathcal{E}\} - 1} = G(\mathcal{E}) \ , \tag{3.83}$$

for $2 \leq n \leq N$. Therefore

$$C_n \ \simeq \ \mathcal{N}_{\rm H} \left(\mathcal{N}_{\rm H}\,\frac{\pi^2}{6}\right)^{n-1} G(\mathcal{E}) = (1.75)^{n-1}\,\mathcal{N}_{\rm H}\,G(\mathcal{E}) \ . \tag{3.84}$$

Upon rescaling

$$\gamma \simeq 0.57 \sum_{j=1}^{N} (1.75\,\gamma_1)^j \ , \tag{3.85}$$

and switching back to dimensionful variables, one finds

$$C(E > M) \ \simeq \ \gamma \, \frac{\mathcal{N}_{\rm H}}{\sqrt{m}} \, \frac{(E-M)/m}{\exp\{(E-M)/m\} - 1} \ . \tag{3.86}$$

This approximation was checked numerically to work extremely well for a wide range of N. The details of the numerical analysis can be found in the Appendix B.

The result in Eq. (3.86) means that one can describe the quantum state of the N-particle system as the (normalised) single-particle state

$$|\Psi_{\rm S}\rangle \simeq \frac{|M\rangle + \gamma\,|\psi\rangle}{\sqrt{1+\gamma^2}} \ , \tag{3.87}$$

where

$$|\psi\rangle = \frac{\mathcal{N}_{\rm H}}{\sqrt{m}} \frac{(E-M)/m}{\exp\{(E-M)/m\} - 1} \, |E\rangle \ . \tag{3.88}$$

Therefore, the BEC BH effectively looks like one particle of very large mass $M = N\,m$ in a superposition of states with "Planckian hair". To have most of the toy gravitons in the ground state, all that needs to be assumed is $\gamma \ll 1$. However, nothing prevents one from also considering the above approximate wave-function for $\gamma \simeq 1$ or even larger.

Partition function and entropy

It is now straightforward to employ the effective wave-function (3.87) to compute expectations values, such as

$$\begin{aligned} \langle\, \hat{H} \,\rangle \ &= \ \frac{1}{1+\gamma^2} \left\{ M + \gamma^2 \, \frac{\mathcal{N}_{\rm H}^2}{m} \int_M^\infty \left[\frac{(E-M)/m}{\exp\{(E-M)/m\} - 1} \right]^2 E \, {\rm d}E \right\} \\ &= \ m_{\rm p} \sqrt{N} \left[1 + \gamma^2 \, \frac{\mathcal{N}_{\rm H}^2}{N} \left(6\zeta(3) - \frac{\pi^4}{15} \right) \right] + O(\gamma^4) \ , \end{aligned} \tag{3.89}$$

where the higher powers of the parameter γ were discarded and the approximation $(1+\gamma^2)^{-1} \simeq 1 - \gamma^2$ was used.

Since

$$\begin{aligned}\langle\,\hat{H}^2\,\rangle &= \frac{1}{1+\gamma^2}\left\{M^2+\gamma^2\,\frac{\mathcal{N}_{\rm H}^2}{m}\int_M^\infty\left[\frac{(E-M)/m}{\exp\{(E-M)/m\}-1}\right]^2\,E^2\,{\rm d}E\right\}\\ &= m_{\rm p}^2\,N\left[1+2\,\frac{\gamma^2}{N}\,\mathcal{N}_{\rm H}^2\,\left(6\,\zeta(3)-\frac{\pi^4}{15}\right)\right.\\ &\qquad\left.+\frac{4}{15}\,\frac{\gamma^2}{N^2}\,\mathcal{N}_{\rm H}^2\,\left(\pi^4-90\,\zeta(5)\right)\right]+O(\gamma^4)\;, \qquad (3.90)\end{aligned}$$

one can easily obtain the uncertainty

$$\begin{aligned}\Delta E=\sqrt{\langle\,\hat{H}^2\,\rangle-\langle\,\hat{H}\,\rangle^2} &= \gamma\,\frac{m_{\rm p}}{\sqrt{N}}\,\mathcal{N}_{\rm H}\sqrt{\frac{4}{15}\,(\pi^4-90\zeta(5))-\mathcal{N}_{\rm H}^2\left(6\zeta(3)-\frac{\pi^4}{15}\right)^2}+O(\gamma^2)\\ &\simeq 0.76\,\gamma\,\frac{m_{\rm p}}{\sqrt{N}}\;. \qquad (3.91)\end{aligned}$$

In the large N limit, one recovers the result [18]

$$\frac{\Delta E}{\langle\,\hat{H}\,\rangle}\sim\frac{\gamma}{N}+O(\gamma^2)\;. \qquad (3.92)$$

From a thermodynamical point of view, Eq. (3.89) can be used to estimate the partition function of the system according to

$$\langle\,\hat{H}\,\rangle=-\frac{\partial}{\partial\beta}\log Z(\beta)\;, \qquad (3.93)$$

where $\beta=T_{\rm H}^{-1}=m^{-1}\simeq\sqrt{N}/m_{\rm p}$. One then finds

$$\begin{aligned}\langle\,\hat{H}(\beta)\,\rangle &= m_{\rm p}^2\,\beta\left(1+\frac{\mathcal{K}\,\gamma^2}{m_{\rm p}^2\,\beta^2}\right)\\ &= \frac{\partial}{\partial\beta}\left[\frac{1}{2}\,m_{\rm p}^2\,\beta^2+\mathcal{K}\,\gamma^2\,\log(k\,\beta)\right]\;, \qquad (3.94)\end{aligned}$$

where $\mathcal{K}=\mathcal{N}_{\rm H}^2\,[6\zeta(3)-\pi^4/15]\simeq 0.81$, and k is an integration constant with dimensions of mass. It is then straightforward to obtain

$$\log Z(\beta)=-\frac{1}{2}\,m_{\rm p}^2\,\beta^2-\mathcal{K}\,\gamma^2\,\log(\beta\,k)\;, \qquad (3.95)$$

and, for $k=m_{\rm p}$, one finds

$$Z(\beta)=(m_{\rm p}\,\beta)^{-\mathcal{K}\gamma^2}\;e^{-\frac{1}{2}\,m_{\rm p}^2\beta^2}\;, \qquad (3.96)$$

which contains two factors. One of the factors has the form $1/\beta = T_{\rm H}$ to some power, which looks like the thermal wave-length of a particle, and is due to the contribution of the excited modes to the energy spectrum. This is consistent with these modes propagating freely, since an external potential was not considered in the model [6]. The exponential damping factor appears because of the bound states which are localised within the classical Schwarzschild radius $R_{\rm H}$.

The statistical canonical entropy can next be obtained from

$$S(\beta) = \beta^2 \, \frac{\partial F(\beta)}{\partial \beta} \ , \tag{3.97}$$

where $F(\beta) = -(1/\beta) \, \log Z$ is the Helmoltz free energy . It is straightforward to get

$$S(\beta) = \frac{1}{2} \, m_{\rm p}^2 \, \beta^2 - \mathcal{K} \, \gamma^2 \log(m_{\rm p} \, \beta) + \mathcal{K} \, \gamma^2 \ , \tag{3.98}$$

which is the usual Bekenstein-Hawking formula [132] plus a logharitmic correction. In fact, $\beta \simeq m^{-1}$ can be written as a function of the Schwarzschild radius,

$$\beta = \frac{R_{\rm H}}{2 \, \ell_{\rm p} \, m_{\rm p}} \ , \tag{3.99}$$

the constant can be rescaled and one can define the area of the horizon as $A_{\rm H} = 4 \, \pi \, R_{\rm H}^2$, hence yielding

$$S = \frac{A_{\rm H}}{4 \, \ell_{\rm p}^2} - \frac{\mathcal{K}}{2} \, \gamma^2 \, \log\left(\frac{A_{\rm H}}{16 \, \pi \, \ell_{\rm p}^2} \right) \ . \tag{3.100}$$

The expression of the entropy depends on the "collective" parameter γ defined in Eq. (3.85), rather than on the single-particle γ_1 which gives the probability for each constituent to be a Hawking mode and which is determined by the details of the scatterings that occur inside the BEC. Therefore, even if the Hawking radiation were detectable, the details of the interactions inside the BEC would hardly show directly. Still, $\gamma_1 = 0$ also implies $\gamma = 0$. The logarithmic correction switches off if the scatterings inside the BEC are negligible (and the Hawking radiation is absent). It needs to be emphasised that in this corpuscular model the number N of bosons is conserved, and this happens because both the BH and its Hawking radiation are made of the same kind of particles.

[6] In other words, the grey-body factors for bosonic Hawking quanta are approximated by one.

The specific heat is given by

$$\begin{aligned} C_V &= \frac{\partial \langle \hat{H} \rangle}{\partial T} \\ &\simeq -m_{\rm p}^2 \beta^2 + \mathcal{K} \gamma^2 \ , \end{aligned} \tag{3.101}$$

which is negative for small γ and large β (or, equivalently, large N), in agreement with the usual properties of the Hawking radiation, but vanishes for $\beta \simeq \gamma/m_{\rm p}$, that is for $N_c \sim \gamma^2$. Assuming for simplicity $1.75\,\gamma_1 \sim 1$, so that $\gamma \sim N$ from Eq. (3.85), one finds that the specific heat vanishes for $N_c \sim 1$. As one would naively expect the Hawking radiation switches off when there are no more particles to emit. This is in agreement with the microcanonical picture of the Hawking evaporation and with the estimate of the backreaction from the next section. One can also find more details on the microcanonical picture in Refs. [143] and references therein.

Horizon wave-function and backreaction

It is interesting to compute the HWF and investigate the existence of a trapping surface in this case. The main result in Ref. [18], also presented in the previous sections, is that the quantum N-particle states considered shows a horizon of size very close to the expected classical value $R_{\rm H}$, with quantum fluctuations that die out for increasing N, as one expects in the context of semiclassical gravity,

$$\langle \hat{r}_{\rm H} \rangle \simeq R_{\rm H} + O(N^{-1/2}) \ , \tag{3.102}$$

The horizon wave function can be written using the spectral coefficients (3.86) as

$$|\Psi_{\rm H}\rangle = \frac{|R_{\rm H}\rangle + \gamma\,|\psi_{\rm H}\rangle}{\sqrt{1+\gamma^2}} \ . \tag{3.103}$$

The state $|R_{\rm H}\rangle$ defined so that

$$\langle R_{\rm H}|\,\hat{r}_{\rm H}\,|R_{\rm H}\rangle = R_{\rm H} \ , \tag{3.104}$$

represents the discrete part of the spectrum and the states

$$\psi_{\rm H}(r_{\rm H} > R_{\rm H}) \equiv \langle\, r_{\rm H} \mid \psi_{\rm H} \,\rangle = \mathcal{N}_{\rm H} \sqrt{\frac{N}{4\,\pi\,R_{\rm H}^3}}\, \frac{(r_{\rm H}-R_{\rm H})/(2\,\ell_{\rm p}\,m/m_{\rm p})}{\exp\left\{\frac{r_{\rm H}-R_{\rm H}}{2\,\ell_{\rm p}\,m/m_{\rm p}}\right\}-1} \tag{3.105}$$

are related to the excited Hawking modes. As usual $\Psi(r_{\rm H} \leq R_{\rm H}) \simeq 0$ and the normalization is fixed by the scalar product (2.10). The expectation value of the gravitational radius is found to be

$$\begin{aligned} \langle\, \hat{r}_{\rm H} \,\rangle \;&=\; 4\pi \int_{R_{\rm H}}^{\infty} |\Psi_{\rm H}(r_{\rm H})|^2 \; r_{\rm H}^3 \, {\rm d}r_{\rm H} \\ &=\; R_{\rm H} \left[1 + \frac{3\,\gamma^2}{N}\, \mathcal{N}_{\rm H}^2 \left(6\,\zeta(3) - \frac{\pi^4}{15} \right) \right] + O(\gamma^4) \;, \end{aligned} \tag{3.106}$$

in which $R_{\rm H}$ is given by Eq. (3.9). We thus see that

$$\langle\, \hat{r}_{\rm H} \,\rangle - R_{\rm H} = 3\,\gamma^2\, \frac{R_{\rm H}}{N} + O\left(\frac{1}{N^2} \right) \;. \tag{3.107}$$

From

$$\langle\, \hat{r}_{\rm H}^2 \,\rangle = R_{\rm H}^2 \left[1 + 4\,\gamma^2\, \mathcal{N}_{\rm H}^2 \left(6\zeta(3) - \frac{\pi^4}{15} \right) \frac{1}{N} \right] + O\left(\frac{1}{N^2} \right) \;, \tag{3.108}$$

one finds

$$\Delta r_{\rm H} = R_{\rm H}\, \frac{\gamma\, \mathcal{N}_{\rm H}}{\sqrt{N}} \sqrt{2 \left(6\zeta(3) - \frac{\pi^4}{15} \right)} + O\left(\frac{1}{N^2} \right) \tag{3.109}$$

and, omitting a factor of order one,

$$\frac{\Delta r_{\rm H}}{\langle\, \hat{r}_{\rm H} \,\rangle} \sim \frac{\gamma}{N} + O(\gamma^2) \;, \tag{3.110}$$

which is the same as the result obtained in Section 3.2.2 (and also Ref. [18]).

Note that $\langle\, \hat{r}_{\rm H} \,\rangle > R_{\rm H}$, even if only by a small amount for large N, which is in agreement with the Hawking quanta adding a contribution to the gravitational radius. The toy gravitons are therefore bound within a sphere of radius slightly larger than the pure BEC value $R_{\rm H}$. This should make the typical energy of the reciprocal $2 \to 2$ scatterings a little smaller, resulting in a slightly smaller depletion rate

$$\begin{aligned} \Gamma \;&\sim\; \frac{1}{\langle\, \hat{r}_{\rm H} \,\rangle} \\ &\simeq\; \frac{1}{\sqrt{N}\, \ell_{\rm p}} \left[1 - \frac{3\,\gamma^2}{N}\, \mathcal{N}_{\rm H}^2 \left(6\,\zeta(3) - \frac{\pi^4}{15} \right) \right] \;. \end{aligned} \tag{3.111}$$

Assuming the above relation still works for small N, the flux would become zero for a number of quanta equal to

$$\begin{aligned} N_c \;&\simeq\; 3\,\gamma^2\, \mathcal{N}_{\rm H}^2 \left(6\,\zeta(3) - \frac{\pi^4}{15} \right) \\ &\simeq\; 2.4\,\gamma^2 \;. \end{aligned} \tag{3.112}$$

Recalling Eq. (3.85), and assuming $1.75\,\gamma_1 \lesssim 1$, so that $\gamma \lesssim N$, one obtains $N_c \gtrsim 1$, which is the same as the flux vanishing for a finite number of constituents. While the above approximations might not hold for small N values, this result was also obtained in the microcanonical description of the Hawking radiation: the emitted flux vanishes for vanishingly small BH mass [143]. This is also in agreement with the thermodynamical analysis from Section 3.2.4, and the vanishing of the specific heat for $N = N_c \sim 1$. However, N_c depends on the collective parameter γ, which is directly related with the single-particle γ_1 for small N.

Chapter 4

Conclusions

Since Schwarzschild solved Einstein's field equations and BHs made their entrance in the scenario of contemporary physics, it was evident that they would have been the main characters in the analogy between large gravitational objects and the geometrical structure of space-time, while bestowing Newtonian gravity with very accurate corrections. When carried to the the Planck scale, though, GR breaks down and fails at giving a consistent description of the laws of nature. Therefore, in consideration of the more reliable explanation of physics given by QM than the one given by classical means, it is unavoidable to seek a theory which gives a feasible quantisation scheme of the gravitational interaction, in order to improve our comprehension of the mechanisms ruling the universe.

In this thesis we presented the HQM and the corpuscular BH model, with its geometrical properties coming from an effective point of view. They are quite powerful tools, which give the standard features of a quantum mechanical object to the gravitational radius.

The HQM is best explained by describing a spherically symmetric massive particle with a Gaussian wave-function, which sounds as a reasonable design for massive sources representing potential BHs around the Planck scale, at least in first approximation. One then finds that a neutral particle has a strong probability to lie inside its own trapped surface (that is to say $P_{\rm BH} \simeq 1$), when the width of the Gaussian ℓ is of the same order of the scale at which quantum gravitational effects are relevant, $\ell \sim \ell_{\rm p}$. Of course, this is the same to say $m \sim m_{\rm p}$. In addition to that, this set-up naturally allows for a GUP and a minimum resolvable length, by linearly combining the characteristic uncertainty in the horizon's size with the usual one on the spatial extension of the quantum wave-packet. This concept is straightforwardly exemplified with corrections to the Hawking decay rate.

This procedure is also applicable to space-times, whose horizons' struc-

ture is more involved, like the Reissner-Nordström metric (Section 2.3.2). When the charge-to-mass ratio $\epsilon < 1$, it follows that for a significantly large interval of masses the outer horizon has a strong probability to exist, and thus the massive particle is a BH, while the inner one has a negligible chance to form. This phenomenological implication stems straightforwardly from the quantum properties of the underlying geometry, albeit being a counter-intuitive argument in a purely classical description. Moreover, this formalism allows an analytical extension to the over-charged regime $\epsilon > 1$, where GR places a naked singularity. Besides being non-unique, this continuation is not maximal, because the upper value of the specific charge is bound by imposing the basic properties of quantum systems to hold, such as unitarity (that is, the normalisability of the HWF).

Another intriguing and direct interpretation of Thorne's hoop conjecture is the possibility of forming BHs through particle collisions, as shown in Section 2.3.3. In particular, this would in principle allow to test the results in modern-day particle accelerators, such as LHC. Exerting some strong approximations, like the one-dimensionality of the target space (or alternatively setting the impact parameter to zero), the probability for an event horizon to form as a consequence of the collision between two gaussian-shaped wave-packet was estimated, supporting a quantum version of the hoop conjecture. The main upgrade with respect to the related classical version is that this model confirms a minimum value for the mass of the BH of the same order of m_{p}, therefore driving the possible BH production by these means way beyond our experimental capabilities, at least at the present day.

Nevertheless, the situation could change in principle when scenarios with extra spatial dimensions are employed. In such cases the "quantum gravitational mass scale" which replaces m_{p} may be indeed within our grasp. The HQM draws notable corrections to the production cross-sections of BHs in large extra-dimensional models, like the ADD one, granting a larger and larger suppression as the number of spatial dimensions grows. In particular, lower-dimensional space-times have been studied thoroughly, due to the recent claims that quantum BHs may effectively behave as one-dimensional objects. The analysis additionally supports the conception that, in $(1+1)$ dimensions, BHs are supposed to be strictly Quantum-Mechanical objects.

As we mentioned the problem of time in Section 1.2.2, it is hard give a feasible dynamical evolution to GR. That is why we mostly analysed static configurations throughout this elaborate, and even the model of particle collisions was treated in this fashion. In any case, this conceptual problem cannot be superseded forever, since an horizon traps matter and energy in its own interior, and this mechanism is meant to have some profound impact on the dynamics of the system. The simplest choice in order to get a

time-dependent HQM, is to construct by means of a suitable modification of Schrödinger equation, in which the probability of the particle to belong inside its own horizon affects the evolution. As expected, even from qualitative arguments, the spread of a Gaussian packet shall be slowed down by the presence of a trapped surface, as states enjoying $P_{\rm BH} = 1$ are not supposed to propagate in time.

All the above cases are interesting applications of the HQM and open up several perspectives for future extensions, like the estimation of the probability that the gravitational collapse of a lump of matter may result in the formation of a BH. Unfortunately, taking a wave-packet and pushing its mass to the Planck scale, $m \to m_{\rm p}$, does not yield a realistic model for a large, semi-classical BH. The fluctuations in the horizon's size are indeed of the same magnitude order of it expectation value, $\Delta r_{\rm H} \sim \langle\, \hat{r}_{\rm H} \,\rangle$, and grow out of control as the latter becomes macroscopical.

A reasonable improvement of this model is to model the structure of a BH as given by many microscopical constituents (gravitons, in a realistic case), which are allow to superpose in the same quantum state, instead of an extremely massive one. This phylosophy is behind the so-called corpuscular BH model, brought to light recently in Refs. [73]. This model incorporates all of the characteristics of a BH as given by its many-body structure, contrary to standard lore, while the geometry of space-time emerges in an effective description of the latter. It was demonstrated that the quantum state for a self-gravitating static massless scalar field [18] is approximately a BEC of the form conjectured in Ref. [73], whose horizon's size was subsequently extimated by means of HQM arguments. The classical description of a Schwarzschild BH is recovered when the number of elements N is large, since the energy of each toy-graviton m is well below $m_{\rm p}$, but the total energy M jumps much above the Planck scale. The uncertainty $\Delta r_{\rm H}$ is typically of the order of the energy of the predicted Hawking quanta, which in turn scale like $1/N$, as claimed in Refs. [73]. This further supports the idea that BHs must be composite objects made of very light constituents.

Starting from this many-body picture, we took back the description of the formation of a BH via the gravitational collapse of a star. In section 3.1 we considered a simplistic model for a Newtonian cluster of ordinary matter: the current $J \sim \rho$ represents the star, while the coupled massless scalar field $\langle g|\, \hat{\phi}\, |g\rangle \simeq \phi_{\rm c} \sim V_{\rm N}$ reproduces the outer Newtonian potential. As an approximation, we made the assumption that the energy contribution of the gravitons is subdominant and can be thus neglected.

In Section 3.1.1 the circumstance is the exact opposite: the gravitational collapse took place and any degree of freedom coming from the matter source is ignored. The Schwarzschild radius affects both the size of the confinement

region of the resulting self-sustained quantum state and its (almost) only allowed wave-number k_c, as given by Eq. (3.39). In addition to that, this state nicely matches the relations (3.8), which have been known to hold for a self-gravitating body near the threshold of BH formation (see, for example, Refs. [133, 140]). As in the analysis of static cases, the time dependence of this treatment is absent and the two configurations can be therefore related just by means of an unphysical mechanism, like a delta-form shock-wave. Nonetheless, the two cases are feasible approximate descriptions of the state of a collapsing star in the asymptotic past and future.

In order to give further physical meaning to this model, one can think about a phase transition for the graviton state around the time when matter and gravitons have comparable weight. Such an analysis might help determine whether or not the state of BEC BH is ever reached (according to Refs. [73, 144], a BH is precisely the state on the verge of a quantum phase transition), and under which conditions. One could deal with this topic starting from the Klein-Gordon equation with both matter and "graviton" currents,

$$\Box\phi(x) = q_{\mathrm{M}}\, J_{\mathrm{M}}(x) + q_{\mathrm{G}}\, J_{\mathrm{G}}(x)\ , \tag{4.1}$$

where J_{M} is the general matter current used in Section 3.1 and J_{G} the graviton current depicted by Eq. (3.36). The latter can be regarded as a perturbation in the “star case" and the formal expansion around the coupling q_{G} could likely lead to perturbative corrections for the Newtonian potential V_{N} near the star, because of the formal analogy between the graviton current (3.36) and an effective mass term for the toy-graviton ϕ. Conversely, in the self-sustained regime it is possible to expand for small q_{M}, since the ordinary matter gives a modest contribution. The effect of such a correction would be the enhancement of the fuzziness of the horizon in the exterior of the BH. A phase transition might happen in the framework of an overlap of these two cases, where no source dominates over the other, and the main features emerging from this picture are to be obtained non-perturbatively. In any case, an order parameter must be identified.

On the brink of the phase transition, before the formation of a BH, one may guess that the case in which all of the constituents are in a slightly excited state above the BEC energy ($\gamma_1 \gtrsim 1$) suggests the physical processes that could take place. The quantum state of an already formed BH is reliably represented by the parameter $\gamma_1 \ll 1$ of Section 3.2.2, or the equivalent Hawking case of Section 3.2.4, one might view the γ_1 (or the collective analogue γ) as an effective order parameter for the phase transition from a spherically symmetric source of matter to a BH. In such a dynamical context, it is necessary that γ is promoted to a time-dependent quantity, which

sees its value decrease from values of order one (or possibly larger) to much smaller values during the collapse. Accordingly, the investigation of the possible dependence of γ on the physical variables, which define the state of matter along the collapse, is supposed to give some interesting implications.

One has to emphasise that the special relativistic scalar equation is manipulated in the Newtonian approximation, while BHs are a product of GR. In this context, the only employed general relativistic result was the condition for the existence of trapping surfaces in spherically symmetric systems which establishes the foundations of the HQM (and the GUP that follows from it [11]). The advantage of such "fuzzy" descriptions of a BH's horizon is that they do not require any knowledge of the quantum state of the source (see [70, 145, 146] and references therein), as further implied by the quantisation of spherically symmetric space-times. Investigations of collapsing thin [147, 148] or thick shells [149], also hint at similar scenarios. The current approach is more general because it allows one to link the causal structure of space-time, encoded by the horizon wave-function $\psi_{\rm H}$, to the presence of a material source in a state $\psi_{\rm S}$. In order to study the time evolution of the system, a "feedback" from $\psi_{\rm H}$ into $\psi_{\rm S}$ must be introduced as in Section 2.4.

Concerning the quantum state describing an evaporating BH made of scalar toy gravitons, it was explained that a Planckian distribution, portraying the depleted modes at the Hawking temperature $T_{\rm H} \sim m$, correctly reproduces the main known properties of Hawking radiation, like the characteristic flux, the Bekenstein-Hawking entropy law and the negative heat capacity, for a large BH mass (or, equivalently, large N). The many-body state is also found to be self-similar with respect to the single particle state, where of course the energy and mass of the single constituent are substituted with their respective totals. By means of this approximation it is possible to compute the leading order corrections to the energy of the system which determine a logarithmic contribution to the entropy, due to the modes that irradiate freely in space, and a vanishing specific heat for N of order one, as we expect the process of evaporation to end after a finite interval of time.

This output is further encouraged by the HWF, which allows to extimate the backreaction of the Hawking radiation onto the horizon radius. Since the latter is connected to the energy scale of the condensate [73], as the Hawking flux is, the extra term in $\langle\, \hat{r}_{\rm H} \,\rangle$ diminishes the emission. In the case of light BHs, this effect will again ensure that the radiation eventually stops. This is precisely what one expects from a microcanonical description of the BH system [143].

Finally, let us stress out once more that the analysis given here does not explicitly consider the dynamical evolution of the BEC, but it only considers

a picture of the system at a given instant of time. Anyway, it is possible to recover an approximation for $N \gg 1$, where the flux is a perturbation, by means of Eq. (3.13), or by the appropriately modified expression that stems from Eq. (3.111) in the limit of $N \to \mathcal{O}(1)$. Concerning this regime, another important aspect is that the model should at least trace the modelisation of BHs as single particle states investigated in Ref. [13].

Appendix A

Useful integrals

In this review, we made use of integrals of the form

$$\mathrm{I}_3 = \int_1^\infty \gamma\left(\frac{3}{2}, A\,x^2\right)\, e^{-x^2}\, x^2\,\mathrm{d}x \tag{A.1}$$

where A is a positive real parameter. From

$$x\, e^{-x^2} = -\frac{1}{2}\,\frac{\mathrm{d}}{\mathrm{d}x} e^{-x^2} \tag{A.2}$$

and

$$\frac{\mathrm{d}}{\mathrm{d}y}\,\gamma(s,y) = y^{s-1}\, e^{-y}\ , \tag{A.3}$$

upon integrating by parts, one obtains

$$\begin{aligned}
\mathrm{I}_3 &= \int_1^\infty \gamma\left(\frac{3}{2}, A^2\,x^2\right)\, e^{-x^2}\, x^2\,\mathrm{d}x \\
&= \frac{1}{2\,e}\,\gamma\left(\frac{3}{2}, A^2\right) + \frac{1}{2}\int_1^\infty e^{-x^2}\,\frac{\mathrm{d}}{\mathrm{d}x}\left[x\,\gamma\left(\frac{3}{2}, A^2\,x^2\right)\right]\,\mathrm{d}x \\
&= \frac{1}{2\,e}\,\gamma\left(\frac{3}{2}, A^2\right) + A^3\int_1^\infty e^{-\left(1+A^2\right)x^2}\, x^3\,\mathrm{d}x + \frac{1}{2}\int_1^\infty e^{-x^2}\,\gamma\left(\frac{3}{2}, A^2\,x^2\right)\,\mathrm{d}x \\
&= \frac{1}{2\,e}\,\gamma\left(\frac{3}{2}, A^2\right) + \frac{A^3\,\Gamma\left(2, 1+A^2\right)}{2\left(1+A^2\right)^2} + \frac{1}{2}\int_1^\infty e^{-x^2}\,\gamma\left(\frac{3}{2}, A^2\,x^2\right)\,\mathrm{d}x\ ,
\end{aligned} \tag{A.4}$$

From the property

$$\begin{aligned}
\gamma\left(\frac{3}{2}, A^2\,x^2\right) &= \frac{1}{2}\gamma\left(\frac{1}{2}, A^2\,x^2\right) - A\,x\,e^{-A^2\,x^2} \\
&= \frac{\sqrt{\pi}}{2}\,\mathrm{erf}(Ax) - A\,x\,e^{-A^2\,x^2}\ ,
\end{aligned} \tag{A.5}$$

the integral

$$\begin{aligned}\int_1^\infty e^{-x^2}\,\gamma\left(\frac{3}{2},A^2\,x^2\right)\,\mathrm{d}x &= \frac{\sqrt{\pi}}{2}\int_1^\infty \mathrm{erf}(Ax)\,e^{-x^2}\,\mathrm{d}x - A\int_1^\infty e^{-(1+A^2)x^2}\,\mathrm{d}x \\ &= -\frac{A\,e^{-(1+A^2)}}{2(1+A^2)} + \frac{\pi}{4}[1-\mathrm{erf}(1)\,\mathrm{erf}(A)] \\ &\quad -\pi\,T\left(\sqrt{2}\,A,\frac{1}{A}\right)\ , \end{aligned} \tag{A.6}$$

where $\mathrm{erf}(x)$ is an error function and $T(a,b)$ is the Owen's T distribution defined as

$$T(a,b) = \frac{1}{2\pi}\int_0^a \frac{e^{-\frac{1}{2}\,b^2\,(1+x^2)}}{1+x^2}\,\mathrm{d}x\ . \tag{A.7}$$

Finally, putting everything together yields

$$\begin{aligned}\mathrm{I}_3 &= \frac{1}{2\,e}\,\gamma\left(\frac{3}{2},A^2\right) + \frac{\pi}{8}[1-\mathrm{erf}(1)\,\mathrm{erf}(A)] + \frac{A^3\,\Gamma\left(2,1+A^2\right)}{2\left(1+A^2\right)^2} \\ &\quad -\frac{A\,e^{-(1+A^2)}}{4(1+A^2)} - \frac{\pi}{2}\,T\left(\sqrt{2}\,A,\frac{1}{A}\right) \\ &= \frac{\pi}{8}\,\mathrm{erfc}(A) + \frac{\sqrt{\pi}}{4}\,\Gamma\left(\frac{3}{2},1\right)\,\mathrm{erf}(A) - \frac{A}{2}e^{-(1+A^2)} + \frac{A^3\,(2+A^2)\,e^{-(1+A^2)}}{2\left(1+A^2\right)^2} \\ &\quad -\frac{A\,e^{-(1+A^2)}}{4(1+A^2)} - \frac{\pi}{2}\,T\left(\sqrt{2}\,A,\frac{1}{A}\right) \\ &= \frac{\pi}{8}\,\mathrm{erfc}(A) + \frac{\sqrt{\pi}}{4}\,\Gamma\left(\frac{3}{2},1\right)\,\mathrm{erf}(A) - \frac{A(3+A^2)}{4(1+A^2)^2}e^{-(1+A^2)} \\ &\quad -\frac{\pi}{2}\,T\left(\sqrt{2}\,A,\frac{1}{A}\right)\ . \end{aligned} \tag{A.8}$$

Appendix B

Numerical analysis of self-sustained quantum states

B.1 Analytical spectrum for $\gamma \gtrsim 1$

We start by noting the spectral coefficient in Eq. (3.66) can be written as

$$\begin{aligned} C(E \geq M) \;&\sim\; \int_m^\infty \mathrm{d}E_1 \cdots \int_m^\infty \mathrm{d}E_N \, \exp\left\{ -\sum_{i=1}^{N} \frac{(E_i - m)^2}{2\,m^2} \right\} \delta\left(E - \sum_{i=1}^{N} E_i \right) \\ &\sim\; \int_m^\infty \mathrm{d}E_1 \cdots \int_m^\infty \mathrm{d}E_{N-1} \, \exp\left\{ -\sum_{i=1}^{N-1} \frac{(E_i - m)^2}{2\,m^2} - \frac{\left(E - \sum_{i=1}^{N-1} E_i - m \right)^2}{2\,m^2} \right\} \\ &\equiv\; \int_m^\infty \mathrm{d}E_1 \cdots \int_m^\infty \mathrm{d}E_{N-1} \, e^{-\frac{F^2(E,\{\mathcal{E}_i\})}{2\,m^2}} \;. \end{aligned} \tag{B.1}$$

In order to proceed, we find it convenient to write the argument of the exponential as

$$\begin{aligned} -2\,m^2\,F^2(E,\{\mathcal{E}_i\}) \;&\equiv\; \sum_{i=1}^{N-1} (E_i - m)^2 + \left(E - \sum_{i=1}^{N-1} E_i - m \right)^2 \\ &=\; \sum_{i=1}^{N-1} (E_i - m)^2 + \left[E - \sum_{i=1}^{N-1} (E_i - m) - N\,m \right]^2 \\ &=\; (E - M)^2 + \sum_{i=1}^{N-1} \mathcal{E}_i^2 \\ &\quad + \left[\sum_{i=1}^{N-1} \mathcal{E}_i - 2\,(E - M) \right] \sum_{j=1}^{N-1} \mathcal{E}_j \;, \end{aligned} \tag{B.2}$$

where $\mathcal{E}_i = E_i - m$, so that

$$\begin{aligned} C(E \geq M) \;&\sim\; e^{-\frac{(E-M)^2}{2\,m^2}} \int_0^\infty \mathrm{d}\mathcal{E}_1 \cdots \int_0^\infty \mathrm{d}\mathcal{E}_{N-1} \\ &\quad \times \exp\left\{ -\sum_{i=1}^{N-1} \frac{\mathcal{E}_i^2}{2\,m^2} - \left[\sum_{i=1}^{N-1} \frac{\mathcal{E}_i}{2\,m} - \frac{(E-M)}{m} \right] \sum_{j=1}^{N-1} \frac{\mathcal{E}_j}{m} \right\} \\ &\equiv\; e^{-\frac{(E-M)^2}{2\,m^2}}\, I(E, M; m) \;. \end{aligned} \tag{B.3}$$

We then note that the above integral contains the Gaussian measure,

$$\int_0^\infty \mathrm{d}\mathcal{E}_1 \cdots \int_0^\infty \mathrm{d}\mathcal{E}_{N-1} \exp\left\{ -\sum_{i=1}^{N-1} \frac{\mathcal{E}_i^2}{2\,m^2} \right\} \sim \int_0^\infty \mathcal{E}^{N-2}\, \mathrm{d}\mathcal{E} \exp\left\{ -\frac{\mathcal{E}^2}{2\,m^2} \right\} \tag{B.4}$$

where $\mathcal{E}^2 = \sum_{i=1}^{N-1} \mathcal{E}_i^2$, and is significantly different from zero only for $\mathcal{E} \lesssim m$. We can therefore approximate

$$\sum_{i=1}^{N-1} \mathcal{E}_i \simeq \mathcal{E} \;, \tag{B.5}$$

from which we obtain

$$\begin{aligned} I(E, M; m) \;&\sim\; \int_0^\infty \mathcal{E}^{N-2}\, \mathrm{d}\mathcal{E} \exp\left\{ -\frac{\mathcal{E}^2}{m^2} + \frac{(E-M)}{m} \frac{\mathcal{E}}{m} \right\} \\ &=\; e^{\frac{(E-M)^2}{4\,m^2}} \int_0^\infty \mathcal{E}^{N-2}\, \mathrm{d}\mathcal{E} \exp\left\{ -\frac{\left[2\,\mathcal{E} - (E-M)\right]^2}{4\,m^2} \right\} \;. \end{aligned} \tag{B.6}$$

This integral can be exactly evaluated in terms of hypergeometric functions, but we can just further approximate it here as

$$\begin{aligned} I(E, M; m) \;&\sim\; m\,(E-M)\, P_{(N-3)}(E, M)\, e^{\frac{(E-M)^2}{4\,m^2}} \\ &\sim\; (E-M)\, e^{\frac{(E-M)^2}{4\,m^2}} \;, \end{aligned} \tag{B.7}$$

where $P_{(N-3)}$ is a polynomial of degree $N-3$. For $N = M/m \gg 1$, we finally obtain,

$$C(E \geq M) \;\sim\; (E-M)\, e^{-\frac{(E-M)^2}{4\,m^2}} \;, \tag{B.8}$$

which is the expression in Eq. (3.67).

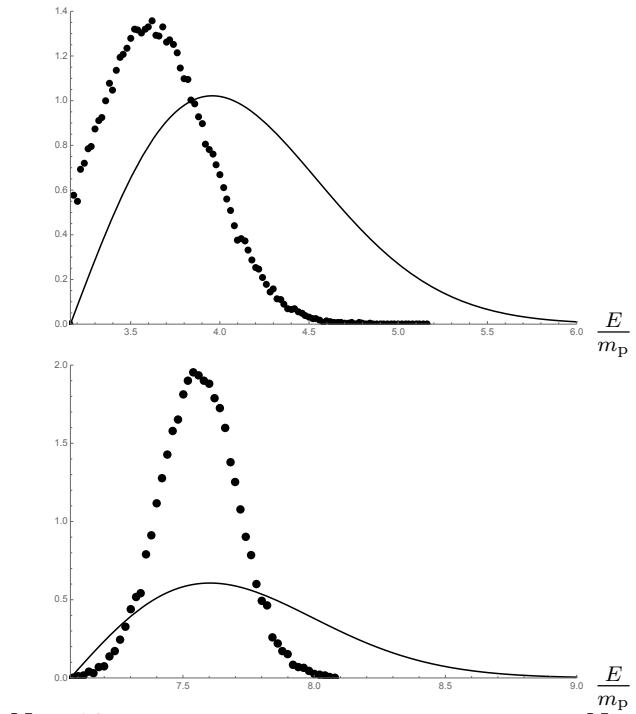

Figure B.1: Monte Carlo estimate of the spectral coefficient in Eq. (B.3) (dots) compared to its analytical approximation (3.67) (solid line), both normalised according to Eq. (B.1), for $N = 10$ and $N = 50$.

B.2 Numerical spectrum for $\gamma \gtrsim 1$

In this Appendix, we estimate the spectral coefficient in Eq. (B.3) [which exactly equals the one in Eq. (3.66)] for various values of N. For this purpose, we have implemented a standard Monte Carlo method in a MATHEMATICA notebook, in which the coefficient is also numerically normalised, so that

$$\int_M^\infty C^2(E)\,\mathrm{d}E = 1\ . \tag{B.1}$$

The dependence of the spectral coefficient on the total energy E is then compared with the analytical approximation (3.67).

Fig. B.1 shows this comparison for $N = 10$ and $N = 50$. For the former value, the analytical approximation overestimates both the location of the peak and (slightly) the width of the curve (thus underestimating the height of the peak). For $N = 50$, the location of the peak is instead very well identified by Eq. (3.67), but the actual width remains narrower than its analytical approximation (resulting in a large discrepancy in the peak values).

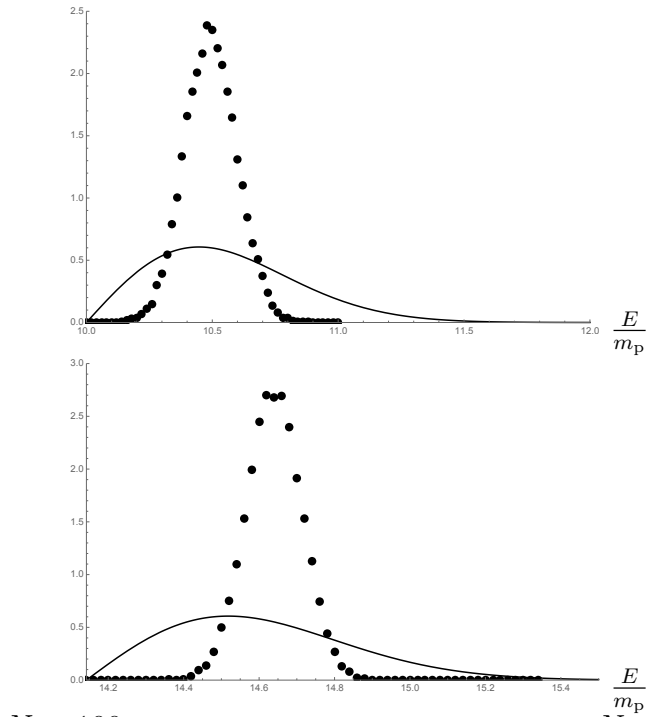

Figure B.2: Monte Carlo estimate of the spectral coefficient in Eq. (B.3) (dots) compared to its analytical approximation (3.67) (solid line), both normalised according to Eq. (B.1), for $N = 100$ and $N = 200$.

Fig. B.2 shows the comparison for $N = 100$ and $N = 200$. From these plots, it is clear that the analytical approximation progressively underestimates the value of the energy at which the spectral coefficients peak, at the same time overestimating more and more the width of the curve (by about a factor of three in these two plots), and consequently underestimates the height of the curve at peak values.

All of these trends are further confirmed in Fig. B.3, which shows the comparison for $N = 300$ and $N = 500$. The peaks of the numerical estimate and the analytical approximation continue to separate further apart, whereas the numerical width becomes narrower than the analytical width for increasing N.

The overall conclusion is that the analytical approximation (3.67) is fairly good for estimating the energy at the peak of the spectral coefficients, but overestimates (underestimates) significantly the width (peak value), for $N \gtrsim 100$.

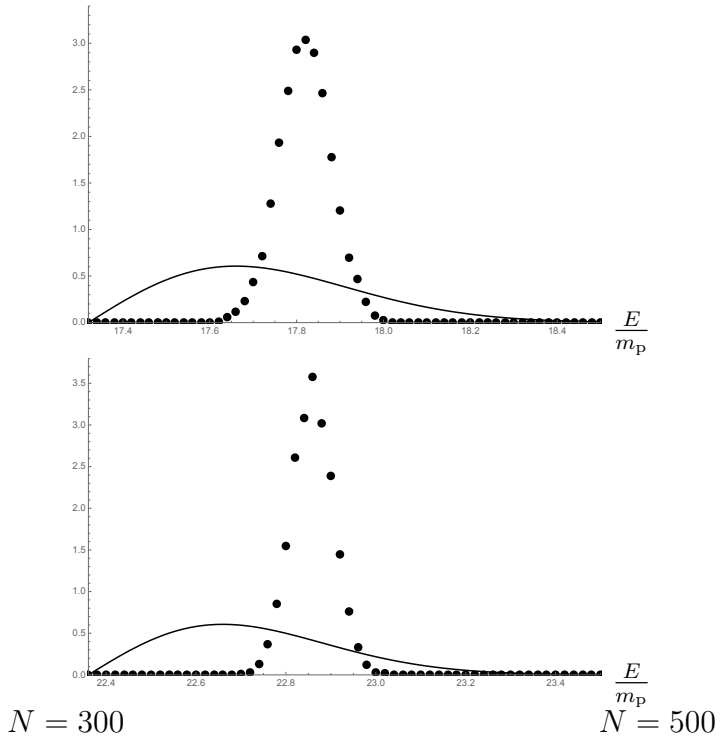

Figure B.3: Monte Carlo estimate of the spectral coefficient in Eq. (B.3) (dots) compared to its analytical approximation (3.67) (solid line), both normalised according to Eq. (B.1), for $N = 300$ and $N = 500$.

B.3 Monte Carlo estimate of spectral coefficients

We have checked the analytical approximation (3.86) by computing directly some of the spectral coefficients (3.81) by means of a Monte Carlo algorithm. Fig. B.4 shows the numerical estimates of $C_5 = C_5(E-M)$ and $C_{10} = C_{10}(E-M)$ along with their analytical approximation for $N = 10$. This comparison immediately shows that the coefficients C_n indeed have a "Planckian" shape, in agreement with their analytical approximation. Finally, Fig. B.5 shows the whole coefficient $C(E > M)$ for $N = 10$. The same quantities for larger values of N, up to $N = 100$ have also been computed and the results are qualitatively the same.

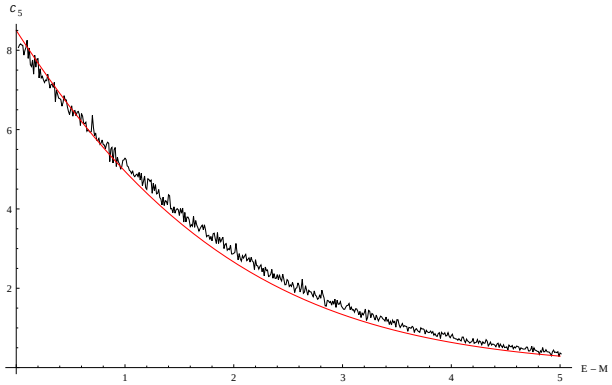

(a) C_5

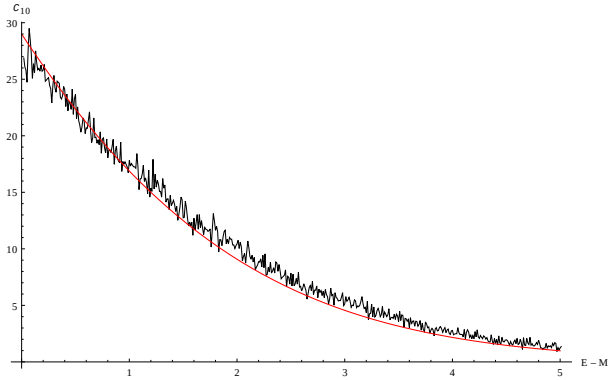

(b) C_{10}

Figure B.4: Numerical estimate of some coefficients in the expansion (3.81) (black lines), and their analytical approximation (red lines), for $N = 10$ (energies are in Planck units).

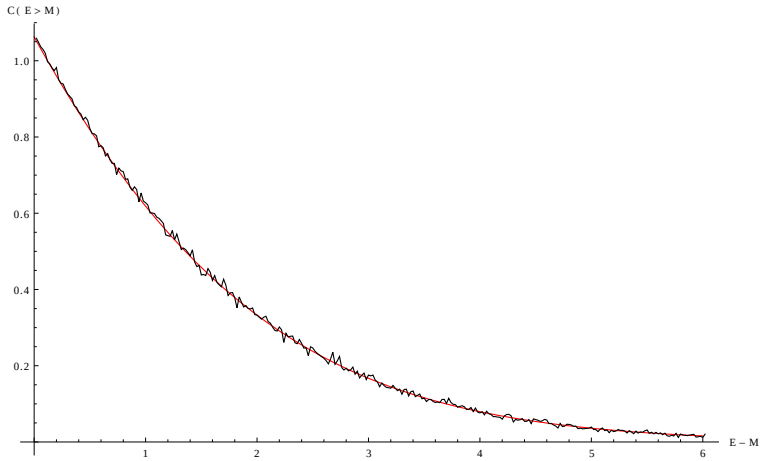

Figure B.5: Numerical estimate of $C(E > M)$ (black line), and its analytical approximation (3.86) (red line) for $N = 10$ (energies are in Planck units).

Bibliography

[1] J.R. Oppenheimer and H. Snyder, Phys. Rev. **56** (1939) 455.

[2] J.R. Oppenheimer and G.M. Volkoff, Phys. Rev. **55** (1939) 374.

[3] P.S. Joshi, "Gravitational Collapse and Spacetime Singularities," Cambridge Monographs on Mathematical Physics (Cambridge, 2007).

[4] J.D. Bekenstein, "Black holes: Physics and astrophysics. Stellar-mass, supermassive and primordial black holes," astro-ph/0407560.

[5] K.S. Thorne, "Nonspherical Gravitational Collapse: A Short Review," in *J.R. Klauder, Magic Without Magic,* San Francisco (1972), 231.

[6] S.W. Hawking, Nature **248**, 30 (1974).

[7] S.W. Hawking, Comm. Math. Phys. **43**, 199 (1975).

[8] G. Dvali and C. Gomez, "Black Hole's Information Group", arXiv:1307.7630.

[9] R. Casadio, A. Giugno, O. Micu and A. Orlandi, Entropy **17** (2015) 6893.

[10] R. Casadio, "Localised particles and fuzzy horizons: A tool for probing Quantum Black Holes," arXiv:1305.3195 [gr-qc].

[11] R. Casadio and F. Scardigli, Eur. Phys. J. C **74** (2014) 1, 2685.

[12] R. Casadio, O. Micu and F. Scardigli, Phys. Lett. B **732** (2014) 105.

[13] R. Casadio, Eur. Phys. J. C **75** (2015) 160.

[14] R. Casadio, O. Micu and D. Stojkovic, JHEP **1505** (2015) 096.

[15] R. Casadio, O. Micu and D. Stojkovic, Phys. Lett. B **747** (2015) 68.

[16] F. Scardigli, Phys. Lett. B **452** (1999) 39.

[17] R. Casadio, A. Giugno and O. Micu, "Horizon Quantum Mechanics: a hitchhiker's guide to quantum black holes," arXiv:1512.04071 [hep-th].

[18] R. Casadio, A. Giugno, O. Micu and A. Orlandi, Phys. Rev. D **90** (2014) 8, 084040.

[19] R. Casadio, A. Giugno and A. Orlandi, Phys. Rev. D **91** (2015) 12, 124069.

[20] A. Einstein, Annalen Phys. **17** (1905) 891 [Annalen Phys. **14** (2005) 194].

[21] A. Einstein, Annalen Phys. **49** (1916) 769 [Annalen Phys. **14** (2005) 517].

[22] A. D. Sakharov, Sov. Phys. Dokl. **12** (1968) 1040 [Dokl. Akad. Nauk Ser. Fiz. **177** (1967) 70] [Sov. Phys. Usp. **34** (1991) 394] [Gen. Rel. Grav. **32** (2000) 365].

[23] P. A. M. Dirac, Proc. Roy. Soc. Lond. A **246** (1958) 333.

[24] P. Bergmann, Phys. Rev. **144** (1966) 1078.

[25] C. Rovelli, Living Rev. Rel. **1** (1998) 1.

[26] B.S. DeWitt, Phys. Rev. **160** (1967) 1113-1148.

[27] P. D. D'Eath and P. N. Payne, Phys. Rev. D **46** (1992) 658.

[28] P. D. D'Eath and P. N. Payne, Phys. Rev. D **46** (1992) 675.

[29] P. D. D'Eath and P. N. Payne, Phys. Rev. D **46** (1992) 694.

[30] J.M.M. Senovilla, Europhys. Lett. **81** (2008) 20004.

[31] G.L. Alberghi, R. Casadio, O. Micu and A. Orlandi, JHEP **1109** (2011) 023.

[32] S.D.H. Hsu, Phys. Lett. B **555** (2003) 92.

[33] B. J. Carr and S. B. Giddings, Sci. Am. **292N5** (2005) 30 [Spektrum Wiss. **2005N9** (2005) 32].

[34] X. Calmet, D. Fragkakis and N. Gausmann, Eur. Phys. J. C **71** (2011) 1781;

[35] X. Calmet, W. Gong and S.D.H. Hsu, Phys. Lett. B **668** (2008) 20.

[36] X. Calmet, Mod. Phys. Lett. A **29** (2014) 1450204.

[37] X. Calmet and R. Casadio, Eur. Phys. J. C **75** (2015) 9, 445

[38] M. Maggiore, Phys. Lett. B **319** (1993) 83.

[39] A. Kempf, G. Mangano, R.B. Mann, Phys. Rev. D **52** (1995) 1108.

[40] R. Casadio and F. Scardigli, Class. Quant. Grav. **20** (2003) 3915.

[41] R. Casadio and F. Scardigli, Int. J. Mod. Phys. D **18** (2009) 319.

[42] M. Bleicher, P. Nicolini, M. Sprenger, Eur. J. Phys. 33 (2012) 853.

[43] H. Stephani, "Relativity: An introduction to special and general relativity," Cambridge University Press (Cambridge, 2004).

[44] V. Faraoni, "Is the Hawking quasilocal energy Newtonian?," arXiv:1510.03789 [gr-qc].

[45] G. Lemaître, Ann. Soc. Sci. Bruxelles A **53** (1933) 51.

[46] P.C. Vaidya, Proc. Indian Acad. Sci., Sect. A, Phys. Sci. **33** (1951a) 254.

[47] C.W. Misner, Phys. Rev. B **137** (1965) 1350;

[48] R.W. Linquist, C.W. Misner and R.A. Schwartz, Phys. Rev. B **137** (1965) 1364.

[49] R. Penrose, Riv. Nuovo Cim. **1** (1969) 252 [Gen. Rel. Grav. **34** (2002) 1141].

[50] E. Poisson and W. Israel, Phys. Rev. D **41** (1990) 1796.

[51] N. D. Birrell and P. C. W. Davies, "Quantum Fields in Curved Space," Cambridge Monographs on Mathematical Physics (Cambridge, 1984).

[52] C. J. Isham, gr-qc/9210011.

[53] K. Schwarzschild, Sitzungsber. Preuss. Akad. Wiss. Berlin (Math. Phys.) **1916** (1916) 189.

[54] K. Schwarzschild, Sitzungsber. Preuss. Akad. Wiss. Berlin (Math. Phys.) **1916** (1916) 424.

[55] G. Dvali, C. Gomez and A. Kehagias, JHEP **1111** (2011) 070.

[56] G. Dvali, G.F. Giudice, C. Gomez and A. Kehagias, JHEP **1108** (2011) 108.

[57] S. Hossenfelder, Living Rev. Rel. **16** (2013) 2.

[58] B. S. DeWitt, Phys. Rev. **162** (1967) 1195.

[59] K. Nakamura, S. Konno, Y. Oshiro and A. Tomimatsu, Prog. Theor. Phys. **90** (1993) 861.

[60] A. Ashtekar, J. Baez, A. Corichi and K. Krasnov, Phys. Rev. Lett. **80** (1998) 904.

[61] S. Carlip, Phys. Rev. Lett. **82** (1999) 2828.

[62] R. H. Price and K. S. Thorne, Phys. Rev. D **33**, 915 (1986).

[63] K. S. Thorne, R. H. Price and D. A. Macdonald, "Black Holes: The Membrane Paradigm," Yale University Press (New Haven, 1986).

[64] C. R. Stephens, G. 't Hooft and B. F. Whiting, Class. Quant. Grav. **11** (1994) 621.

[65] L. Susskind, J. Math. Phys. **36** (1995) 6377.

[66] P. Hajicek, Phys. Rev. D **30** (1984) 1178.

[67] A. Tomimatsu, Phys. Lett. B **289** (1992) 283.

[68] R. Casadio, Phys. Lett. B **511** (2001) 285.

[69] K. V. Kuchar, Phys. Rev. D **50** (1994) 3961.

[70] A. Davidson and B. Yellin, Phys. Lett. B **736** 267.

[71] R. Brustein and A. J. M. Medved, JHEP **1406** (2014) 057.

[72] G. Dvali and C. Gomez, Fortsch. Phys. **61** (2013) 742.

[73] G. Dvali and C. Gomez, JCAP **01** (2014) 023 .

[74] G. Dvali and C. Gomez, Eur. Phys. J. C **74** (2014) 2752.

[75] G. Dvali and C. Gomez, Phys. Lett. B **716**, (2102) 240.

[76] F. Kühnel and B. Sundborg, JHEP **1412** (2014) 016.

[77] R. Casadio and A. Orlandi, JHEP **1308** (2013) 025.

[78] W. Mück and G. Pozzo, JHEP **1405** (2104) 128.

[79] R. Di Criscienzo, S.A. Hayward, M. Nadalini, L. Vanzo and S. Zerbini, Class. Quant. Grav. **26** (2009) 062001.

[80] F. Scardigli, Nuovo Cim. B **110** (1995) 1029.

[81] R.J. Adler, P. Chen and D.I. Santiago, Gen. Rel. Grav. **33** (2001) 2101.

[82] M. Cavaglia, S. Das and R. Maartens, Class. Quant. Grav. **20** (2003) L205.

[83] F. Scardigli, "Hawking temperature for various kinds of black holes from Heisenberg uncertainty principle", gr-qc/0607010.

[84] K. Nouicer, Class. Quant. Grav. **24**, (2007) 5917.

[85] F. Scardigli, "Glimpses on the micro black hole planck phase", arXiv:0809.1832 [hep-th].

[86] P. Chen, C. Gruber and F. Scardigli, Phys. Rev. D **83**, (2011) 063507.

[87] P. Jizba, H. Kleinert, F. Scardigli, Phys. Rev. D **81**, (2010) 084030.

[88] M.K. Parikh and F. Wilczek, Phys. Rev. Lett. **85**, (2000) 5042.

[89] M. Angheben, M. Nadalini, L. Vanzo and S. Zerbini, JHEP **0505**, (2005) 014.

[90] R. Casadio and B. Harms, Phys. Rev. D **58** (1998) 044014.

[91] R. Casadio and B. Harms, Entropy **13** (2011) 502.

[92] E. Greenwood and D. Stojkovic, JHEP 032P 0408.

[93] A. Saini and D. Stojkovic, Phys. Rev. D **89** (2014) 044003.

[94] L. M. Krauss, D. Stojkovic and T. Vachaspati, Phys. Rev. D **76** (2007) 024005.

[95] D. Stojkovic and T. Vachaspati, Phys. Lett. B **663** (2008) 107.

[96] E. Greenwood, D. Stojkovic and J. E. Wang, Phys. Rev. D **80** (2009) 124027.

[97] H. Reissner, Annalen der Phys. **50** (1916) 106.

[98] G. Nordström, Verhandl. Koninkl. Ned. Akad. Wetenschap., Afdel. Natuurk., **26** (1918) 1201.

[99] V. I. Dokuchaev, Class. Quant. Grav. **31** (2014) 055009.

[100] E. Brown and R. B. Mann, Phys. Lett. B **694** (2011) 440.

[101] E. G. Brown, R. B. Mann and L. Modesto, Phys. Rev. D **84** (2011) 104041.

[102] S. B. Giddings and S. D. Thomas, Phys. Rev. D **65** (2002) 056010.

[103] S. Dimopoulos and G. L. Landsberg, Phys. Rev. Lett. **87** (2001) 161602.

[104] N. Arkani-Hamed, S. Dimopoulos and G. R. Dvali, Phys. Lett. B **429** (1998) 263.

[105] I. Antoniadis, N. Arkani-Hamed, S. Dimopoulos and G. R. Dvali, Phys. Lett. B **436** (1998) 257.

[106] L. Randall and R. Sundrum, Phys. Rev. Lett. **83** (1999) 3370.

[107] L. Randall and R. Sundrum, Phys. Rev. Lett. **83** (1999) 4690.

[108] K. Koyama and R. Maartens, Living Rev. Rel. **13** (2010) 5.

[109] R. Casadio, R.T. Cavalcanti, A. Giugno and J. Mureika, "Horizon of quantum black holes in various dimensions," arXiv:1509.09317 [gr-qc].

[110] J. R. Mureika, Phys. Lett. B **716**, 171 (2012).

[111] R. Loll, Nucl. Phys. Proc. Suppl. **94** (2001) 96.

[112] J. Ambjorn, J. Jurkiewicz, R. Loll, Phys. Rev. D **72** (2005) 064014.

[113] J. Ambjorn, J. Jurkiewicz, R. Loll, "Quantum Gravity, or The Art of Building Spacetime," in *Approaches to Quantum Gravity*, ed. D. Oriti, Cambridge University Press (2006).

[114] L. Modesto and P. Nicolini, Phys. Rev. D **81** (2010) 104040.

[115] P. Nicolini and E. Spallucci, Adv. High Energy Phys. **2014** (2014) 805684.

[116] B. J. Carr, J. Mureika and P. Nicolini, JHEP **1507** (2015) 052.

[117] J. Mureika and P. Nicolini, Eur. Phys. J. Plus **128** (2013) 78.

[118] L.A. Anchordoqui, D.C. Dai, M. Fairbairn, G. Landsberg and D. Stojkovic, Mod. Phys. Lett. **A 27** (2102) 1250021.

[119] L.A. Anchordoqui, D.C. Dai, H. Goldberg, G. Landsberg, G. Shaughnessy, D. Stojkovic and T.J. Weiler, Phys. Rev. D **83** (2011) 114046.

[120] J.R. Mureika and D. Stojkovic, Phys. Rev. Lett. **106** (2011) 101101.

[121] J.R. Mureika and D. Stojkovic, Phys. Rev. Lett. **107** (2011) 169002.

[122] N. Afshordi and D. Stojkovic, Phys. Lett. B **739** (2014) 117.

[123] D. Stojkovic, Mod. Phys. Lett. A **28** (2013) 1330034.

[124] W. Mück, Eur. Phys. J. **C73**, (2013) 2679.

[125] V. Foit and N. Wintergerst, "Self-similar Evaporation and Collapse in the Quantum Portrait of Black Holes", arXiv:1504.04384 [hep-th].

[126] S. Hofmann and T. Rug, "A Quantum Bound-State Description of Black Holes", arXiv:1403.3224 [hep-th].

[127] F. Kühnel, Phys. Rev. D **90** (2014) 084024.

[128] F. Kühnel and B. Sundborg, "Modified Bose-Einstein Condensate Black Holes in d Dimensions", arXiv:1401.6067 [hep-th].

[129] F. Kühnel and B. Sundborg, Phys. Rev. D **90** (2014) 064025.

[130] G. Dvali and C. Gomez, Phys. Lett. B **719**, 419 (2013).

[131] G. Dvali, C. Gomez and S. Mukhanov, "Black Hole Masses are Quantized," arXiv:1106.5894 [hep-ph].

[132] J. D. Bekenstein, "Quantum black holes as atoms," gr-qc/9710076.

[133] R. Ruffini and S. Bonazzola, Phys. Rev. **187** (1969) 1767.

[134] F. Kuhnel and M. Sandstad, "Baryon number conservation in Bose-Einstein condensate black holes," arXiv:1506.08823 [gr-qc].

[135] M. Colpi, S. L. Shapiro and I. Wasserman, Phys. Rev. Lett. **57** (1986) 2485.

[136] M. Membrado, J. Abad, A. F. Pacheco and J. Sanudo, Phys. Rev. D **40** (1989) 2736.

[137] J. Balakrishna, "A Numerical study of boson stars: Einstein equations with a matter source," arXiv:gr-qc/9906110.

[138] T. M. Nieuwenhuizen, Europhys. Lett. **83** (2008) 10008.

[139] T. M. Nieuwenhuizen and V. Spicka, "Bose-Einstein condensed supermassive black holes: A Case of renormalized quantum field theory in curved space-time," arXiv:0910.5377 [gr-qc].

[140] P.-H. Chavanis and T. Harko, Phys. Rev. D **86** (2012) 064011.

[141] M. J. Duff, Phys. Rev. D **7**, 2317 (1973).

[142] S. Deser, Gen. Rel. Grav. **42**, 641 (2010).

[143] B. Harms and Y. Leblanc, Phys. Rev. D **46**, (1992) 2334.

[144] D. Flassig, A. Pritzel, and N. Wintergerst, Phys. Rev. D **87**, (2013) 084007.

[145] R. Brustein, Fortsch. Phys. **62** (2014) 255.

[146] R. Brustein and M. Hadad, Phys. Lett. B **718** (2012) 653.

[147] R. Torres and F. Fayos, Phys. Lett. B **733** (2014) 169.

[148] R. Torres, Phys. Lett. B **733** (2014) 21.

[149] R. Brustein and A. J. M. Medved, JHEP **1309** (2013) 015.